GEOLOGICA ULTRAIECTINA

Mededelingen van de
Faculteit Aardwetenschappen
Universiteit Utrecht

No. 187

STRUCTURAL ANALYSIS OF SOME MARINE KEROGENS THROUGH A COMBINED CHEMICAL AND THERMAL DEGRADATION APPROACH

Ingeborg M. Höld

GEOLOGICA ULTRAIECTINA

Mededelingen van de
Faculteit Aardwetenschappen
Universiteit Utrecht

No. 187

STRUCTURAL ANALYSIS OF SOME MARINE KEROGENS THROUGH A COMBINED CHEMICAL AND THERMAL DEGRADATION APPROACH

STRUCTURAL ANALYSIS OF SOME MARINE KEROGENS THROUGH A COMBINED CHEMICAL AND THERMAL DEGRADATION APPROACH

Gecombineerde chemische en thermische degradatie:
een methode voor de structuuropheldering van mariene kerogen

(Met een samenvatting in het Nederlands)

Proefschrift
ter verkrijging van de graad van doctor
aan de Universiteit Utrecht
op gezag van de Rector Magnificus, Prof. Dr. H.O. Voorma
involge het besluit van het College voor Promoties
in het openbaar te verdedigen
op maandag 13 maart 2000 des namiddags te 4:15 precies

door
Ingeborg Maria Höld
geboren op 20 oktober 1968
te 's-Gravenhage

Promotor: Prof. Dr. J.W. de Leeuw
Co-promoter: Dr. Ir. J.S. Sinninghe Damsté

The investigations were supported by a PIONIER grant to Dr. Ir. J.S. Sinninghe Damsté from the Netherlands Organization for Scientific Research (NWO).

ISBN 90-5744-045-8

Aan mijn ouders

CONTENTS

SUMMARY

Approximately 95% of the sedimentary organic matter in the geosphere exists in the form of kerogen, a macromolecular substance that is insoluble in water and normal organic solvents. There have been numerous attempts to elucidate the chemical structure of kerogens since kerogen is the main precursor of crude oil. However, since kerogens consist of high-molecular weight compounds that are not amenable to chromatographic analysis, it is difficult to elucidate their structures. The objective of the research described in this thesis was to gain a better insight in the chemical composition of marine kerogens the predominant precursors of crude oils. In the first part (Chapters 2-3) two different combinations of techniques, i.e. combined pyrolysis and stable carbon isotope analysis and combined chemical and thermal degradation, are introduced. These techniques are used to study several kerogens of different ages and origins in order to determine the various constituents present in kerogen and in order to gain information on the origin and importance of these constituents. In the second part (Chapters 4-7) some of these constituents present in kerogen and the reactions during thermal degradation are studied in more detail.

In **Chapter 2** the off-line pyrolysis products of several marine kerogens were analysed. The stable carbon isotopic composition of the released *n*-alkanes (C_{10}-C_{25}) are quite similar to those of the *n*-alkenes (C_{13}-C_{20}), suggesting that they have a common origin such as algal biopolymers. The isoprenoid alkanes also have similar isotopic compositions but can differ significantly from those of the *n*-alkanes and *n*-alkenes. These isoprenoids could be derived from an isoprenoid algaenan similar to that biosynthesized by the freshwater algae *Botryococcus braunii* race *L*.

Flash pyrolysis and sequential chemical degradation were combined in **Chapter 3** in order to study the molecular composition of an immature Type II-S kerogen from the Miocene Monterey Formation. Firstly, base hydrolysis was performed in order to hydrolyse ester bonds, in the second step aliphatic ethers were cleaved and in the third step sulfur-sulfur and sulfur-carbon bonds in the kerogen were broken. Linear and isoprenoid alkanes and alkenes were partially released upon cleavage of ether-bonds and are probably derived from *n*-alkyl and isoprenoid algaenans, respectively, biosynthesized by marine algae. The precursor moieties of the alkylthiophenes generated upon pyrolysis were released upon cleavage of sulfide-bonds indicating that their precursors, probably sugars, were sulfur-bound to the kerogen. Upon ether- as well as sulfur-bond cleavage, alkylpyrroles were released indicating that their precursors, probably tetrapyrrole pigments, occur ether- as well as sulfur-bound in the kerogen. Furthermore, prist-1-ene as well as tocopherols were removed from the flash pyrolysate after ether-bond cleavage, indicating that ether-bound tocopherols are probably a major source of prist-1-ene in

kerogen pyrolysates. In addition, ester-, ether- and sulfur-bound low-molecular-weight biomarkers attached to the kerogen were identified. However, the release of these biomarkers into the extract has hardly any impact on the residue pyrolysate and thus most of the compounds identified in the extracts are probably quantitatively less important constituents of the kerogen.

As is indicated in Chapter 2 and 3, the principal isoprenoid hydrocarbons found in flash pyrolysates of immature kerogens are prist-1-ene and, to a lesser extent, prist-2-ene. Chemical degradation experiments on a sulfur-rich kerogen, described in **Chapter 4,** show that at least two precursors can generate pristenes upon pyrolysis of sulfur-rich kerogens: ether-bound precursors, probably tocopherols, and a sulfur-bound precursor. Prist-2-ene is likely formed by the double bond isomerization of prist-1-ene. This isomerization of prist-1-ene into prist-2-ene depends on the amount of protons available for the formation of the intermediate carbonium ion. These protons can be derived from (acidified) aluminosilicates (e.g. the clay minerals montmorillonite and kaolinite) present in the sediment or from an inorganic acid (e.g. HI, HCl). The degree of isomerization depends on the amount of protons available versus the total organic carbon content of the sediment.

In **Chapter 5** a number of products were identified in several kerogen pyrolysates (e.g Green River, Monterey Formation) that (partially) were also found in the pyrolysate of the sodium salt of retenoic acid, a compound thought to mimic the pyrolysis behaviour of non-aromatic cyclic carotenoids. This suggests that non-aromatic cyclic carotenoids such as β-carotene are present in kerogens. Selective chemical degradation results suggest that ether-bound non-aromatic cyclic carotenoids are present in some kerogens and are probably the precursors of these compounds. Also relatively high amounts of a number of methylated benzenes (*e.g.* 1,2,3-trimethylbenzene) were identified in these kerogen pyrolysates. These methylated benzenes are partly derived from aromatized products formed during diagenesis.

The Huqf oil from Oman and other time-equivalent oils are characterized by relatively high amounts of mid-chain branched monomethyl alkanes. In **Chapter 6** the Huqf oil, the saturated hydrocarbon fractions, the desulfurized polar fractions of the bitumens and the kerogen pyrolysates of three potential source rocks from the Huqf Formation (Oman) were analyzed in order to resolve the origin of these mid-chain branched monomethyl alkanes. Using off-line pyrolysis and chemical degradation in combination with compound specific carbon isotope analysis, it was assessed that the mid-chain branched monomethyl alkanes are probably derived from lipids with C_{28+} carbon skeletons and methyl branching at the 12- or 13-position. These lipids were incorporated in the kerogen through reactions of sulfur with functional groups at different positions in the precursor lipid(s).

The presence of kerogen bound cyclic monoterpenoids (α-terpineol, borneol and fenchylalcohol) and tricyclic diterpenoids has been established in Tertiary, Cambrian and Late Proterozoic marine kerogens in **Chapter 7** through flash pyrolysis, alkaline hydrolysis and authentic standards. The unsaturated and aromatic terpenoids in the kerogen pyrolysate are formed from rearrangement reactions of the ester bound precursors followed by aromatisation. However, there are serious doubts if these terpenoids are indigenous to these marine kerogens.

SAMENVATTING

Ongeveer 95% van het sedimentair organisch materiaal in de geosfeer bestaat uit kerogeen, een macromoleculaire substantie die onoplosbaar is in water en normale organische oplosmiddelen. Er zijn vele pogingen gedaan om de chemische structuur van kerogeen op te helderen omdat kerogeen het uitgangsmateriaal voor ruwe olie is. Echter, omdat kerogeen bestaat uit verbindingen met een hoog molecuul gewicht die slecht ontvankelijk zijn voor chromatografische analyse, is deze chemische samenstelling moeilijk te bepalen. Het doel van dit onderzoeksproject was om een beter inzicht te verkrijgen in de chemische samenstelling van marine kerogenen. In het eerste gedeelte (hoofdstukken 2-3) worden twee verschillende combinaties van technieken, i.e. een combinatie van pyrolyse en stabiele koolstof isotoop bepaling en een combinatie van chemische en thermische degradatie, geïntroduceerd. Deze technieken worden gebruikt om diverse kerogenen van verschillende leeftijd en oorspong te bestuderen om daarmee de verschillende bestanddelen waaruit deze kerogenen zijn opgebouwd te bepalen en informatie omtrent de oorspong en belangrijkheid van deze bestanddelen te verkrijgen. In het tweede gedeelte (hoofdstukke 4-7) worden enkele van deze in kerogeen aanwezige bestanddelen en de reacties die plaatsvinden tijdens thermische degradatie in meer detail bestudeerd.

In **Hoofdstuk 2** zijn de (off-line) pyrolyse producten van diverse marine kerogenen geanalyseerd. De stabiele koolstof isotopen samenstelling van de losgemaakte *n*-alkanen (C_{10}-C_{25}) is min of meer gelijk aan die van de *n*-alkenen (C_{13}-C_{20}). Dit suggereert dat de oorsprong van beide waarschijnlijk van algen afkomstige biopolymeren zijn. De isoprenoid alkanen hebben onderling ook een min of meer gelijke stabiele koolstof isotopen samenstelling die echter kan verschillen van die van de *n*-alkanen en *n*-alkenen. Deze isopenoiden zouden afkomstig kunnen zijn van een, op het door de zoetwater alg *Botryococcus Braunii* race *L* gelijkend, isoprenoid algaenan.

Flash pyrolyse en chemische degradatie zijn gecombineerd in **Hoofdstuk 3** om de moleculaire samenstelling van een Type II-S kerogeen van de Miocene Monterey Formatie te bestuderen. Ten eerste is een basische hyrolyse uitgevoerd om te ester bindingen te hydrolyseren. In de tweede stap zijn de alifatische ethers verbroken en in de derde stap zijn de in het kerogeen aanwezige zwavel-zwavel en de zwavel-koolstof bindingen verbroken. Het verbreken van ether bindingen resulteert in loslaten van lineaire en isopenoid alkanen en alkenen. Deze verbindingen zijn waarschijnlijk afkomstig van door marine algen gebiosynthetiseerde *n*-alkyl en isoprenoid biopolymeren. De voorlopers van de tijdens pyrolyse gevormde alkylthiophenen werden losgelaten na het verbreken van de sulfide bindingen in het kerogeen. Deze voorlopers van alkylthiophenen zijn waarschijnlijk afkomstig van suikers. Zowel na het verbreken van ether- als na het

verbreken van zwavel bindingen, werden alkylpyrrolen losgemaakt van het kerogeen. Dit suggereert dat de voorlopers, waarschijnlijk tetrapyrrool pigmenten, zowel ether- als zwavel gebonden in het kerogeen zitten. Verder werden na het verbreken van ether bindingen zowel prist-1-een als de tocopherolen verwijderd uit het flash pyrolysaat van het kerogeen wat suggereert dat ether-gebonden tocopherolen de meest waarschijnlijke voorlopers zijn van prist-1-een in het kerogeen pyrolysaat van de Miocene Monterey Formatie. Bovendien zijn ester-, ether- en zwavel gebonden biomarkers met een laag-moleculair gewicht geïdentificeerd in de losgemaakte fractie. Echter, het losmaken van deze biomarkers van het kerogeen heeft nauwelijks effect op de samenstelling van het residu pyrolysaat en daarom zullen deze in het extract aanwezige verbindingen waarschijnlijk kwantitatief minder belangrijke bestanddelen van het kerogeen zijn.

Zoals al is vermeld in hoofdstuk 2 en 3 zijn de belangrijkste isoprenoid koolwaterstoffen die in het flash pyrolysaat van onrijpe kerogenen gevonden zijn prist-1-een en, in mindere mate, pris-2-een. Chemische degradatie experimenten op zwavelrijke kerogenen, beschreven in **Hoofdstuk 4**, laten zien dat minstens twee soorten voorlopers pristenen kunnen genereren tijdens pyrolyse van zwavel-rijke kerogenen: ether-gebonden voorlopers, waarschijnlijk tocopherolen, en een zwavel-gebonden voorloper. Prist-2-een wordt waarschijnlijk gevormd door een dubbele band isomerizatie van prist-1-een. Deze isomerizatie van prist-1-een in prist-2-een is afhankelijk van de aanwezige hoeveelheid, voor de formatie van het intermediair carbonium ion benodigde, protonen. Deze protonen kunnen afkomstig zijn van in sediment aanwezige (aangezuurde) aluminosilcaten (e.g.. de kleimineralen montmorilloniet en kaoliniet) of van een anorganisch zuur (e.g. HI, HCl). De mate van isomerizatie is afhankelijk van de hoeveelheid beschikbare protonen versus de totale in het sediment aanwezige hoeveelheid organisch koolstof.

In **Hoofdstuk 5** zijn in verschillende kerogeen pyrolysaten een aantal producten geïdentificeerd die (gedeeltelijk) ook in het pyrolysate van een natrium zout van retinoic zuur, een verbindingen die het pyrolyse gedrag van niet-aromatische cyclische carotenoiden nabootst, voorkomen. Dit suggereert dat niet-aromatische cyclische carotenoiden,zoals β-caroteen, aanwezig zijn in sommige kerogenen en dat deze waarschijnlijk de voorlopers zijn van de geïdentificeerde verbindingen. Ook zijn relatief hoge hoeveelheden van een aantal gemethyleerde benzenen (e.g. 1,2,3-trimethylbenzeen) geïdentificeerd in deze kerogeen pyrolysaten. Deze gemethyleerde benzenen zijn gedeeltelijk afkomstig van tijdens diagenese gearomatizeerde producten.

De Huqf olie uit Oman en andere uit dezelfde tijd afkomstige oliën worden gekarakteriseerd door een relatief hoog gehalte aan in het midden van de keten vertakte monomethyl alkanen. In **Hoofdstuk 6** zijn de Huqf olie, de verzadigde koolwaterstof fracties, de ontzwavelde polaire fracties van de bitumen en de kerogeen pyrolysaten van drie potentiële source rocks van de Huqf Formatie geanalyseerd om de oorspong van deze in het midden van de keten vertakte monomethyl alkanen te achterhalen. Met behulp van

off-line pyrolyse en chemische degradatie in combinatie met component specifieke stabiele koolstof isotoop bepalingen, is bepaald dat deze vertakte monomethyl alkanen waarschijnlijk afkomstig zijn van lipiden met C_{28+} koolstof skeletten met een methyl vertakking op de 12- of 13-positie. Deze lipiden zijn opgenomen in het kerogeen via een reactie van zwavel met op verschillende in de voorloper lipiden aanwezige functionele groepen.

In **Hoofdstuk 7** is, in Tertiaire, Cambrische en Laat Protezoische marine kerogen, de aanwezigheid van in het kerogeen gebonden cyclische monoterpenoiden (α-terpineal, borneol en fenchylalcohol) en tricyclische diterpenoiden, met behulp van flash pyrolyse, basische hydrolyse en autentieke standaarden, vastgesteld. De onverzadigde en aromatische terpenoiden in het kerogeen pyrolysaat kunnen gevormd zijn via een herschikkingsreactie van de ester gebonden voorlopers gevolgd door aromatiseren. Echter, er zijn ernstige twijfels of deze terpenoiden authentiek zijn voor deze marine kerogenen.

CHAPTER 1

Introduction

1.1 Sedimentary organic matter

Large quantities of organic matter are biosynthesised every day by primary producers like plants, algae and bacteria. When this organic matter settles on the sea floor, it is subjected to a wide range of (bio)chemical reactions. A large portion of the sedimentary organic matter is reworked by organisms living on the sea floor or in the top layer of the sediment. A small fraction (<0.5%), however, may escape the biosphere and will become part of the geosphere where it is stored in sediments (Fig. 1.1). During geological time, the organic matter is buried and matures when it is subjected to increasing subsurface temperatures. Initially, this causes mild (bio)chemical transformations known as diagenetic reactions. Later, more severe reactions, including even C-C bond cleavage, may take place. This latter process can ultimately lead to the formation of crude oils.

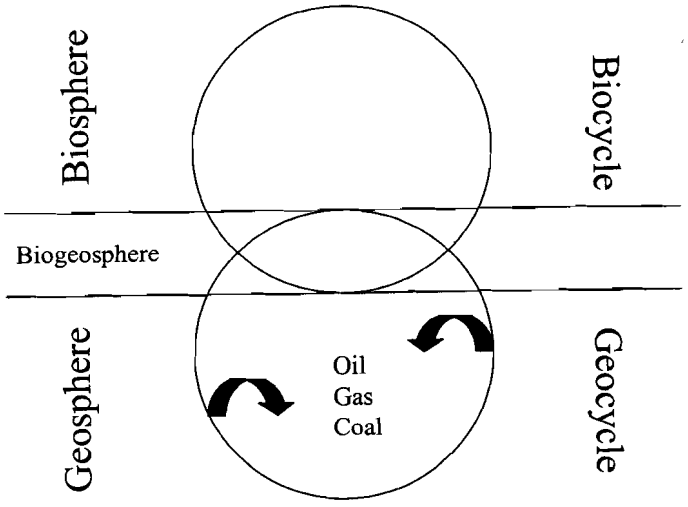

Figure 1.1 Organic carbon cycle.

Ca. 5% of the sedimentary organic matter consists of bitumen, the part extractable by organic solvents (Durand, 1980). The identification of these extractable low-molecular-weight compounds has been one of the dominant research areas in organic geochemistry. These low-molecular-weight compounds are either originally present in the sedimentary organic matter or have formed from thermal breakdown of kerogen. *Ca.* 95% of the sedimentary organic matter in the geosphere exists in the form of kerogen, a macromolecular substance that is insoluble in water and normal organic solvents (Durand, 1980). There have been numerous attempts to elucidate the chemical structure of kerogens since kerogen is the main precursor of crude oil. However, since kerogens consist of high-molecular weight compounds that are not amenable to chromatographic analysis, it is difficult to elucidate their structures. With the limited amount of data available a number of models have been proposed for the origin and structure of kerogen.

1.2 Origin and structure of kerogen

According to the classical model (Tissot and Welte, 1984), it is thought that during early diagenesis the organic material from primary production is broken down into smaller constituents by microbial action, which are then incorporated into new polymeric structures. With increasing time and burial depth most of this material becomes progressively insoluble due to increasing polycondensation and defunctionalisation, resulting in the formation of kerogen. Indeed, several studies showed that low-molecular-weight lipids may become linked via ester or ether bonds to kerogens (*e.g.* Michaelis and Albrecht, 1979; Mycke *et al.*, 1987; Koopmans et al., 1996a) although they usually only comprise a small fraction of the kerogen.

In the last decade, the recognition and identification of highly resistant, aliphatic biomacromolecules in higher plant cuticles and cell walls of fresh-water algae, led to the proposition of the selective preservation model (e.g. Tegelaar et al., 1989). This model suggests that a significant fraction of lacustrine kerogen is derived from mixtures of selectively preserved resistant biomacromolecules. Although these biomacromolecules are only minor constituents of living organisms, it is believed that in the long term their refractory nature causes them to accumulate in sediments. Such a pathway was first suggested by Philp and Calvin (1976) based on their studies of algal macromolecular constituents. The identification of resistant aliphatic biomacromolecules in cell walls of several marine microalgae, i.e. Chlorophyceae and Eustigmatophyceae, was thought to provide evidence for a major contribution of such biomacromolecules (algaenans) to marine kerogens as well (Derenne et al., 1992a,b; de Leeuw en Largeau, 1993; Gelin et al., 1996a, 1997). However, since both of these classes of microalgae are not considered to be ubiquitous in marine environments, the occurrence of algaenans in other classes of

marine microalgae were studied and only a limited occurrence was found (Gelin et al., 1999). Therefore, it may well be the case that preserved biopolymers in sediments are derived from perhaps only a few species.

Besides these pathways for kerogen formation there is a third way in which parts of especially marine kerogens may be formed, i.e. natural vulcanisation. The identification of organic sulfur compounds with specific carbon skeletons unambiguously related to known precursor lipids was the first indication of the occurrence of a natural vulcanisation reaction (e.g. Valisolalao et al., 1984; Brassell et al, 1986; Sinninghe Damsté et al., 1988). Additional evidence for the sulfurisation of lipids has been obtained from laboratory experiments and both ionic and radical mechanisms have been proposed (e.g. Vairavamurthy and Mopper, 1987; Fukushima et al., 1992; de Graaf et al., 1992, 1995; Rowland et al., 1993; Schouten et al., 1993, 1994; Krein and Aizenhtat, 1994, 1995; Adam et al., 1998). Since then, it has become generally accepted that organic sulfur compounds occurring in the geosphere are formed during early diagenesis from the reaction of functionalized molecules with reduced inorganic sulphur species. Sulfurisation can occur (i) intramolecularly, resulting in the formation of low-molecular-weight organic sulfur compounds with e.g. thiophene, thiolane or thiane moieties, and (ii) intermolecularly, resulting in the formation of macromolecules consisting of carbon skeletons linked by (poly)sulfide bridges (Sinninghe Damsté et al., 1988, 1990a). Recently, it was suggested that not only functionalised lipids but also carbohydrates can react with reduced inorganic sulphur species through their functional groups, generating a sulfur cross-linked insoluble macromolecular network of carbohydrate skeletons and thus end up in kerogens (Sinninghe Damsté et al., 1999). The contribution to sulfur-rich kerogens of hetero-atoms-containing compounds, like porphyrins, has also been proposed (Schaeffer et al., 1993; Gelin et al., 1996b). In addition, evidence has been presented that functionalized molecules may be attached simultaneously by oxygen and sulfur bonds (Richnow et al., 1992, 1993; Schaeffer et al., 1995; Koopmans et al., 1997a). Recently, the occurrence of an oxygen incorporation process was proposed which may compete or proceed the sulfurization processes of organic matter at an early stage of diagenesis (Jenisch et al., 1999).

In conclusion, presently it is believed that marine kerogens are mixtures of (i) compounds originally biosynthesised as macromolecules (algaenans), and (ii) compounds which became macromolecularly bound during diagenesis (Fig 1.2). However, much work remains to be done in order to resolve the exact chemical composition of especially marine kerogens.

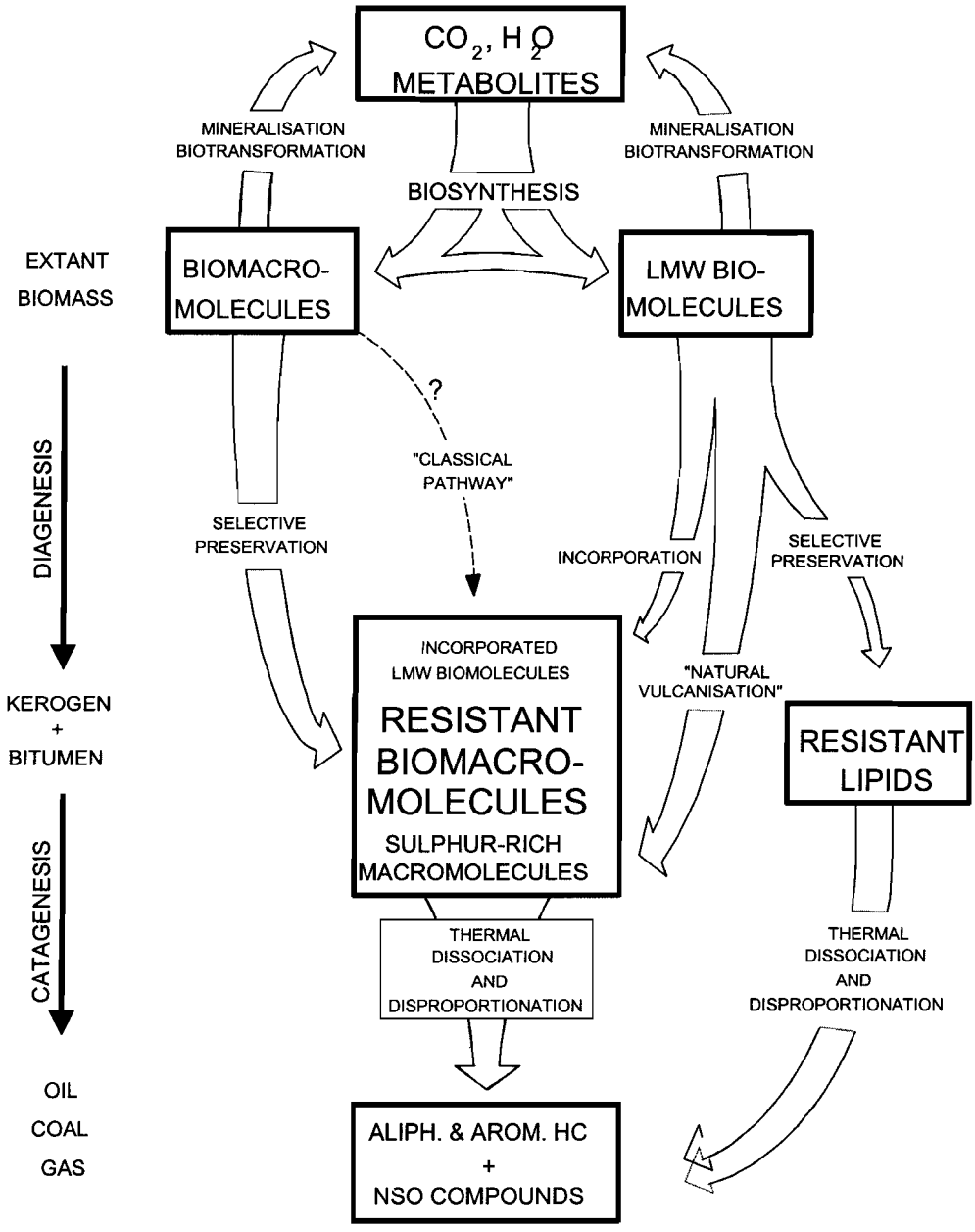

Figure 1.2 Mechanism for kerogen formation.

1.3 Kerogen degradation techniques

In order to resolve the chemical composition of kerogens, several techniques are available, especially degradation techniques which can break down the macromolecules thermally or chemically. The structural elements released can provide information concerning the origin and structure of the kerogens.

1.3.1 Thermal degradation

Pyrolysis is defined as thermal degradation in an inert atmosphere. The most commonly used method to identify pyrolysis products involves the on-line coupling of a pyrolysis unit with a gas chromatograph-mass spectrometer system (Py-GC-MS; e.g. Maters et al., 1977; Larter, 1984; Boon et al., 1987; Horsfield, 1989). Pyrolysis of kerogens also generates non-GC-amenable compounds, *i.e.* high-molecular-weight and polar components and, therefore, typically only *ca.* 10% of the pyrolysed starting material can be analysed by Py-GC-MS. However, several studies have demonstrated that pyrolytic fragments are structural representative of the kerogen as a whole (e.g. Goth et al., 1988; Horsfield, 1989; Eglinton et al., 1990, 1991; Sinninghe Damsté et al., 1990b; Larter and Horsfield, 1993). In many cases the total pyrolysate is very complex and separation of the total pyrolysate into different fractions is necessary. To this end, off-line pyrolysis can be performed to allow detailed analysis of the pyrolysis products. In this way, it can still provide information concerning the different contributors to the kerogen (e.g Hartgers et al., 1994a; Gelin et al., 1996b).

1.3.2 Chemical degradation

Although thermal degradation yields information on the presence of certain moieties in kerogens, it yields no information on how the thermally released molecules were linked to the kerogen. Selective chemical degradation can overcome this problem. Several studies have been published on different methods where selectively ester-, ether- or sulfur-bonds in high-molecular-weight aggregates were cleaved and the released extracts were studied, in order to find out how specific biomarkers were bound to macromolecules.

Oxygen-linked structural units can be investigated by several ether- and/or ester-bond degrading reagents. Ester bonds are simply cleaved by acidic or alkaline hydrolysis. A stepwise alkaline saponification and acid hydrolysis of extracted sediments released lipids bound to the kerogen by ester- and amide- or glycosidic bonds, respectively (Goossens et al., 1989). Compounds released were predominantly acyclic monocarboxylic acids, with small amounts of among others hopanoic- and biphytanic acids. $BCl_3/LiAlH_4$ and $HI/LiAlH_4$ degradation have been used to cleave ester and ether linkages in macromolecular organic matter (*e.g* Jenisch et al., 1990; Richnow et al., 1992, 1993;

Koopmans et al., 1998). Compounds released are predominantly *n*-alkanes, acyclic isoprenoids and smaller amounts of steranes, hopanes and biphytanes.

S-bound moieties can be released by several desulfurizing reagents. Richnow et al. (1992) used nickel(0)cene/$LiAlH_4$ to desulfurize polar fractions, asphaltenes and, to some extent, kerogens. However, reaction times are long and some side reactions have been noted. Lithium in ethylamine is used to desulfurize asphaltenes and kerogens (*e.g.* Hoffman et al., 1992; Gelin et al., 1995, 1996b; Koopmans et al., 1997a). The disadvantages of this method are contamination problems with the lithium, requiring the use of liquid ammonia in the purification process and the relative long preparation and reaction times. Schouten et al. (1993) reported the successful use of nickel boride to desulfurize geomacromolecules. Since the active desulphurization agent is prepared *in situ* problems with the activity of the agent (like with Raney nickel) are absent. Therefore, the efficiency of Ni_2B for the desulfurization of geomacrocolecules is higher (Schouten et al., 1993; Hefter et al., 1995). Typical compounds released with desulfurizing reagents are *n*-alkanes, phytane and smaller amounts of steranes, hopanes, biphytanes and carotenoid derivatives.

Ruthenium tetroxide has been applied in catalytic oxidative breakdown of kerogens (Standen et al., 1991; Richnow et al., 1992). It oxidizes certain types of aromatic structures releasing aliphatic alkyl substituents as carboxylic acids in high yields. These aliphatic carboxylic acids receive an additional carbon atom from the aromatic ring system. Furthermore, this reagent oxidizes different types of ethers, primary alcohols and olefins (Schouten et al., 1997; Blokker et al., 1998).

In order to get a better insight in the total composition of the kerogen and the different types of linkages of the constituents in the kerogens, sequential chemical degradations of kerogen have been performed (e.g. Richnow et al., 1992; Hefter et al., 1995; Schaeffer et al., 1995). This technique cleaves subsequently and selectively ester-, ether-, (poly)sulfide- and possibly aryl-bonds and allows in this way the identification of the different types of linkages of the constituents in the kerogen. Some constituents are linked exclusively *via* sulfur, oxygen or aromatic entities to the kerogen. However, upon desulfurization of a residue some alcohols were detected, indicating that these compounds must have been bound simultaneously by both oxygen and sulfur-bonds (e.g Richnow et al., 1992; Jenisch et al., 1999).

Thus, chemical degradation is useful in determining some of the mode of binding of a number of structural moieties in kerogens. However, all these studies were concerned with the identification of the released compounds. Studies of the effect of chemical degradations on the structure of the remaining kerogen residues are very limited. Analysis of a kerogen pyrolysate of a hypersaline sediment before and after desulfurization has been performed (Gelin et al., 1995, 1996b; Kenig et al., 1995; Schaeffer et al., 1995). Significant variations in the relative contributions and abundances of pyrolysis products

were observed. The series of normal hydrocarbons contributed relatively more to the pyrolysate of the desulfurised kerogens suggesting an enrichment of lineair algaenans biosynthesised by marine algae. Also, in order to obtain information about the precursors of free pristane, Koopmans et al. (1999) studied the relative abundance of prist-1-ene and prist-2-ene in marine kerogens, released upon pyrolysis, before and after desulfurization and/or ether-bond cleavage. Depending on the kerogen samples, the precursor of the pristenes was ether-bound and/or sulfur-bound in the kerogen. Oxygen-bound tocopherol and sulfur- and oxygen-bound pristane were identified as the precursors of free pristane.

These studies show that valuable information may be gained by the combination of chemical and thermal degradation of kerogens, where both the released compounds and the effect on the kerogens are studied. Thus this combination may provide a powerful tool in identifying sources and mode of binding of moieties in kerogens.

1.4 Stable carbon isotope monitoring

Although structures of released moieties can sometimes reveal their sources, this is often not the case. In this respect the stable carbon isotopic composition of these moieties can provide additional information on their origin. Carbon occurs on earth in three forms: ^{12}C (*ca.* 98.9 %), ^{13}C (*ca.* 1.1 %) and ^{14}C (< 0.1 %). Only the first two isotopes, ^{12}C and ^{13}C, occur in a natural stable form. The relative amounts of ^{12}C and ^{13}C in organic matter, however, may change through various physical and biochemical processes: e.g. the relative amounts of ^{12}C and ^{13}C of the carbon source used in photosynthesis, isotope effects associated with carbon uptake and biosynthesis and/or isotope effects associated with chemical alterations during diagenesis (e.g. Hayes, 1993; Freeman et al., 1994; Schouten et al., 1997). In order to express the variation in ^{12}C and ^{13}C the amount of ^{13}C is divided by the amount of ^{12}C and compared to the ratio of a standard, a marine limestone (PDB) with a $^{13}C/^{12}C$ of 0.0112372 (Craig, 1957). The difference between these ratios is expressed in per mills and termed $\delta^{13}C$:

$$\delta^{13}C_{compound} = \frac{R_{compound} - R_{PDB}}{R_{PDB}} * 1000$$

Where $R = {}^{13}C/{}^{12}C$

In organic geochemical studies $\delta^{13}C$-values of total organic matter are often used as indicators for sources and diagenetic process (e.g. Schidlowski et al., 1984; Peters and Moldowan, 1993). The disadvantage of measuring the carbon isotopic composition of

total organic matter or kerogens is, however, that it represents an average of $\delta^{13}C$-values of structural moieties of diverse origins. The development of isotope-ratio-monitoring gas chromatography-mass spectrometry (irm-GCMS) to determine the stable carbon isotopic compositions of individual compounds (e.g. Hayes et al., 1990) has led to numerous applications of this technique in organic geochemistry as it provides valuable information on the origin of individual compounds present in sediments (e.g. Freeman et al., 1990; Kohnen et al., 1992). Besides determining the sources of free biomarkers, the natural variations in stable carbon isotopic values of the individual compounds released by thermal or chemical degradation of kerogens can be used to distinguish between different contributions of the moieties present in kerogens (e.g. Eglinton, 1994; Hartgers et al., 1994; Hoefs et al., 1995; van Kaam-Peters et al., 1997a, Schouten et al., 1997).

1.5 Scope and framework of the thesis

The objective of the research described in this thesis was to gain a better insight in the chemical composition of marine kerogens. Two different combinations of techniques, i.e. combined pyrolysis and stable carbon isotope analysis and combined chemical and thermal degradation, were used to study several kerogens of different ages and origins in order to determine the various constituents present in kerogen and in order to gain information on the origin and importance of these constituents. In Chapter 2 the isotopic analysis of off-line pyrolysis products of several marine kerogens reveal the presence of different alganaens. Flash pyrolysis and sequential chemical degradation were combined in Chapter 3 in order to study the effects of different bond-cleavages on the molecular composition of an immature Type II-S kerogen from the Miocene Monterey Formation. In Chapter 4 it is shown that at least two precursors in sulfur-rich kerogens can generate pristenes upon, an ether-bound and a sulfur-bound precursor. It is also demonstrated that prist-2-ene originates from prist-1-ene through acid clay catalysis. In Chapter 5 a number of products were identified in several kerogen pyrolysates (e.g Green River, Monterey Formation) that are also found in the pyrolysate of the sodium salt of retenoic acid, a compound thought to mimic the pyrolysis behaviour of non-aromatic cyclic carotenoids. This suggests that non-aromatic cyclic carotenoids such as β-carotene are present in kerogens. In Chapter 6 the Huqf oil, the saturated hydrocarbon fractions, the desulfurized polar fractions of the bitumens and the kerogen pyrolysates of three potential source rocks from the Huqf Formation (Oman) are analyzed in order to provide clues to the origin of mid-chain branched monomethyl alkanes present in kerogens from the Huqf Formation. The presence of kerogen bound cyclic monoterpenoids and tricyclic diterpenoids is established in Tertiary, Cambrian and Late Proterozoic marine kerogens in Chapter 7

through flash pyrolysis, alkaline hydrolysis and authentic standards. However, there are serious doubts if these terpenoids are indigenous to these marine kerogens.

CHAPTER 2

Changes in the molecular structure of a type II-S kerogen (Monterey Formation, USA) during sequential chemical degradation

Ingeborg M. Höld, Niels J. Brussee, Stefan Schouten, and Jaap S. Sinninghe Damsté

2.1 Abstract

Flash pyrolysis and sequential chemical degradation were combined to study the molecular composition of an immature Type II-S kerogen from the Miocene Monterey Formation. Firstly, base hydrolysis was performed in order to hydrolyse ester bonds, in the second step aliphatic ethers were cleaved and in the third step sulfur-sulfur and sulfur-carbon bonds in the kerogen were broken. Linear and isoprenoid alkanes and alkenes were partially released upon cleavage of ether-bonds and are probably derived from *n*-alkyl and isoprenoid algaenans, respectively, biosynthesized by marine algae. The precursor moieties of the alkylthiophenes generated upon pyrolysis were released upon cleavage of sulfide-bonds indicating that their precursors, probably sugars, were sulfur-bound to the kerogen. Upon ether- as well as sulfur-bond cleavage, alkylpyrroles were released indicating that their precursors, probably tetrapyrrole pigments, occur ether- as well as sulfur-bound in the kerogen. Furthermore, prist-1-ene as well as tocopherols were removed from the flash pyrolysate after ether-bond cleavage, indicating that ether-bound tocopherols are probably a major source of prist-1-ene in kerogen pyrolysates. Furthermore, our degradation approach resulted in the recognition of specific ester-, ether- and sulfur-bound low-molecular-weight biomarkers attached to the kerogen. However, the release of these biomarkers into the extract has hardly any impact on the residue pyrolysate and thus most of the compounds identified in the extracts are probably less important constituents of the kerogen.

2.2 Introduction

Kerogen comprises ca. 95% wt of the sedimentary organic matter (Durand, 1980). However, the precise origin of especially marine kerogens is still far from understood. A significant fraction of kerogen may be derived from algal resistant biomacromolecules, composed of polymethylenic chains with linear or isoprenoid carbon skeletons and crosslinked *via* ether bridges through selective preservation (Goth *et al.*, 1988; Derenne

et al., 1992a,c; Gelin *et al.*, 1996a,b). In addition to these biomacromolecules (so-called algaenans), substantial amounts of high-molecular-weight sulfur compounds can also be present in especially marine kerogens. These kerogens have been classified on basis of their elemental composition as Type II-S kerogens (Orr, 1986). The sulfur compounds are formed *via* "vulcanization" of lipids (Sinninghe Damsté *et al.*, 1989; Boussafir *et al.*, 1995) and carbohydrates (Kok *et al.*, 1997) during early diagenesis. It is thought that this process transfers these compound classes from the labile to the refractory organic matter pool and in this way leads to preservation. Orr (1986) postulated that preferential cleavage of the weak S-S and S-C bonds present in these Type II-S kerogens produces larger fragments, leading to high initial amounts of asphaltenes, resins and sulfur-rich aromatics together with smaller amounts of saturated hydrocarbons during the maturation process.

Because of its macromolecular structure, kerogen is insoluble in common organic solvents (Durand, 1980; Durand and Nicaise, 1980) and is as such difficult to analyze. Flash pyrolysis is a widely used tool to study the composition of kerogens (*e.g.* van de Meent *et al.*, 1980; Larter, 1984; Eglinton *et al.*, 1991) and requires only a few milligrams of starting material. Although only a small fraction of the pyrolysed starting material can be analyzed by Py-GC-MS, due to the loss of non-GC-amenable compounds, NMR and other spectroscopic techniques have shown that the structural information recovered from this small amount is generally representative of the bulk of the starting material (*e.g.* Goth *et al.*, 1988; Horsfield, 1989; Larter and Horsfield, 1993). However, the flash-pyrolysis technique yields no information on how the thermally released molecules were linked to the kerogen. Sequential selective chemical degradation of kerogen can overcome this problem. This technique cleaves selectively ester-, ether- and (poly)sulfide-bonds subsequently and allows in this way the identification of the different types of linkages of structural building blocks in the macromolecular structure. Several studies showed that some biomarkers are linked exclusively *via* sulfur, oxygen or aromatic entities to the macromolecular network and that some compounds (*e.g.* hopanoids and *n*-alkanes) are bound simultaneously by sulfur and oxygen bonds (*e.g.* Richnow *et al.*, 1992; Hefter *et al.*, 1995; Schaeffer *et al.*, 1995). However, yields of chemical degradation are often very low because chemical degradation reagents react only at the outer edge of the kerogen particles.

In this study flash pyrolysis and sequential chemical degradation were combined to study the molecular composition of an immature Miocene Type II-S kerogen from the Monterey Formation. The variety of compound classes present in the flash pyrolysate of this kerogen, *e.g.* normal, branched and cyclic hydrocarbons, alkyl aromatic hydrocarbons, alkylthiophenes and alkylpyrroles and the fact that its sediments were extensively studied previously (Rullkötter and Isaacs, 1998), made this kerogen appropriate to study the influence of the different chemical degradation steps on the

chemical structure of kerogen. This is the first study in which chemical degradation methods and degradation sequence were chosen to differentiate between ester-, ether- and sulfur bound structural units present in the kerogen and in the mean time the residue pyrolysates were monitored after each degradation step. This study resulted in the identification of predominantly linear and isoprenoid algaenans and probably of sulfur-bound carbohydrates and sulfur- and ether-bound porphyrins in the Type-II-S Monterey kerogen.

2.3 Experimental

Sample

A sediment sample (KG-1) was taken from a fresh outcrop of the middle Miocene carbonaceous marls of the Monterey Formation at Naples Beach (USA; Isaacs *et al.*, 1992). The sample has a TOC content of 9.6 %. Elemental analysis of the isolated kerogen indicated that it is an immature Type II-S kerogen with an atomic H/C ratio of 1.27, an atomic O/C ratio of 0.15, and an atomic S/C ratio of 0.05 (Isaacs, personal communication).

Extraction and kerogen isolation

The powdered sample was Soxhlet extracted with dichloromethane/methanol (DCM/MeOH; 7.5:1, v/v) for 32 h. Carbonates were removed by treatment with 4N HCl at room temperature and ultrasonically extracted with water (3x), MeOH (3x) and finally DCM (3x; Hartgers *et al.*, 1992). Kerogen isolation was performed by HCl/HF treatments of the solvent-extracted sediment (Eglinton, 1988). The isolated kerogen was ultrasonically extracted with MeOH, DCM/MeOH (1:1) and DCM.

Sequential chemical degradation

The different sequential chemical degradation steps are schematically shown in Fig. 2.1.

Firstly, an alkaline hydrolysis was performed in order to hydrolyze ester bonds within the kerogen (Goossens *et al.*, 1989). 30 ml 1N KOH in methanol (MeOH) was added to 400 mg kerogen, refluxed for 1 h at 65°C under a nitrogen atmosphere and then cooled to room temperature. The pH was adjusted to 3 by adding 4 N HCl(H_2O) /MeOH (1:1,v/v). The residue R_1 was washed with H_2O/MeOH (1:1, v/v, 3x), with MeOH (3x) and with ethyl acetate (3x). The residue R_1 was dried under nitrogen. The combined extracts were washed with saturated NaCl-solution (3x) and with H_2O (2x). The extract E_1 was dried with Na_2SO_4 and concentrated by distillation.

During the second step, aliphatic ethers were cleaved by treatment with HI (March, 1985). 35 ml 56% HI-solution (in H_2O) was added to 370 mg residue R_1, refluxed for 1 h under a nitrogen atmosphere and then cooled to room temperature. Residue R_2 was obtained as described above for R_1. The combined extracts were washed with H_2O saturated with NaCl, with 5 wt % $Na_2S_2O_3$-solution in order to remove I_2 and then with H_2O. 30 ml 1,4-dioxane was added to the extract and the ethyl acetate was distilled off. 700 mg $LiALH_4$ was added to the extract, refluxed for 1.5 h and then cooled to room temperature. Ethyl acetate was added to deactivate the remaining $LiALH_4$ and the reaction mixture was centrifuged. The supernatant was washed with H_2O saturated with NaCl (3x) and with H_2O (2x). The extract E_2 was dried with Na_2SO_4 and concentrated by distillation.

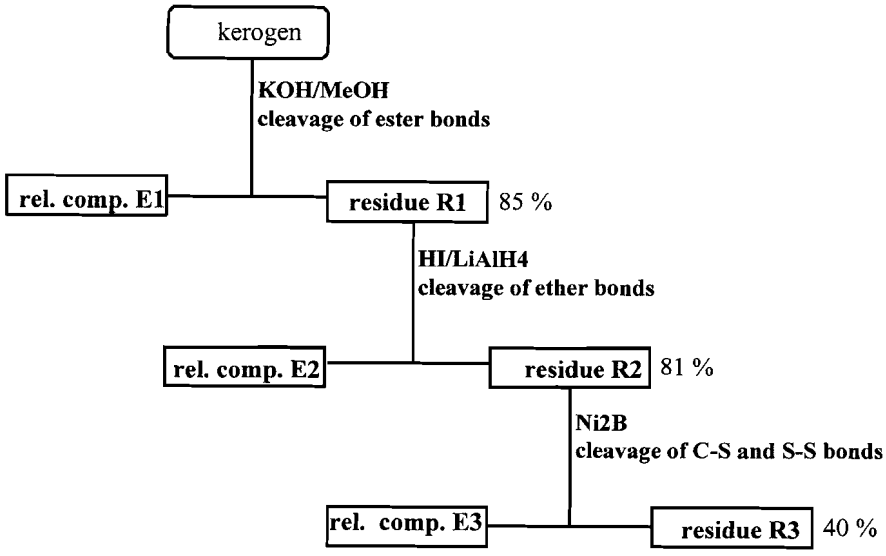

Figure 2.1 Flow diagram of the sequential chemical degradation of the Monterey kerogen. Yield of the residues are indicated.

In the third step, (poly)sulfide bonds in the kerogen were cleaved by treatment with Ni_2B (Schouten *et al.*, 1993). 25 ml MeOH/THF (1:1), 500 mg $NiCl_2$ and 500 mg $NaBH_4$ were added to 350 mg residue R_2. The mixture was refluxed for 1 h under stirring and N_2 atmosphere and then cooled down to room temperature. The residue R_3 and extract E_3 were obtained as described above for R_1 and E_1. In order to remove the Ni salts present in

the residue, 10 ml concentrated HNO_3 was added and left to react for 12 h. The residue R_3 washed with H_2O/MeOH (1:1, v/v, 3x), with MeOH (3x) and with ethyl acetate (3x).

After all three degradation steps the extracts were derivatised by treatment with CH_2N_2 and BSTFA/pyridine to derivatise fatty acids and alcohols, respectively. Extracts and residues were analyzed by GC-MS and flash pyrolysis-GC-MS, respectively.

Gas chromatography (GC)

GC was performed on a Hewlett Packard 6890 or a Hewlett Packard 5890 instrument, both equipped with on-column injectors. A fused silica capillary column (25 m x 0.32 mm) coated with CP Sil-5 (film thickness 0.12 μm) was used with helium as carrier gas. Compounds analyzed on the HP 6890 were detected by a flame ionization detector (FID). Compounds analyzed on the HP 5890 were detected simultaneously by FID and sulfur-selective flame photometric detector (FPD), using a stream-splitter at the end of the column (split ratio FID:FPD=1:2). The samples were dissolved in hexane before they were injected at 35°C (5 min) and the oven was subsequently heated to 310°C (10 min) at 4°C/min.

Flash pyrolysis-gas chromatography (Py-GC)

Py-GC was carried out using a Curie point pyrolysis device (FOM-4LX) using a high frequency generator (Fischer 9425). The pyrolysis unit was directly mounted on the injector block of a Hewlett Packard 5890 gas chromatograph. The temperature of the injector block was 250°C. The sample material was applied to ferromagnetic wires by pressing the dry sample onto the wire (Venema and Veurink, 1985). On-line pyrolysis was performed by inductive heating of the wires within 0.1 s to their Curie point temperatures (610°C) and were kept at those temperatures for 10 s. Separation of the pyrolysis products was accomplished by a fused silica capillary column (25 m x 0.32 mm) coated with CP Sil-5 (film-thickness 0.45 μm) using helium as carrier gas. The temperature was programmed from 0°C (5 min), by using a cryogenic unit, to 300°C (10 min) at a rate of 3°C/min. Compounds were detected by a FID at a temperature of 320°C.

Gas chromatography-mass spectrometry (GC-MS)

GC-MS was carried out on a Hewlett Packard 5890 gas chromatograph connected to a mass spectrometer (VG-Autospec Ultima) operated at 70 eV with a mass range *m/z* 40-800 and a cycle time of 1.8 s. The resolution was set to 1000. The gas chromatograph was equipped with a fused silica capillary column (25 m x 0.32 mm) coated with CP Sil-5 (film thickness 0.12 μm) using helium as carrier gas. The samples were injected at 35°C. After 5 minutes at 35°C the oven was heated to 310°C at 4°C/min and was held at 310°C for 10 minutes.

Flash pyrolysis-gas chromatography-mass spectrometry (Py-GC-MS)

Py-GC-MS analysis were performed on a Hewlett Packard 5890 gas chromatograph connected to a mass spectrometer (VG-Autospec Ultima). Pyrolysis and chromatographic conditions were identical to those described above for py-GC. The MS-conditions used for pyrolysis-GC-MS were the same as for GC-MS.

Compounds were identified by comparison of mass spectra and retention times with those reported in literature. References to the relevant papers are given at appropriate places in the text.

2.4 Results

Sequential selective chemical degradation of a Type II-S kerogen from the Monterey Formation was performed to provide insight into the molecular structure of marine sulfur-rich kerogens. As a first step, alkaline hydrolysis (KOH/MeOH) was performed in order to hydrolyse the ester bonds present in the kerogen (Fig. 2.1). In the second step ether bonds were cleaved using $HI/LiAlH_4$. In the third step, (poly)sulfide bonds in the kerogen were cleaved with Ni_2B. This latter step was chosen as the final one because Ni salts are generated during the desulfurization experiment and are left with the kerogen residue. These Ni salts can only be removed by HNO_3 treatment which may cause oxidation and nitrification of the organic matter. Since $HI/LiAlH_4$ is known to hydrolyze ester bonds as well as cleaving ether bonds, alkaline hydrolysis was chosen as the first step before $HI/LiAlH_4$ treatment. After all three degradation steps both extracts and residues were analyzed by GC-MS and flash pyrolysis-GC-MS, respectively. The composition of the flash pyrolysates was determined by integration of specific mass chromatograms characteristic for the major compound classes present in the pyrolysates (*cf.* Hartgers *et al.*, 1994b).

Kerogen

GC/MS analysis of the flash pyrolysate of the kerogen revealed a range of different components (Fig. 2.2a). The major components comprise of C_8-C_{28} *n*-alkanes and *n*-alk-1-enes with a maximum around C_{15} (Fig. 2.3a), C_{11}-C_{20} isoprenoid alkanes and alkenes with 2,6,10-trimethyldecane and pris-1-ene present in the highest relative abundance (Fig. 2.3a), C_0-C_4 alkylated benzenes (Hartgers *et al.*, 1992) with a relatively high 1-methyl-4-isopropylbenzene (Fig. 2.4a), C_1-C_4 alkylated thiophenes (Fig. 2.4a; Sinninghe Damsté *et al.*, 1988), C_0-C_4 alkylated pyrroles (Fig. 2.4a; Sinninghe Damsté *et al.*, 1992), C_0-C_3 alkylated naphthalenes, C_0-C_3 alkylated benzothiophenes, α– and γ–tocopherol (Fig. 2.2a), C_{27}-C_{29} steranes/sterenes (Fig. 2.2a) and 22,29,30-trisnorhop-17(21)-ene and 30-norhop-17(21)-ene (Fig. 2.2a).

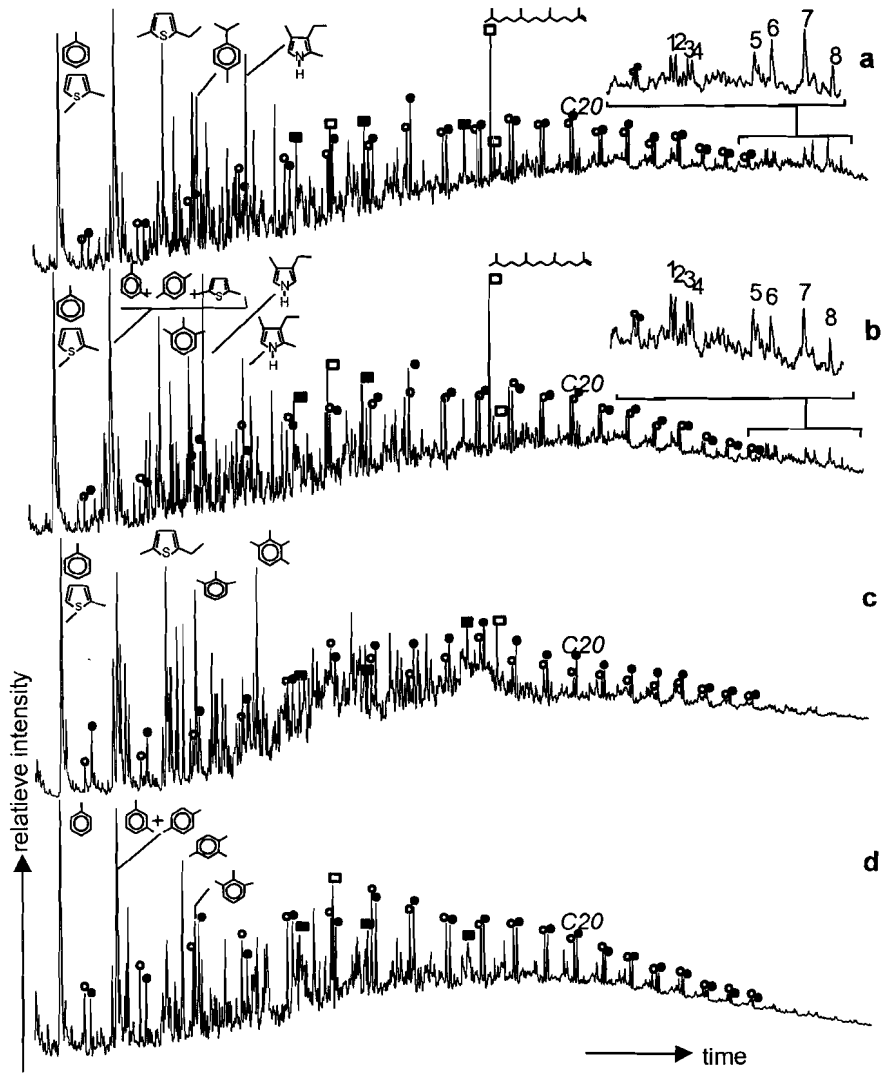

Figure 2.2 Partial Total Ion Current (TIC) trace of the flash pyrolysate (Curie temperature 610 °C) of (**a**) the isolated kerogen, (**b**) the residue R_1 after alkaline hydrolysis, (**c**) the residue R_2 after ether-bond cleavage, (**d**) the residue R_3 after desulfurization. Filled and open circles indicate the homologous series of *n*-alkanes and *n*-alk-1-enes, respectively. Their number of carbon atoms is indicated with italic numbers. Filled and open squares indicate pseudo homologous series of isoprenoid alkanes and alk-1-enes, respectively. Key: 1 = cholestan-3-ol , 2 = 5α-cholestane, 3 = trisnorhop-17(21)-ene, 4 = cholestadiene, 5 = 30-norhop-17(21)-ene, 6 = γ-tocopherol, 7 = α-tocopherol, 8 = cholest-4-en-3-one.

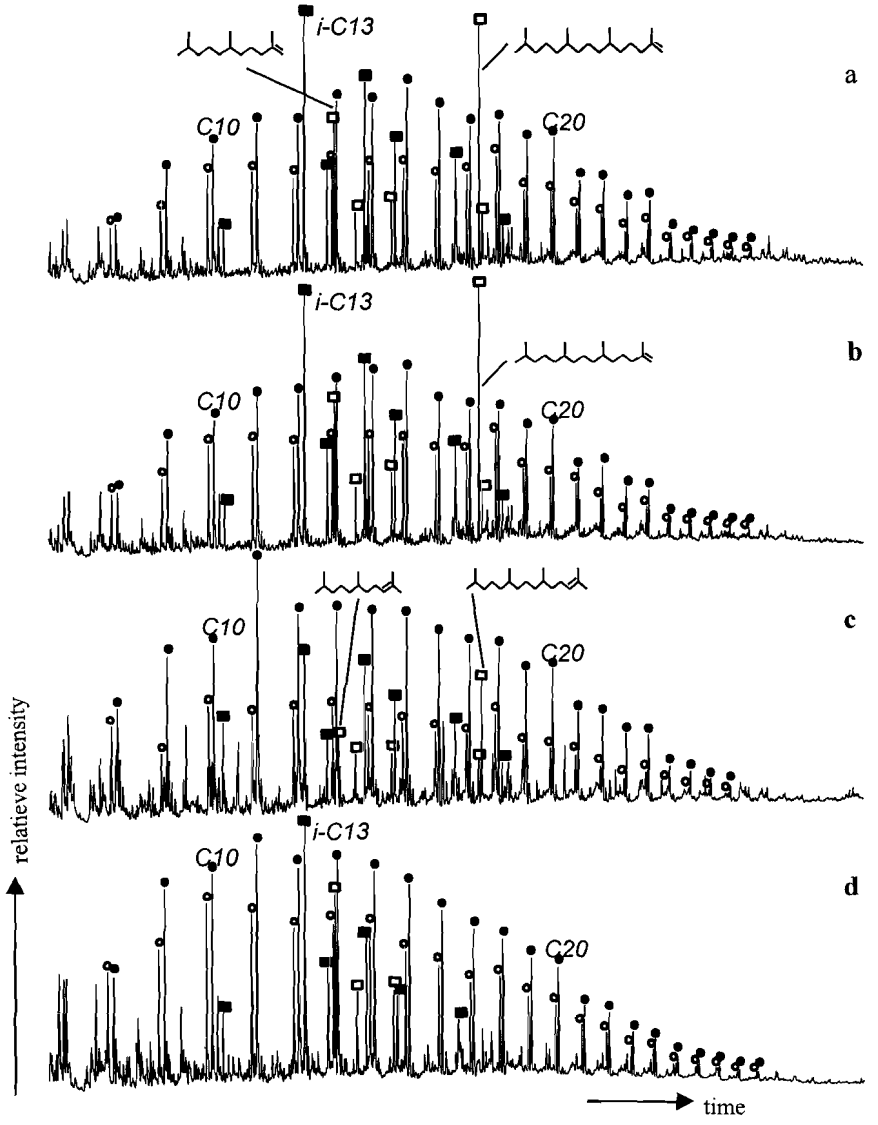

Figure 2.3 Mass chromatogram of the alkenes and alkanes (*m/z 55+57)* of (**a**) the isolated kerogen, (**b**) the residue R_1 after base hydrolysis, (**c**) the residue R_2 after ether-bond cleavage, (**d**) the residue R_3 after desulfurization. Filled and open circles indicate the homologous series of *n*-alkanes and *n*-alk-1-enes, respectively. Their number of carbon atoms is indicated with italic numbers. Filled and open squares indicate homologous series of isoprenoid alkanes and alk-1-enes, respectively.

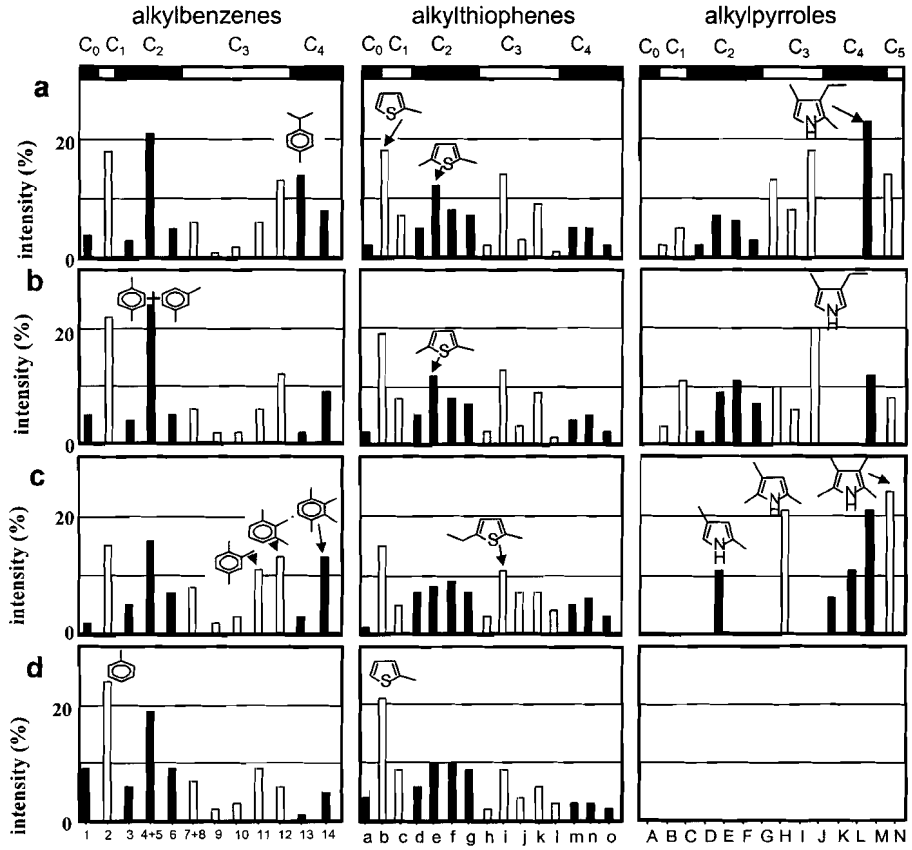

Figure 2.4 Bar diagram of the relative abundances of alkylbenzenes, alkylthiophenes and alkylpyrroles in (**a**) the isolated kerogen, (**b**) the residue after hydrolysis, (**c**) the residue after ether-bond cleavage, (**d**) the residue after desulfurization. Relative abundances were determined by integration of summed mass chromatograms of *m/z 78+91 +92+105+106+119+120+133+134+147+148+161+162* for alkylbenzenes, *m/z 84+97+98+111+112+125+126+139+140+153+154* for alkylthiophenes and *m/z 67+80+81+94+95+108+109+122+123+136+137* for alkylpyrroles, respectively. The relative abundances are expressed as their percentage of the sum of the quantified members of a compound class.
Key alkylbenzenes: 1 = benzene; 2 = toluene; 3 = ethylbenzene; 4 = 1,3-dimethylbenzene; 5 = 1,4-dimethylbenzene; 6 = 1,2-dimethylbenzene; 7 = 1-ethyl-3-methylbenzene; 8 = 1-ethyl-4-methylbenzene; 9 = 1,3,5-trimethylbenzene; 10 = 1-ethyl-2-methylbenzene; 11 = 1,2,4-trimethylbenzene; 12 = 1,2,3-trimethylbenzene; 13 = 1-methyl-4-isopropylbenzene; 14 = 1,2,3,4- tetramethylbenzene.
Key alkylthiophenes: a = thiophene; b = 2-methylthiophene; c = 3-methylthiophene; d = 2-ethylthiophene; e = 2,5-dimethylthiophene; f = 2,4-dimethylthiophene; g = 2,3-dimethylthiophene; h = 2-propylthiophene; i = 2-ethyl-5-methylthiophene; j = 2-ethyl-4-methylthiophene; k = 2,3,5-trimethylthiophene; l = 2,3,4-trimethylthiophene; m = isopropylmethylthiophene; n = 2-methyl-5-propylthiophene; o = 5-ethyl-2,3-dimethylthiophene.
Key alkylpyrroles: A = pyrrole; B = 2-methylpyrrole; C = 3-methylpyrrole; D = 2,5-dimethylpyrrole; E = 2,4-dimethylpyrrole; F = 2,3-dimethylpyrrole; G = 3,4-dimethylpyrrole; H = 2,3,5-trimethylpyrrole; I = 2,3,4-trimethylpyrrole; J = 3-ethyl-4-methylpyrrole; K = dimethylethylpyrrole; L = 2,3-dimethyl-4-ethylpyrrole; M = 2,4-dimethyl-3-ethylpyrrole; N = 3-ethyl-2,4,5-trimethylpyrrole.

Furthermore, small amounts of monoterpenes like limonene, terpinolene and cyclofenchene could also be identified in the kerogen pyrolysate (Höld *et al.*, unpublished results) as well as a small amounts of 6,10,14-trimethyl-2-pentadecanone and small amounts of a series of C_7-C_{25}-alkan-2-ones maximizing at C_9 and C_{17}. The thiophene ratio (=[2,5-dimethylthiophene]/([1,2-dimethylbenzene]+[*n*-non-1-ene]); Eglinton *et al.*, (1990)) of the kerogen, known to provide a rapid estimation of the organic sulfur content of kerogens, is 1.2 indicating a high S_{org}/C ratio in the kerogen.

Alkaline hydrolysis - Released compounds E_1

Compounds released from the kerogen by alkaline hydrolysis (Table 2.1; Fig. 2.5a) are predominantly monocarboxylic acids (C_9-C_{34}) with a strong even-over-odd carbon number predominance and a maximum around C_{16} and C_{18}. Furthermore, relatively small amounts of dicarboxylic acids (C_9-C_{28}), isoprenoid monoacids (C_{14}-C_{20}), 17β,21β(H)-bishomohopanoic acid, 17β,21β(H)-homohopanoic acid and 17β,21β(H)-trishomohopanoic acid were detected as well as acyclic and cyclic biphytanyl dicarboxylic and monocarboxylic acids (C_{40}) previously identified by Meunier-Christman (1988) and reported by Ahmed *et al.* (1998) and Schouten *et al.* (1998). Small amounts of cholest-5-en-3β-ol and 24-ethylcholest-5-en-3β-ol were present in the extract as well as 6,10-dimethylundecan-2-one and 6,10,14-trimethylpentadecan-2-one.

Alkaline hydrolysis - Residue R_1

Alkaline hydrolysis of the kerogen resulted in a 85% yield of residue R_1. GC/MS analysis of the flash pyrolysate of the residue R_1 revealed a similar pattern of components as in the pyrolysate of the initial kerogen except for the hopanoids which are almost absent in the pyrolysate of residue R_1 (Fig. 2.2b). Hardly any changes in relative abundance between the different compound classes could be observed (Fig. 2.6).
1-Methyl-4-isopropylbenzene has almost disappeared from the residue pyrolysate (*cf.* Figs. 2.4a-b) as well as the monoterpenes (limonene, terpinolene and cyclofenchene; Höld *et al.*, unpublished results). Other alkylbenzenes (Figs. 2.4a-b), as well as *n*-alkanes and *n*-alk-1-enes (Figs. 2.3a-b), alkylthiophenes (Figs. 2.4a-b), alkylnaphthalenes and alkylbenzothiophenes showed no changes in distribution pattern, nor did changes occur in the relative amounts of tocopherols, alkan-2-ones and steranes/sterenes. However, a small change in the distribution of the alkylpyrroles did occur. 3-Methyl-4-ethyl-pyrrole increased in abundance relative to the other pyrroles (*cf.* Figs. 2.4a-b). The thiophene ratio remained almost constant at 1.3.

Table 2.1: Yields of selected released compounds.

Fraction	Compound	µg/g yield residue
E_1	C_{16} monocarboxylic acid	66
	6,10,14-trimethylpentadecanone	25
	C_{16} dicarboxylic acid	<10
	4,8,12-trimethyltridecanoic acid	16
	17β,21β(H)-bishomohopanoic acid	23
	monoterpenoid	110
	acyclic biphytanyl dicarboxylic acid	<10
	cholest-5-en-3β-ol	<10
E_2	C_{16} monocarboxylic acid	35
	C_{16} alkyl ester acetic ester	140
	phytane	26
	acyclic biphytanes	19
	5α-cholestane	<10
	cholestadiene	<10
	C_{24}-*n*-alkane	27
E_3	C_{16} monocarboxylic acid	22
	phytane	30
	acyclic biphytanes	85
	5α-cholestane	17
	C_{24}-*n*-alkane	77
	C_{16}-alkan-2-ol	22
	C_{16}-alkan-3-ol	<10
	C_{16}-alkan-4-ol	<10

Cleavage of ether-bonds - Released compounds E_2

Compounds released from the kerogen by ether-bond cleavage (Table 2.1; Fig. 2.5b) are predominantly monocarboxylic acids (C_9-C_{34}) with a strong even-over-odd carbon number predominance, maximizing at C_{16} and C_{18}. However, it is surprising to detect acids in this extract since acids are converted to alcohols upon treatment with $LiAlH_4$ (Wade, 1987). Furthermore, a series of alkyl ester acetic acids (C_{14}-C_{20}) with a very strong even-over-odd predominance was identified (Fig. 2.5b). Possibly, the ethyl acetate used contained traces of acetic acid. This acetic acid may have reacted with the alcohols originating from monocarboxylic acids (as mentioned previously, acids are converted to alcohols upon treatment with $LiAlH_4$). The same hypothesis may explain the presence of 2-methyl-benzylacetic acid in the extract reflecting the presence of 2-methylbenzylalcohol. Phytane, acyclic and cyclic biphytanes (Hoefs *et al.*, 1997) and small amounts of 5α and 5β steranes (C_{27}-C_{29}), with a higher abundance of the 5α isomers, as well as small amounts of cholestadiene were present in the extract. Predominantly even carbon numbered *n*-alkanes (C_9-C_{34}; mainly C_{24} and C_{30}) were also released.

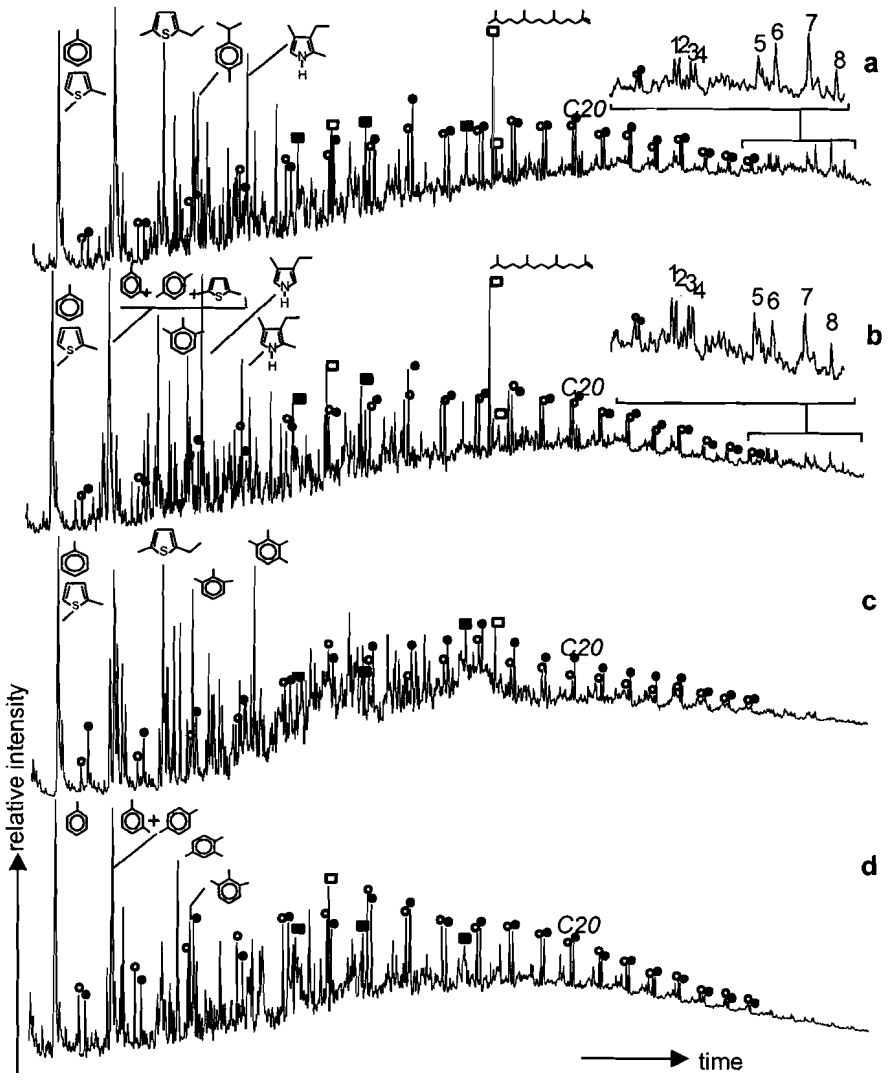

Figure 2.5 Total Ion Current (TIC) traces of (**a**) the extract after ester-bound cleavage, (**b**) the extract after ether-bond cleavage, (**c**) the extract after sulfur-bond cleavage. Filled circles indicate the homologous series of *n*-alkanes. Their number of carbon atoms is indicated with numbers. Crossed squares indicate isoprenoid acids. Stars indicate linear monocarboxylic acids Open circles indicate contamination. Open triangles indicate alkan-2-ols. Filled triangles indicate alkan-1-ols.

Cleavage of ether-bonds - Residue R_2

Ether-bond cleavage of R_1 resulted in a 95% yield of residue R_2. GC/MS analysis of the flash pyrolysate of the residue R_2 revealed similar components as present in the pyrolysate of the initial kerogen and residue R_1 (Fig. 2.2c), except for α– and γ–tocopherol and C_{27}-C_{29} steranes and sterenes, which have disappeared almost completely. Large changes in relative abundance of the different compound classes could also be observed (Fig. 2.6). In the pyrolysate of the residue R_2 *n*-alkanes, *n*-alk-1-enes, isoprenoid alkanes and alkenes as well as the alkan-2-ones have decreased significantly in abundance relative to the other compounds. However, the isoprenoid alkanes and alkenes have decreased relatively more in abundance compared to the linear alkanes and alkenes (*cf.* Figs. 2.3b-c). Furthermore, alkylpyrroles decrease slightly in abundance relative to the other compound classes (Fig. 2.6).

Prist-1-ene and 2,6,10-trimethylundec-1-ene as well as α– and γ– tocopherol have almost disappeared from the residue pyrolysate in contrast to prist-2-ene and 2,6,10-trimethylundec-2-ene which have significantly increased in their relative abundance (*cf.* Figs. 2.2b-c, 2.3b-c). Furthermore, the distribution of the *n*-alkan-2-ones has changed from maximizing at C_9 as well C_{17} to maximizing at C_9 only. The C_3-C_4 alkylated benzenes have increased in relative abundance compared to the C_0-C_2 alkylbenzenes (Figs. 2.4b-c). A significant fraction of the alkylpyrrole isomers (2-methylpyrrole, 3-methylpyrrole, 2,5-dimethylpyrrole, 2,3-dimethylpyrrole, 3,4-dimethylpyrrole, 2,3,4-trimethylpyrrole and 3-ethyl-4-methylpyrrole) disappeared from the residue pyrolysate (Figs. 2.4b-c). However, 2,4-dimethylpyrrole, an ethylmethylpyrrole, 2,3,5-trimethylpyrrole, a dimethylethylpyrrole, 2,3-dimethyl-4-ethylpyrrole and 3-ethyl-2,4,5-trimethylpyrrole were still present in the residue pyrolysate. Alkylnaphthalenes and alkylbenzothiophenes showed no changes in their distribution pattern. The thiophene ratio remained relatively constant at 1.1.

Desulfurization - Released compounds E_3

Compounds released upon desulfurization (Table 2.1; Fig. 2.5c) are similar to those released upon ether-bond cleavage, i.e. predominantly fatty acids (C_9-C_{34}), phytane, acyclic and cyclic biphytanes, 5α and 5β steranes (C_{27}-C_{29}) as well as predominantly even carbon numbered (mainly C_{24} and C_{30}) *n*-alkanes. Furthermore, C_{10}-C_{28} alkan-2-ols, alkan-3-ols and mid-chain alkanols with an even carbon number predominance and a maximum around C_{14} could be identified in the extract after desulfurization. Compounds released after HNO_3 treatment of the residue are predominantly linear fatty acids (C_{10}-C_{30}) and isoprenoid fatty acids (C_{14}-C_{18}).

Desulfurization - Residue R_3

Desulfurization of the residue R_2 resulted in only a 50 % yield of residue R_3. GC/MS analysis of the flash pyrolysate of the residue R_3 indicated major changes in relative abundance between the different compound classes (Fig. 2.6). In the pyrolysate of the residue after desulfurization, alkylthiophenes (Fig. 2.6) and alkylbenzothiophenes have decreased significantly in abundance relative to the other compound classes. This is consistent with the drop of the thiophene ratio from 1.1 to 0.3. Furthermore, alkylpyrroles have almost completely disappeared from the residue pyrolysate (Fig. 2.6). The linear and isoprenoid alkanes and alkenes as well as the alkylbenzenes and alkylnaphthalenes are now dominating the residue pyrolysate after desulfurization (Figs. 2.2 and 2.6).

Both prist-1-ene and prist-2-ene have disappeared from the residue pyrolysate (Fig. 3c-d). Furthermore, the relative intensity of the C_3-C_4 alkylated benzenes compared to the other alkylbenzenes has decreased (Figs. 2.4c-d).

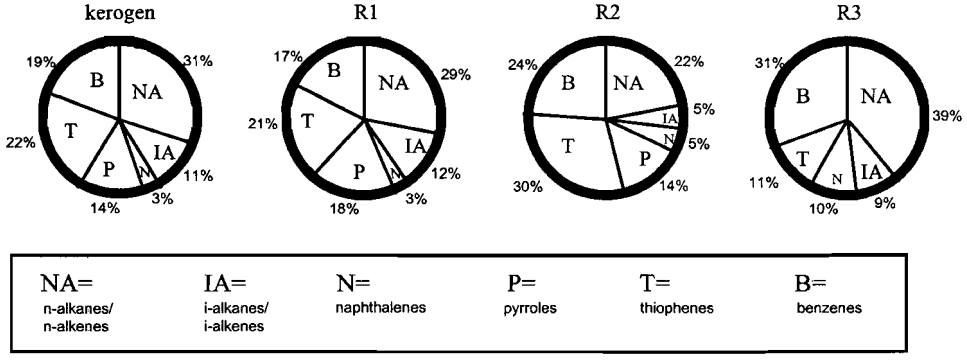

Figure 2.6 Relative abundances of the different component classes in the pyrolysate of the initial kerogen and residues after sequential chemical degradation.

2.5 Discussion

n-Alkenes and n-alkanes

The pyrolysate of the residue R_2 (after ether bond cleavage), revealed a lower relative abundance of *n*-alk-1-enes/*n*-alkanes (Fig. 2.6), indicating that part of the *n*-alkyl skeletons in the kerogen are ether-bound. This is consistent with the fact that predominantly even carbon numbered (mainly C_{24} and C_{30}) *n*-alkanes were released upon treatment with HI. These *n*-alkanes and *n*-alk-1-enes are probably derived from non-hydrolyzable aliphatic macromolecules with linear carbon skeletons (most likely linear algaenans biosynthesized by marine algae) forming an ether-linked macromolecule (*e.g.*

Derenne *et al.*, 1992a,b,c; Gelin *et al.*, 1996a, 1997). Thermal rearrangement reactions of the ether bridges during pyrolysis account for the formation of the *n*-alkan-2-ones (Gelin *et al.*, 1993). It was recently demonstrated that the marine eustigmatophyte *Nanochloropsis salina* biosynthesizes highly aliphatic algaenans composed of ether-linked C_{30}-C_{32} units (Gelin *et al.*, 1996a). A similar type of algaenan may be the precursor of the C_{30} *n*-alkane released upon ether bond cleavage.

The strong relative enrichment of the *n*-alkanes and *n*-alkenes in the pyrolysate of the residue R_3 (after desulfurization) is probably due to the strong decrease of alkylthiophenes and alkylpyrroles (Fig. 2.5). The abundance of the *n*-alkanes and *n*-alkenes relative to the alkylnaphthalenes (Table 2.2) is indeed decreasing slightly upon desulfurization which is consistent with the release of *n*-alkyl skeletons. Kerogen-bound alkylnaphthalene precursors are assumed to remain constant during the degradation steps and are therefore used as an 'internal' standard. If, however, the alkylnaphthalenes would have decreased upon desulfurization than the *n*-alkanes and *n*-alkenes would have decreased even more. The presence of *n*-alkanes and *n*-alkenes in the residue pyrolysates after alkaline hydrolysis, ether-bond cleavage and desulfurization is consistent with the observation that fresh, diagenetically unaltered algaenans consisting of ether-linked macromolecules of linear carbon skeletons release only < 20% of their monomeric units upon hydrolysis and ether-bond cleavage (Blokker *et al.*, 1998).

Table 2.2: The abundance normalized to naphthalenes of different compound classes in the kerogen and residue pyrolysates.

	Kerogen	R_1	R_2	R_3
n-alkanes and *n*-alkenes	10	9	5	4
i-alkanes and *i*-alkenes	4	4	1	1
naphthalenes	1	1	1	1
pyrroles	5	6	3	0
thiophenes	7	7	6	1
benzenes	6	6	5	3

The even carbon numbered (mainly C_{24} and C_{30}) *n*-alkanes released upon desulfurization are probably derived from non-hydrolyzable aliphatic macromolecules with *n*-alkyl carbon skeletons (most likely linear algaenans biosynthesized by marine algae) forming an ether- and sulfur- linked network (*e.g.* Derenne *et al.*, 1992a,b,c; Gelin *et al.*, 1996a). A relatively high amount of sulfur-bound C_{24} *n*-alkane was also identified in a Monterey oil resin but its origin is unknown (Hefter *et al.*, 1995). The precursors of the C_{30} *n*-alkane released upon desulfurization are probably sulfur-bound 1,15-C_{30}-diols or keto-1-ols (*e.g.* de Leeuw *et al.*, 1981; ten Haven *et al.*, 1992; Koopmans *et al.*, 1996), biosynthesized by eustigmatophyte algae (Volkman *et al.*, 1992; Gelin *et al.*, 1996a). Furthermore, alkan-2-ols, alkan-3-ols and mid-chain alcohols were released upon

desulfurization. These alcohols may have been simultaneously ester- or ether- and sulfur-bound to the kerogen (Hefter *et al.*, 1995).

The predominantly even carbon numbered linear fatty acids with a distribution maximizing at C_{16} that occur in all released fractions (E_1, E_2, E_3) are probably contaminants because they occur in every extract with the same distribution, and they do not occur in the kerogen pyrolysate, although it cannot totally be excluded that part of these fatty acids occur ester-bound in the kerogen.

Acyclic isoprenoids

Flash pyrolysis of the residue R_2 after ether-bond cleavage indicates a decrease of C_{11}-C_{18} acyclic isoprenoids relative to other pyrolysis products (Fig. 2.5). These isoprenoid alkanes and alkenes are probably derived from non-hydrolyzable aliphatic macromolecules with isoprenoid carbon skeletons (isoprenoid algaenans) that form an ether-linked macromolecule (*e.g.* Derenne *et al.*, 1989, 1990; Höld *et al.*, 1998). One explanation for the relatively larger decrease in abundance of C_{11}-C_{18} isoprenoids relative to the linear alkanes might be that the isoprenoid algaenans are less densely cross-linked than the *n*-alkyl algaenans.

Flash pyrolysis of the residue after hydrolysis and ether-bond cleavage indicates that, together with a large fraction of prist-1-ene, both α– and γ–tocopherol disappeared from the residue pyrolysate, indicating that their precursors occur ether- and not ester-bound to the kerogen. Since bound tocopherols can thermally generate prist-1-ene *via* a Retro-Diels Alder reaction (Goossens *et al.*, 1984), this suggest that ether-bound tocopherols are a major source of prist-1-ene in kerogen pyrolysates. Surprisingly, however, no tocopherols could be identified among the products released by ether-bond cleavage. Desulfurization released the precursor of prist-2-ene and the residual fraction of the prist-1-ene, indicating that their precursors are sulfur-bound. We propose two different precursors for pristenes: an ether-bound (probably tocopherol) as the precursor for the major fraction of prist-1-ene and a sulfur-bound precursor for prist-2-ene. This is in contrast with Regtop *et al.* (1986) who proposed the same precursor for prist-1-ene and prist-2-ene, with prist-2-ene being formed from prist-1-ene in the presence of clay. Phytane was also released in the extract upon desulfurization, whilst phytenes disappeared from the residue pyrolysate, indicating that its precursors are sulfur-bound phytane skeletons. This is in agreement with a previous study of Type II-S kerogens of the Gessoso solfifera Formation (Gelin *et al.*, 1995).

6,10-Dimethylundecan-2-one and 6,10,14-trimethylpentadecan-2-one were identified in the extract after alkaline hydrolysis. Ten Haven *et al.* (1987) and Rontani *et al.* (1992) reported also the release of 6,10,14-trimethylpentadecan-2-one after alkaline treatment of recent sediments. Rontani *et al.* (1992) explained its formation as a byproduct from alkaline hydrolysis of the phytyl side-chain of photooxidized chlorophyll-

a. It is assumed thus that phytol or derivatives are the precursors of this ketone. However, the release of these isoprenoid ketones is not accompanied by the disappearance of certain compounds in the pyrolysate of the residue and therefore the precursors of these isoprenoid ketones contribute for only a small part to the kerogen.

Alkylthiophenes

A large part of the alkylthiophenes present in the pyrolysate of the kerogen has disappeared after desulfurization (Fig. 2.5) and the thiophene ratio decreased from 1.1 to 0.3 upon desulfurization. This is in agreement with previous desulfurization studies on Type II-S kerogens (Gelin *et al.*, 1996b) and consistent with the idea that ascribes C_1-C_4 alkylated thiophenes in kerogen pyrolysates, at least partly, to small (i.e. C_5-C_7), predominantly linear carbon skeletons (probably derived from monosacharides) linked to the kerogen by sulfide linkages (van Kaam-Peters *et al.*, 1997; Kok *et al.*, 1997). Small amounts of thiophenes are left in the flash pyrolysate of the kerogen after the treatment with Ni_2B, probably because the reagent cannot completely access the solid substrate. In the extract the C_5-C_7 *n*-alkyl carbon skeletons could not be identified probably due to evaporation. From this study it can not be definitely concluded that the precursors of the alkylthiophenes are solely sulfur-bound since the precursors could be both sulfur- and ether- and/or ester-bound to the kerogen. However, in another study by Gelin *et al.* (1996b), the precursor moieties of the thiophenes were released from the kerogen upon desulfurization without preceding alkaline hydrolysis and ether-bond cleavage and it is thus likely that their precursors (probably carbohydrates), occur predominantly solely sulfur-bound.

Alkylpyrroles

Alkylpyrroles in kerogen flash pyrolysates have been reported before, *i.e.* in kerogen pyrolysates of sediments from the Miocene Monterey Formation (Sinninghe Damsté *et al.*, 1992) and in a kerogen pyrolysate of a recent diatomaceous ooze from the Namibian Shelf (Klok *et al.*, 1984). The distribution pattern of the alkylpyrroles, with the very abundant 3-ethyl-2,4,5-trimethylpyrrole, found in the kerogen pyrolysate indicates that these products originate from tetrapyrrole pigments derived from chlorophylls (Sinninghe Damsté *et al.*, 1992). The abundance of these pyrroles relatively to the naphthalenes decreased upon ether-bond cleavage (Table 2.2) suggesting that their precursors were (partly) ether-bound to the kerogen. After ether-bond cleavage the distribution pattern of the residual alkylpyrroles is different from the distribution pattern after alkaline hydrolysis. However, the pyrrole distribution and especially the abundance of 3-ethyl-2,4,5-trimethylpyrrole indicates that their precursors are in both cases related to tetrapyrrole pigments. Perhapse, the HI treatment is also influencing the conjugated double bond system of the tetrapyrrole pigments in such a way, that different pyrolysis

products are obtained. A similar phenomenon has been reported in the desulfurization of a kerogen with $Li/EtNH_2$ (Gelin *et al.*, 1996b), where alkylpyrroles appeared in the pyrolysate of the residue, probably due to hydrogenation of double bonds in the tetrapyrrole pigment.

Upon desulfurization, the precursors of the alkylpyrroles are completely released from the residual kerogen. This suggests that these precursors, probably tetrapyrrole pigments, were preserved in the sediments by incorporation into macromolecules *via* sulfur-bonds or sulfur- and ether-bonds. Indeed, the presence of sulfur-bound porphyrins in other sulfur-rich sediments supports this hypothesis (Schaeffer *et al.*, 1993). No tetrapyrrole pigments were found in the extract after desulfurization probably due to the fact that they are not GC-amenable under the analytical conditions used for this study.

Alkylbenzenes

The relative abundance of the alkylbenzenes increases during the different chemical degradation steps (Fig. 2.5). This indicates that most of their precursors are not ester-, ether- or sulfur- bond to the kerogen but more likely secondary pyrolysis products originate from the cyclisation and aromatisation of the macromolecule. Due to the disappearance of other compound classes, alkylbenzenes and alkylnaphthalenes become more enriched in the residual kerogen. Only upon desulfurization the relative abundance of alkylbenzenes compared to alkylnaphthalenes decreases (Table 2.2, Fig. 2.5), mainly due to the loss of C_3-C_4 alkylbenzenes (Figs. 2.4c-4d). It is known that sulfur-bound carbohydrates can generate, apart from alkylthiophenes, also alkylbenzenes upon pyrolysis (Kok *et al.*, 1997). Upon desulfurization these sulfur-bound carbohydrate skeletons may be released in the extract and thus do not generate any alkylbenzenes anymore upon pyrolysis. C_0-C_2 alkylated benzenes are somewhat less abundant after ether-bond cleavage, indicating that some of their unknown precursors are ether bound (Figs. 2.4b-c). This is consistent with the fact that the relative abundance of the alkylbenzenes compared to the alkylnaphthalenes decreases slightly upon ether-bond cleavage (Table 2.2). It is well known that in pyrolysates of algaenans and type I kerogens the alkylated benzene distribution is dominated by C_0-C_2 alkylated benzenes (Hartgers *et al.*, 1994a). Upon ether-bond cleavage the algaenans are partially broken down and consequently the predominance of the C_0-C_2 alkylated benzenes decreases. After desulfurization the remaining algaenan fraction may become more enriched again due to removal of other compound classes and therefore the C_0-C_2 alkylated benzenes may become more predominant. Furthermore, 1-methyl-4-isopropylbenzene almost completely disappears after hydrolysis indicating that its precursor(s) must occur ester linked to the kerogen. This disappearance co-occurs with the release of monoterpenoids, indicating that this alkylbenzene is formed upon pyrolysis from ester-bound monoterpenoids (Höld *et al.*, unpublished results).

Steroids and hopanoids

Cholest-5-en-3β-ol (Table 2.1) and small amounts of 24-methylcholest-5-en-3β-ol and predominantly 24-ethylcholest-5-en-3β-ol were released from the kerogen by hydrolysis. However, the amounts released are low (<1 μg/mg kerogen) and, therefore, these sterols contribute for only a small part to the kerogen. After ether-bond cleavage almost all the 5α and 5β C_{27}-C_{29} steranes and all C_{27}-C_{29} sterenes and C_{27}-C_{29} cholesten-3-ones were removed from the residue whilst in the extract 5α and 5β steranes were released. Flash pyrolysis with standard ether compounds have revealed that ketones result from pyrolytic cleavage of secondary ether bonds (Gelin *et al.*, 1993; Gelin *et al.*, 1994). This suggests that 5α and 5β C_{27}-C_{29} steranes are ether-bound to the kerogen. After desulfurization, 5α and 5β C_{27}-C_{29} steranes were no longer present in the residue pyrolysate, as reported previously for other type II-S kerogens (Gelin *et al.*, 1996b). This is consistent with the fact that these steranes were identified in the desulfurized products, indicating that they have been sulfur-bound to the kerogen. Therefore, steroids occur predominantly ether- and/or sulfur-bound but also, in smaller amounts, ester-bound to the kerogen.

In the residue pyrolysate after hydrolysis, C_{31}-C_{33} 17β,21β(H) hopanoids have decreased in relative abundance. This is consistent with the fact that C_{31}-C_{33} hopanoid acids were present in the products of the alkaline hydrolysis. These acids are probably diagenetic products of bacteriohopanepolyols found in bacteria such as bacteriohopanetetrol. (Ourisson *et al.*, 1979, 1982; Rohmer *et al.*, 1992).

Cyclic and acyclic biphytanes

Relatively small amounts of diacids with biphytanyl skeletons, containing 0-3 cyclopentane rings were released from the kerogen by alkaline hydrolysis. Therefore, these diacids occur ester-bound in the kerogen. In archaea, lipids with these carbon skeleton have only been found ether-bound to polyols (DeRosa and Gambacorta, 1988; Koga *et al.*, 1993). Either these ether lipids have been oxidized to form compounds with carboxylic acid groups or the fatty acids are biosynthesized in archae or other microorganisms, although they have not yet been identified (Meunier-Christman, 1988; Schouten *et al.*, 1998). After ether bond cleavage relatively small amounts of these biphytane skeletons could be identified. Sulfur bond cleavage released relatively large amounts of the same biphytanyl skeletons previously identified in desulfurization products (Richnow *et al.*, 1992). It can thus be concluded that ester-, ether- and sulfur-bound C_{40} biphytanes are present in the kerogen, most likely indicating a contribution of planktonic archaea (Hoefs *et al.*, 1997; Schouten *et al.*, 1998).

2.6 Conclusions

n-Alkyl moieties in the kerogen are partly released upon cleavage of ether-bonds and are probably derived from linear algaenans biosynthesized by marine algae. The abundance of the C_{30} *n*-alkane in the extract after cleavage of ether-bonds might be an indicator for the presence of the algaenan biosynthesized by marine eustigmatophytes. Acyclic isoprenoid moieties are also released upon cleavage of ether-bonds and are probably derived from isoprenoid algaenans biosynthesized by marine algae. However, the isoprenoid algaenan is probably less densely cross-linked compared to the linear algaenan because the isoprenoid algaenan is less persistent towards chemical degradation than the linear algaenan.

Ether-bound tocopherols occur in the kerogen and these are probably a major source of prist-1-ene in kerogen pyrolysate. However, for prist-2-ene a sulfur-bound precursor is proposed. Thiophenes are predominantly released upon desulfurization and their precusors are probably sulfur-bound carbohydrate skeletons. The release of the sulfur-bound carbohydrates also accounts for the decrease in C_3-C_4 alkylated benzenes upon desulfurization. Precursors of alkylated pyrroles are ether and sulfur-bound to the kerogen and are likely derived from tetrapyrrole pigments.

The immature Miocene Type-II kerogen from the Monterey Formation used in this study consists predominantly of linear and isoprenoid algaenans and probably of sulfur-bound carbohydrates and sulfur- and ether-bound porphyrins. Most of the products released from the kerogen upon chemical degradation are to volatile or non-GC amenable and therefore could not be identified in the extract, emphasizing the usefulness of our approach. Furthermore, the degradation sequence resulted in the recognition of specific ester-, ether- and sulfur-bound low-molecular-weight biomarkers attached to the kerogen. However, the release of these biomarkers has no significant impact on the residue pyrolysate and thus most of the compounds identified in extracts are probably less important constituents of the kerogen.

2.7 Acknowledgements

Dr. S. Derenne and Dr. H. Richnow are thanked for suggestions to improve the manuscript. Dr. C.M. Isaacs is thanked for provision of the Monterey KG-1 sample. Dr. W. Pool is thanked for technical assistance and M. Dekker is acknowledged for performing GC-MS analyses. This study was supported by a PIONIER grant to JSSD from the Netherlands Organization for Scientific Research (NWO). This is a NIOZ Contribution no. 3222.

CHAPTER 3

Recognition of *n*-alkyl and isoprenoid algaenans in marine sediments by stable carbon isotopic analysis of pyrolysis products of kerogens

Ingeborg M. Höld, Stefan Schouten, Heidy M.E. van Kaam-Peters and Jaap S. Sinninghe Damsté

3.1 Abstract

Analysis of the pyrolysis products of several marine kerogens revealed that the stable carbon isotopic composition of the *n*-alkanes (C_{10}-C_{25}) are quite similar to those of the *n*-alkenes. This suggests that they have a common origin such as algal biopolymers. The isoprenoid alkanes (C_{13}-C_{20}) also have similar isotopic compositions but can differ significantly from the values of the *n*-alkanes and *n*-alkenes. These isoprenoids could be derived from an isoprenoid algaenan similar to that biosynthesized by the freshwater algae *Botryococcus braunii* race *L*.

3.2 Introduction

Kerogen is the organic matter in sediments which is insoluble in common organic solvents (Durand, 1980; Durand and Nicaise, 1980) and is thought to be derived from the remains of a wide variety of organisms (e.g. algae, bacteria, higher plants). In immature sediments it usually comprises ca. 95% by weight of the sedimentary organic matter (Durand, 1980). However, the exact origin of especially marine kerogens is still not clear. According to the classical theory (Tissot and Welte, 1984), it is thought that during early diagenesis the organic material from primary production is broken down into smaller constituents by microbial action, which are then incorporated into new polymeric structures. With increasing time and burial depth most of this material becomes progressively insoluble due to increasing polycondensation and defunctionalisation, resulting in the formation of kerogen.

The classical model for the formation of kerogen has undergone reappraisal in the light of other recent evidence. It appears that a significant fraction of kerogen may be derived from mixtures of selectively preserved resistant biomacromolecules (*e.g.* Philp and Calvin, 1976; Hatcher *et al.*, 1983; Largeau *et al.*, 1984, 1986; Tegelaar *et al.*, 1989; de Leeuw and Largeau, 1993). During diagenesis the insoluble non-hydrolyzable macromolecular aliphatic organic matter becomes increasingly more prominent (Klok *et*

al., 1984). Several studies have revealed that resistant aliphatic biopolymers are biosynthesized by specific organisms and appear to serve as protective envelopes or cell walls. As such they are highly resistant to (bio)chemical degradation (*e.g.* Largeau *et al.*, 1984, 1986, 1990a, 1990b; Goth *et al.*, 1988; Dubreuil *et al.*, 1989; Tegelaar *et al.*, 1989; de Leeuw *et al.*, 1991; Derenne *et al.*, 1991, 1992a; Gelin *et al.*, 1994, 1996a).

A number of insoluble and resistant aliphatic biomacromolecules have now been isolated from organisms and have, among others, been identified in higher plant leaf cuticles ("cutan", *e.g.* Nip *et al.*, 1986a, 1986b) and in freshwater and marine algae ("algaenan', *e.g.* Berkaloff *et al.*, 1983; Goth *et al.*, 1988; Kadouri *et al.*, 1988; Derenne *et al.*, 1989, 1992b; Gelin *et al.*, 1996a, 1996b). Most of these aliphatic biopolymers are thought to be built from polymethylenic (*n*-alkyl) chains crosslinked *via* ether bridges. However, an aliphatic biopolymer with an isoprenoid carbon skeleton was identified in the *L* race of the freshwater algae *Botryococcus braunii* (Derenne *et al.*, 1990, 1992a, 1994; Gelin *et al.*, 1994).

Rapid thermal dissociation ("flash pyrolysis") is widely used as a method which can provide useful information on the structure and composition of algaenans and kerogens. Several studies have demonstrated that pyrolytic fragments are structurally representative of the kerogen macromolecule as a whole (Horsfield, 1989; Eglinton *et al.*, 1990, 1991; Sinninghe Damsté *et al.*, 1990; Standen *et al.*, 1992; Larter and Horsfield, 1993). Pyrolysis of resistant aliphatic biopolymers predominantly yield homologous series of *n*-alkanes and *n*-alkenes (*e.g.* Largeau *et al.*, 1984; Goth *et al.*, 1988), whereas the aliphatic biopolymer comprised of an isoprenoid carbon skeleton described above yields upon pyrolysis C_{13} to C_{19} regular isoprenoid hydrocarbons and C_{40} isoprenoid hydrocarbons and ketones (Derenne *et al.*, 1990). The relationship between a resistant *n*-alkyl biopolymer from *B. braunii* and a kerogen was shown by Largeau *et al.* (1984, 1986) using pyrolysis. Recently, isoprenoid biopolymers originating from the *L* race of *B. Braunii* were recognized to be a major component in some lacustrine kerogens (Derenne *et al.*, 1994). Observations in other sediments were also consistent with fossilization of resistant biopolymers via selective preservation of algaenan (see for an overview de Leeuw and Largeau, 1993).

Natural variations in stable carbon isotope values may also be used to distinguish between different contributions to kerogen (Fry and Sherr, 1984; Schoell, 1984; Gearing, 1988). The bulk stable carbon isotope value represents a composite carbon isotope value. In order to resolve the separate contributions, the abundance and isotopic compositions of the individual constituents must be determined. Pyrolysis is used as a method to obtain these individual constituents. Flash pyrolysates of biopolymers comprised of polymethylenic chains and of some kerogens yield *n*-alkanes which show a close similarity in carbon isotopic composition of the individual pyrolysis products across the carbon number range measured (Eglinton, 1994). This isotopic uniformity implies a

common origin for *n*-alkanes, supporting the theory that such kerogens are partly derived from aliphatic biopolymers.

In this study, the aliphatic pyrolysis products of a set of thermally immature marine kerogens of various ages and geographical origins are studied in order to obtain information on the origin and extent of the contributions of *n*-alkyl and isoprenoid algaenans to marine kerogens.

3.3 Experimental

Samples

The samples studied are listed in Table 3.1. The Ci/FMM/16.5-21.5 and S//452-457 samples are from marl layers of the Salt IV Formation of the Eocene-Oligocene Mulhouse Potash Basin (Alsace, France; Blanc-Valleron, 1986; Hofmann *et al.*, 1993). The KG-1 sample was taken from a fresh outcrop of the middle Miocene carbonaceous marl member of the Monterey Formation at Naples Beach (USA; Isaacs *et al.*, 1992). The Monterey-TEMO25 sample is from the Upper Miocene Monterey Formation (USA; Sinninghe Damsté *et al.*, 1992). The G6-5-6 sample is from the Lower Toarcian shale, Paris Basin (France; Mackenzie *et al.*, 1980). The sample of the Phosphoria Retort Shale is a phosphatic mudstone of Permian age from the north-western part of Montana (USA; McKelvey, 1959). The KCF-11 is an oil shale from the Jurassic Kimmeridge Clay Formation in Dorset (England; Cox and Gallois, 1981). The NP3726 is a mid Cretaceous, Lower Albian, Niveau Paquier black shale in the Ravel section from the Vocontian Basin (SE France; Bréhéret, 1994).

Extraction, decalcification and kerogen isolation

The powdered sediments were Soxhlet extracted with dichloromethane /methanol (7.5/1, v/v) for 25-40 h. The residues were decalcified by treatment with 4N HCl at room temperature and ultrasonically reextracted with water (3x), methanol (3x) and finally dichloromethane (3x). Kerogen isolation was performed by HCl/HF treatments of the solvent-extracted sediment as described previously by (Eglinton, 1988). The kerogen was ultrasonically extracted with methanol and dichloromethane.

Off-line pyrolysis

The decalcified and extracted sediments or kerogens were placed in a glass boat which was placed in a glass tubereactor. The reactor tube was heated in an oven (Carbolite Tubeoven MTF 12/38A) at 400°C for 1 h under a nitrogen flow. The pyrolysis products were collected in two traps filled with hexane/dichloromethane (7/1, v/v). The second trap was cooled with acetone/CO_2(s). The pyrolysis products of the two traps were

Table 3.1: TOC and bulk stable carbon isotopic compositions of the kerogens/decalcified sediments and pyrolysis residues.

Sample	Location	Type	Age	TOC[a)] (%)	TOC[b)] (%)	$\delta^{13}C$[c)] (‰)	$\delta^{13}C$[d)] (‰)	Py yield (%)	HI mg HC/g Org.-C	i/n ratio
Ci/FMM/16.5-21.5	Mulhouse Basin, France	decalc. sed.	Oligocene	1.2	1.5	-25.0	-25.1	4	288	0.7
S//452-457	Mulhouse Basin, France	decalc. sed.	Oligocene	3.0	6.5	-24.9	-24.6	26	487	0.1
NP3726	Vocontian Basin, France	decalc. sed.	l. Albian	3.0	4.6	-24.0	-24.0	3	*c.* 300	0.6
KG-1	Monterey, USA	decalc. sed.	m. Miocene	9.6	18.1	-22.7	-22.0	10	490	0.4
TEMO25	Monterey, USA	kerogen	m. Miocene	17	56	-22.8	-22.1	n.d.	352	0.3
G6-5-6	Paris Basin, France	decalc. sed.	l. Toarcian	11	16	-27.2	-27.6	12	n.d	0.1
Phosphoria	Phosphoria Retort Shale, USA	decalc. sed.	Permian	16	18.4	-30.5	-29.5	11	n.d	0.2
KCF-11	Kimmeridge Clay, UK	decalc. sed.	Jurassic	24.1	26.8	-22.9	-23.2	40	832	0.9

a) Total Organic Carbon (TOC) of the sediment
b) TOC of the decalcified and extracted sediment or kerogen
c) Isotopic composition of the decalcified and extracted sediment/kerogen before pyrolysis
d) Isotopic composition of the residue

combined to yield the total pyrolysate. The pyrolysis yields were determined from the TOC values, the weight of the initial sediments and the weight of the residues.

Separation of pyrolysis products

Most of the solvent in which the pyrolysates were trapped was distilled off and the pyrolysis products were separated to an apolar and a polar fraction using a column (V_0 = 35ml) packed with Al_2O_3 by elution with 140 ml hexane/dichloromethane (7/1, v/v) and 140 ml methanol/dichloromethane (1/1, v/v), respectively. Throughout the separation procedure special care was taken to allow analysis of the light ends of the pyrolysate by concentrating fractions using distillation. The apolar fraction was further separated into a saturated hydrocarbon and residual fraction using a column (V_0 = 5ml) packed with $AgNO_3$ (10 %) impregnated SiO_2 by elution with 15 ml hexane and 15 ml ethyl acetate, respectively. The residual fraction was separated into an alkene fraction and an aromatic hydrocarbon fraction by column chromatography (Al_2O_3) eluting with hexane and hexane/dichloromethane (7/1,v/v) respectively. The unsaturated hydrocarbon fraction was hydrogenated using PtO_2 as a catalyst and H_2 bubbled through for 1 h. The mixture was then stirred for another 24 h (Sinninghe Damsté *et al.*, 1990). For some fractions the isoprenoid alkanes were isolated from the *n*-alkanes using silicalite adduction (West *et al.*, 1990). The various pyrolysate fractions obtained were analyzed by GC, GC-MS and irm GC-MS.

Gas chromatography (GC)

GC was performed on a Hewlett Packard 6890 or a Hewlett Packard 5890 instrument, both equipped with on-column injectors. A fused silica capillary column (25 m x 0.32 mm) coated with CP Sil-5 (film thickness 0.12 μm) was used with helium as carrier gas. Compounds analyzed on the HP 6890 were detected by a flame ionization detector (FID). Compounds analyzed on the HP 5890 were detected by simultaneously FID and sulfur-selective flame photometric detector (FPD), using a stream-splitter at the end of the column (split ratio FID:FPD=1:2). The fractions (in hexane) were injected at 35°C. After 5 minutes at 35°C, the oven was heated to 310°C at 4°C/min and was held at 310°C for 10 min.

Flash pyrolysis-gas chromatography (Py-GC)

Py-GC was carried out using a FOM-4LX Curie point pyrolysis device using high frequency generator (Fischer 9425). The pyrolysis unit was directly mounted on the injector block of a Hewlett Packard 5890 gas chromatograph. The temperature of the injector block was 250°C. The sediments were applied to ferromagnetic wires by pressing the dry sediment onto the wire (Venema and Veurink, 1985). On-line pyrolysis was performed by inductively heating the wires, within 0.1 s, to their Curie point temperatures

(610°C) and were kept at those temperatures for 10 s. Separation of the pyrolysis products was accomplished on a fused silica capillary column (25 m x 0.32 mm) coated with CP Sil-5 (film-thickness 0.45 μm) using helium as carrier gas. The temperature was programmed from 0°C (5 min), to 300°C (10 min) at a rate of 3°C/min. Compounds were detected by a FID at a temperature of 320°C.

Gas chromatography-mass spectrometry (GC-MS)

GC-MS was carried out as in van Kaam-Peters and Sinninghe Damsté (1997) except that fractions were injected at 35°C. After 5 minutes at 35°C the oven was heated to 310°C at 4°C/min and was held at 310°C for 10 minutes.

Flash pyrolysis-gas chromatography-mass spectrometry (Py-GC-MS)

Py-GC-MS analyses were performed on a Hewlett Packard 5890 gas chromatograph connected to a VG-Autospec Ultima double focusing mass spectrometer. Pyrolysis and chromatographic conditions were identical to those described above for py-GC. Electron impact mass spectra were obtained at 70 eV with a cycle time of 1.8 s and a mass range *m/z* 40-800 at a resolution of 1000.

Bulk stable carbon isotopic analyses

Concentrations of TOC and stable carbon isotopic compositions for the decalcified and extracted sediments and kerogen were determined by automated on-line combustion (Carlo Erba CN analyzer 1502 series) followed by conventional isotope ratio-mass spectrometry (Fisons optima; Fry *et al.*, 1992).

Isotope ratio monitoring-GC-MS (irmGC-MS)

These analyses were carried out as described in van Kaam Peters and Sinninghe Damsté (1997) except that fractions were injected at 35°C. After 5 min at 35°C the oven was programmed to 310 °C at 4°C/min and was held at 310°C for 10 min. The stable carbon isotopic compositions of components were determined from separately integrated ion currents of masses 44, 45 and 46 (Merrit *et al.*, 1994). Values were calibrated against those of deuterated *n*-alkane isotopic standards (co-injection with the sample) as well as an external CO_2 reference gas. The standard error in the mean of the deuterated standards was ≤ 0.12 and the standard error in a single observation of the deuterated standards was ≤ 0.64. Isotopic compositions are reported relative to the Pee Dee Belemnite (PDB) standard and $\delta^{13}C$ values are averaged from duplicate or triplicate measurements.

3.4 Results

Flash pyrolysis

Eight kerogens (Table 3.1) were analyzed by py-GC-MS. The FID and TIC traces of the flash pyrolysates revealed significant differences in their compositions (*e.g.* Fig. 3.1). Homologous series of *n*-alkanes and *n*-alkenes dominate the pyrolysates of most kerogens. These homologous series drop off after C_{20} like pyrolysates of marine kerogens generally do (*e.g.* Behar and Pelet, 1985; Solli and Leplat, 1986; Goth *et al.*, 1988; Horsfield, 1989; Gray *et al.*, 1991). Series of isoprenoid alkanes and alkenes were also detected in all eight flash pyrolysates and consist of regular C_8-C_{20} isoprenoids. They are especially abundant in the flash pyrolysates of the Kimmeridge Clay and the Vocontian Basin (Figs. 3.1c and 3.1d). In the Phosphoria Retort shale also C_{20+} isoprenoid alkanes, and an unusual series of C_9-C_{21} desmethyl (2-nor) isoprenoid alkanes (see below) were found. Only in the flash pyrolysate from the Vocontian Basin kerogen were three irregular isoprenoid alkanes, 2,6,10,15,19-pentamethylicosane, 2,6,15,19-tetramethylicosane and 10-ethyl-2,6,15,19-tetramethylicosane identified (Vink *et al.*, unpublished results). Alkylated benzenes, naphthalenes and indenes are present in all eight flash pyrolysates, but only in the Monterey, the Vocontian Basin and in the Phosphoria Retort Shale pyrolysates do they represent abundant pyrolysis products. Furthermore, the kerogens of the Monterey Formation, the Paris Basin and the Phosphoria Retort Shale are organic sulfur-rich and their flash pyrolysates contain high amounts of alkylated thiophenes, benzo[*b*]thiophenes and thiolanes (Sinninghe Damsté *et al.*, 1989). C_3 - C_5 alkylated pyrroles are only found in high amounts in the flash pyrolysate of the Monterey-TEMO25 kerogen (Sinninghe Damsté *et al.*, 1992).

Off-line pyrolysis

Because the total pyrolysates are far too complex to enable the determination of ^{13}C contents of individual pyrolysis products, separation of the total pyrolysate into different fractions was necessary. To this end, off-line pyrolysis was performed on all kerogens. Depending on the kerogens the off-line pyrolysis yields varied between 3-40% (Table 3.1) which is co-varying with the hydrogen indices (HI, between 288 and 832 mg HC/g organic C). The total off-line pyrolysates were separated into saturated and unsaturated hydrocarbon. fractions. The latter were subsequently hydrogenated. The FID traces of the saturated hydrocarbon fraction of the kerogen pyrolysates reveal, except for the abundance of the isoprenoid alkanes compared to the *n*-alkanes, no significant differences in their general composition (*e.g.* Fig. 3.2). To determine the relative abundance of the isoprenoid hydrocarbons, a so called i/n ratio (isoprenoid over *n*-alkane ratio) was calculated by dividing the summed peak areas of C_{11}-C_{20} isoprenoid alkanes by the summed peak areas of the C_{8+} *n*-alkanes (Table 3.1). The kerogen pyrolysates of the

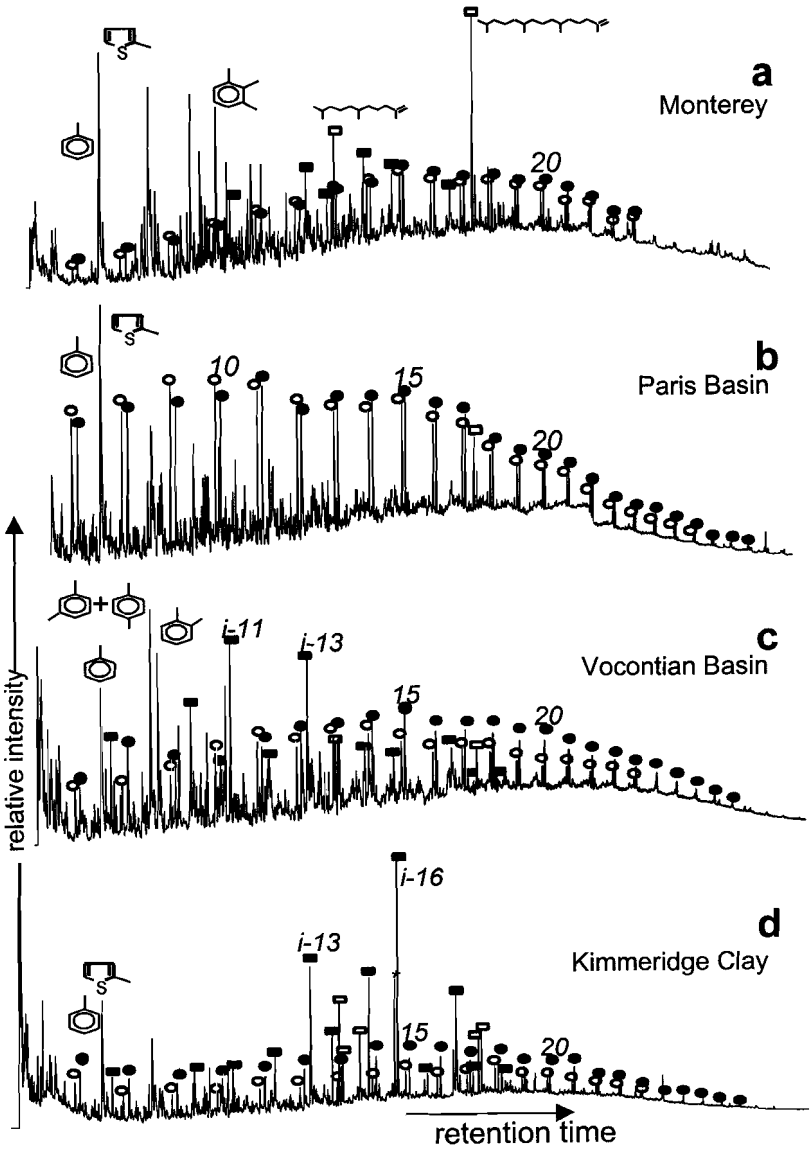

Figure 3.1 Total Ion Current (TIC) traces of the flash pyrolysates (Curie temperature 610 °C) of the kerogen of (**a**) the Monterey Formation (KG-1), (**b**) the Paris Basin, (**c**) the Vocontian Basin and (**d**) the Kimmeridge Clay. Filled and open circles indicate the homologous series of *n*-alkanes and *n*-alk-1-enes, respectively with the number of carbon atoms indicated. Filled and open rectangles indicate pseudo homologous series of isoprenoid *(i-)* alkanes and *i*-alk-1-enes, respectively.

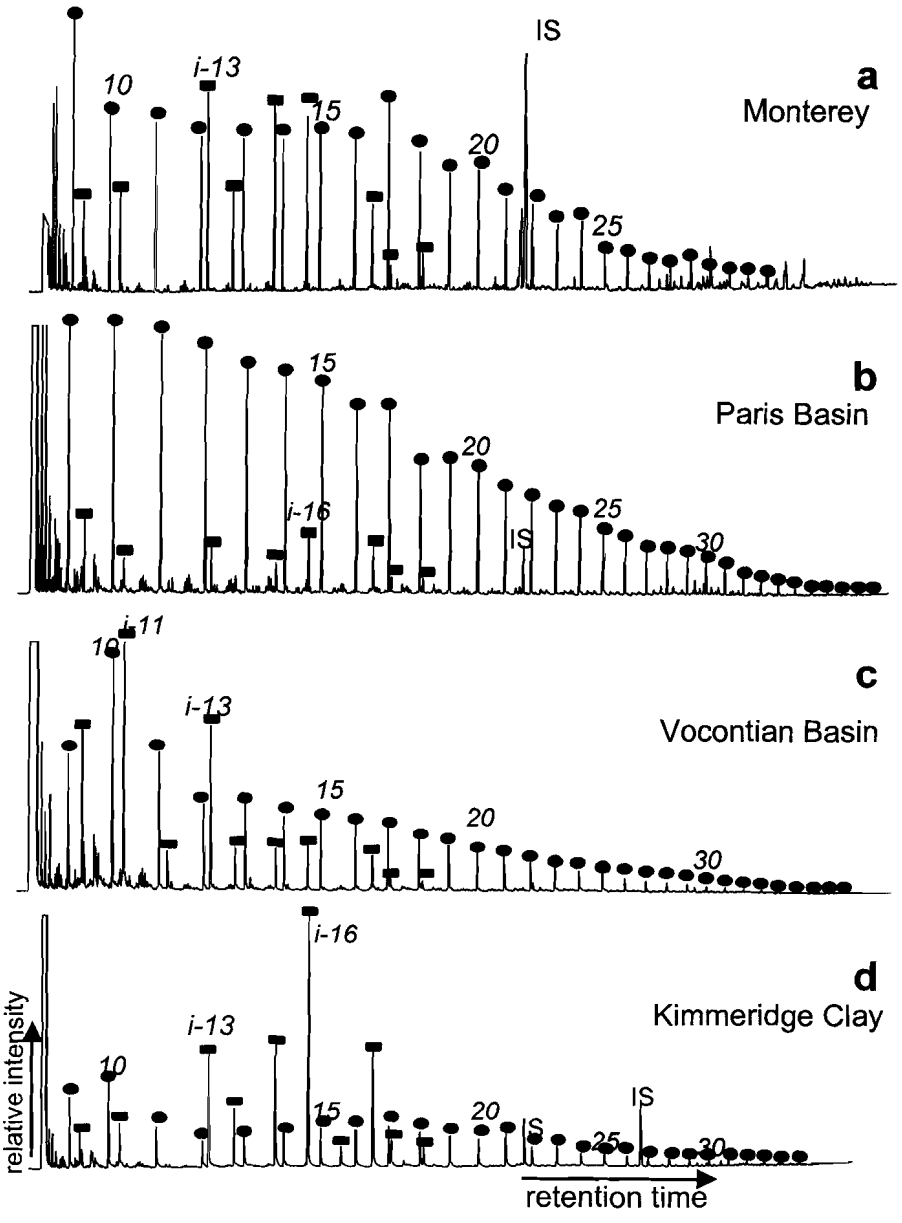

Figure 3.2 FID chromatograms of the saturated hydrocarbon fraction of the off-line pyrolysates of the kerogens of (**a**) the Monterey Formation (KG-1), (**b**) the Paris Basin, (**c**) the Vocontian Basin and (**d**) the Kimmeridge Clay. Filled circles indicate the homologous series of *n*-alkanes with the number of carbon atoms indicated. Filled rectangles indicate pseudo-homologous series of *i*-alkanes. Internal Standards (I.S.): 6,6-d_2-2-methylhenicosane and phenyldodecane (Kimmeridge Clay).

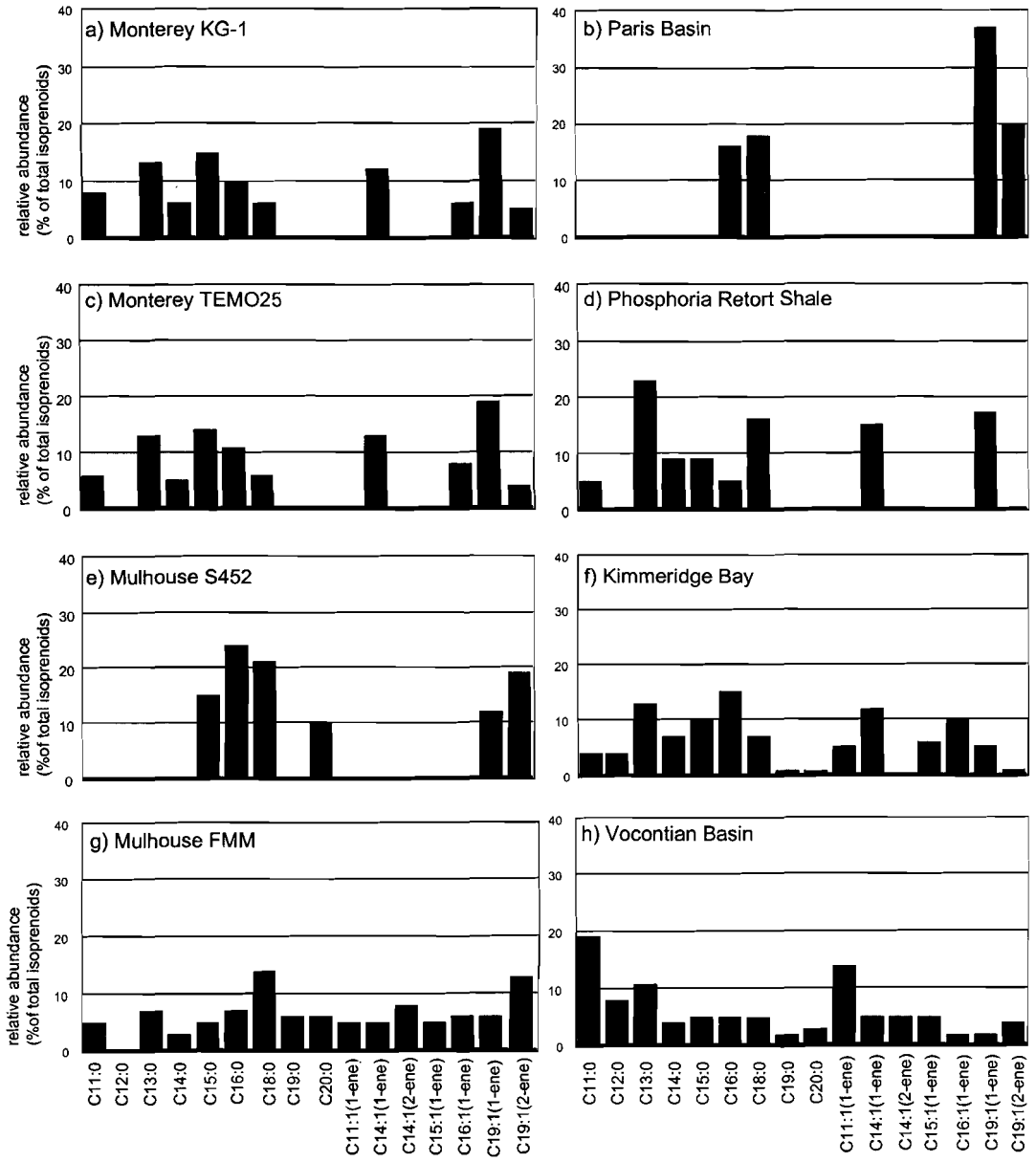

Figure 3.3. Bar plots of the relative abundance of the isoprenoid hydrocarbons in flash pyrolysates of the kerogens of (**a**) the Monterey Formation (KG-1), (**b**) the Paris Basin, (**c**) the Monterey Formation (TEMO25), (**d**) the Phosphoria Retort Shale, (**e**) the Mulhouse Basin (S//452), (**f**) the Kimmeridge Clay, (**g**) the Mulhouse Basin (Ci/FMM/16.5) and (**h**) the Vocontian Basin.

Kimmeridge Clay, Vocontian Basin and Mulhouse Basin (Ci/FMM/16.5-21.5) have much higher i/n ratios compared to the other kerogen pyrolysates. In contrast, the Paris Basin and the other Mulhouse Basin (S//452-457) kerogen pyrolysates have low i/n ratios. The most abundant saturated isoprenoid hydrocarbon differs also between the kerogen pyrolysates (Fig. 3.3). The C_{11} isoprenoid alkane is relatively abundant in the kerogen pyrolysate of the Vocontian Basin. The C_{13} isoprenoid alkane is abundant in all kerogen pyrolysates except in those of the Paris and Mulhouse Basins. In the Paris Basin and in the Mulhouse Basin (Ci/FMM/16.5-21.5) pyrolysates, the C_{16} and C_{18} isoprenoid alkanes are relatively abundant and the C_{15} isoprenoid alkane is relatively abundant in both Monterey and the Mulhouse Basin (S//452-457) pyrolysates.

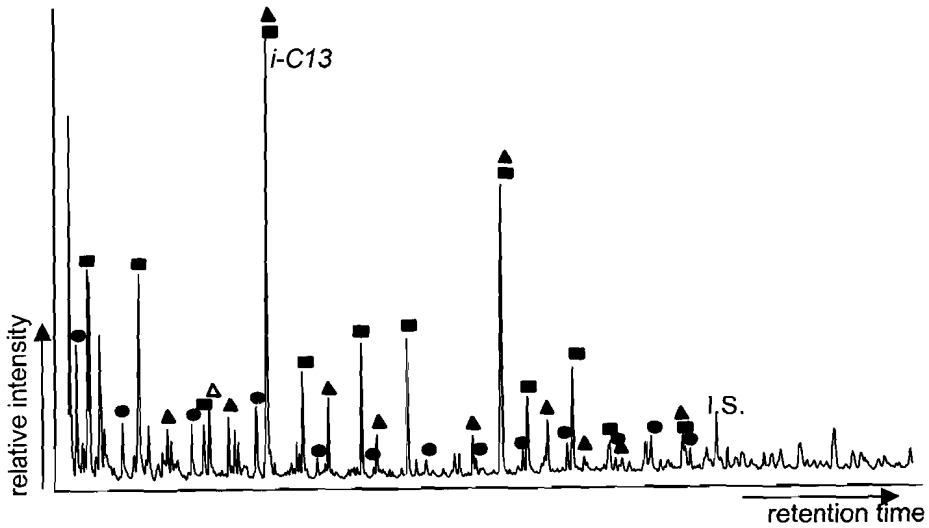

Figure 3.4 Summed mass chromatogram of *m/z* 55+57 of the branched/cyclic saturated hydrocarbon fraction of the off-line pyrolysate of the kerogen of the Phosphoria Retort Shale. Filled circles indicate the homologous series of *n*-alkanes, not fully removed by the silicalite adduction. Filled rectangles indicate the pseudo-homologous series of *i*-alkanes. Filled triangles indicate the pseudo-homologous serie of 2-nor isoprenoids, the open triangle corresponds to 3,7-dimethyldecane. Internal Standard (I.S.): 6,6-d_2-2-methylhenicosane.

An unusual series of methylated alkanes (C_9- C_{21}), was tentatively identified in the branched/cyclic saturated hydrocarbon fraction of the kerogen pyrolysate of the Phosphoria Retort Shale (Fig. 3.4). A common feature of all mass spectra of this series (*e.g.* Fig. 3.5) is the even mass peak at *m/z* 98 corresponding to a C_7H_{14} radical ion. The

formation of such a dominant even mass fragment is typical for branched alkanes (Beynon, 1960, 1968). The mass spectrum shown in Fig. 3.5a reveals also a slightly dominant even mass fragment at *m/z* 70. Furthermore, it has two dominant odd mass fragments at *m/z* 141 and 169. Therefore, this compound was tentatively identified as 4,8-dimethyltridecane. The mass spectrum shown in Fig. 3.5b has two predominant mass fragments at *m/z* 127 and 169, suggesting 3,7-dimethyldodecane as the most likely structure. All compounds of this pseudo homologous series are consistent with regular isoprenoid alkanes which have lost the methyl group at C-2. Kovats indices determined for these C_9- C_{21} 2-nor isoprenoid alkanes fit with those calculated (Table 3.2; Kissin *et al.*, 1986), further confirming their identification.

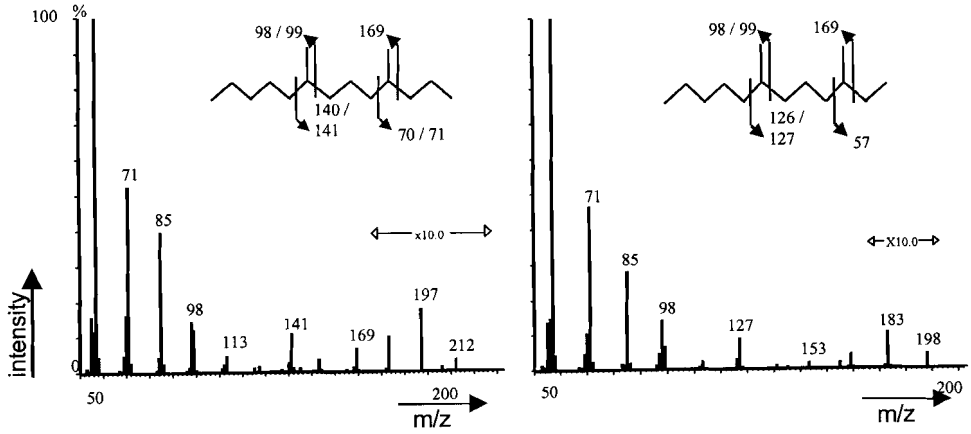

Figure 3.5 Mass spectra of two 2-nor isoprenoids (4,8-dimethyltridecane and 3,7-dimethyldodecane) from the isoprenoid fraction from the off-line kerogen pyrolysate of the Phosphoria Retort Shale sample.

The FID-traces of the unsaturated hydrocarbon fractions reveal only small differences in the general composition of the kerogen pyrolysates. In all alkene fractions, pristene is relatively abundant except in the alkene fractions of the Kimmeridge Clay and Vocontian Basin pyrolysates. The relative abundance of the C_{11}-isoprenoid alkene is, like its saturated counterpart, high in the kerogen pyrolysate of the Vocontian Basin. The relative abundance of the unsaturated C_{14}-isoprenoid is high in all alkene fractions except in those of the Paris Basin and Mulhouse Basin pyrolysate. The large amounts of 2,6,10-trimethylundec-2-ene and prist-2-ene present in the alkene fractions of the Mulhouse Basin and Vocontian basin pyrolysates are noteworthy.

Tabel 3.2: Kovats indexes (KI) for C_9-C_{21} 2-nor isoprenoid alkanes.

2-nor isoprenoids	KI flash-pyrolysate	KI calculated
3-methyloctane	872	872
4-methylnonane	963	962
5-methyldecane	1059	1058
6-methylundecane	1156	1156
2,6-dimethylundecane	1216	1219
3,7-dimethyldodecane	1320	1325
4,8-dimethyltridecane	1407	1411
6,10-dimethylpentadecane	1593	1598
2,6,10-trimethylpentadecane	1652	1663
3,7,11-trimethylhexadecane	1755	1767
4,8,12-trimethylheptadecane	1836	1850
6,10,14-trimethyloctadecane	1928	1936

Stable carbon isotope analysis

Results of bulk carbon isotopic analyses of the kerogens, or decalcified sediments before and after off-line pyrolysis (Table 3.1), suggest that in most samples the residual material after pyrolysis is isotopically heavier than the starting material, indicating that isotopically light organic material is released from the kerogen. Carbon isotopic data derived from compound-specific measurements of individual hydrocarbons in the off-line pyrolysates is shown in Fig. 3.6. Because of their potential susceptibility to fractionation effects, the isotopic compositions of compounds with carbon numbers below C_{10} were excluded (Eglinton, 1994). Except for the samples from Kimmeridge Bay and the Vocontian Basin all samples release hydrocarbons upon pyrolysis which are isotopically lighter than the TOC.

The *n*-alkanes in all kerogen pyrolysates, except for those of the Mulhouse Basin (Ci/FMM/16.5-21.5) and the Kimmeridge Clay, have a uniform isotopic composition with a standard deviation of $\leq$ 1.0‰. The alkene fractions of four selected kerogens were hydrogenated since some of the mid-chain *n*-alkenes, present in minor concentrations, partially coeluted with *n*-alk-1-enes prohibiting the reliable determination of the isotopic values of the *n*-alk-1-enes only. The hydrogenated *n*-alkenes in the off-line pyrolysates of both Monterey, the Paris Basin and the Phosphoria Retort Shale kerogens also have standard deviations of $\leq$ 1.0‰ and their average values are virtually the same as for the *n*-alkanes. The isoprenoid alkane series in all kerogen pyrolysates have a more or less uniform isotopic distribution.

The differences in isotopic composition of isoprenoid and *n*-alkanes vary from insignificant to *ca.* 9‰ (Kimmeridge Clay and Vocontian Basin; Figs. 3.7f and 3.7h). In these latter kerogen pyrolysates the isoprenoid alkanes are also isotopically heavier than the TOC. In all kerogen pyrolysates the isoprenoids are heavier than the *n*-alkanes except that of the Mulhouse Basin (S//452-457) where the isoprenoids are 1.5‰ lighter than the

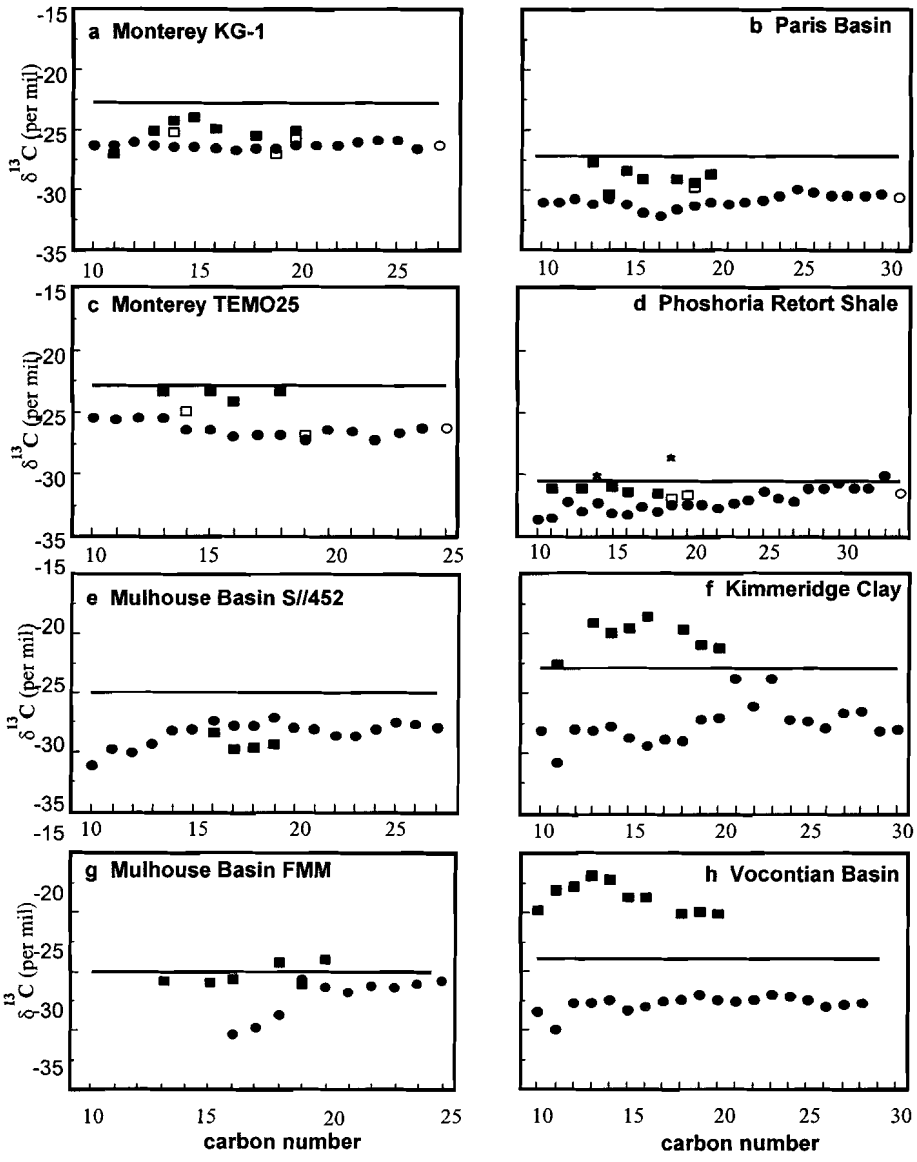

Figure 3.6 Plot of $\delta^{13}C$ values as a function of carbon number for aliphatic hydrocarbon pyrolysis products from (**a**) the Monterey Formation (KG-1), (**b**) the Paris Basin, (**c**) the Monterey Formation (TEMO25), (**d**) the Phosphoria Retort Shale, (**e**) the Mulhouse Basin (S//452), (**f**) the Kimmeridge Clay, (**g**) the Mulhouse Basin (Ci/FMM/16.5) and (**h**) the Vocontian Basin. Filled and open circles indicate the homologous series of *n*-alkanes and *n*-alk-1-enes, respectively. Filled and open squares indicate homologous series of *i*-alkanes and *i*-alk-1-enes, respectively. The straight line indicates the bulk TOC value.

that of the Mulhouse Basin (S//452-457) where the isoprenoids are 1.5‰ lighter than the *n*-alkanes. The difference in the isotopic composition of the released hydrocarbons and the $\delta^{13}C_{TOC}$ varies. In the Monterey kerogen pyrolysate the hydrogenated C_{14} and C_{20} unsaturated isoprenoids have similar isotopic compositions to their saturated counterparts *e.g.* in KG-1: -25.1‰ (C_{14}) and -25.7‰ (C_{20}) and in TEMO25: -24.9‰ (C_{14}). The isotopic composition of pristene (measured as pristane), *e.g.* in KG-1: -26.7‰ and in TEMO25: -26.9‰, is different from its saturated counterpart. However, the isotopic compositions for prist-1-ene in the Paris Basin (-26.7‰) and in the Phosphoria Retort Shale (-31.9‰) are comparable with those of their saturated counterparts.

Because of their low concentration, the isotopic composition from only two alkanes of the 2-nor isoprenoid alkane series (C_9-C_{21}) present in the Phosphoria Retort Shale sediment sample could be determined. Both of these 2-nor isoprenoids are isotopically heavier (-28.6‰ and -30.1‰) then the TOC value (-30.5‰).

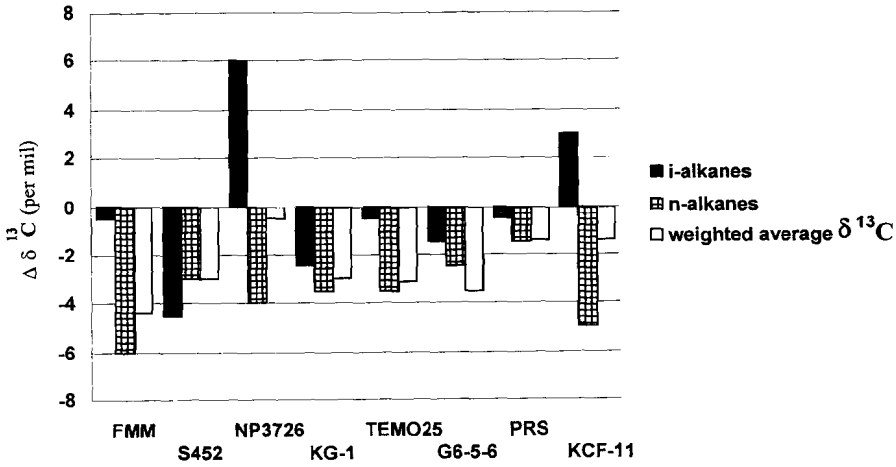

Figure 3.7 Plot of the differences between the average stable carbon isotopic composition of the *n*-alkyl algaenans and isoprenoid algaenans compared to the stable carbon isotopic composition of the bulk TOC. The third bar indicates the weighted average $\delta^{13}C$ of algaenan.

3.5 Discussion

n-Alkanes and n-alkenes

The *n*-alkanes in all kerogen pyrolysates, except for the Mulhouse Basin (Ci/FMM/16.5-21.5) and the Kimmeridge Clay, have a uniform carbon isotopic composition indicating the presence of linear polymethylenic carbon skeletons with presumably identical origins. The *n*-alkenes in both the Monterey, Paris Basin and Phosphoria Retort Shale kerogens are isotopically uniform and their average values are virtually the same as for the *n*-alkanes, indicating that they originate from the same biopolymer as their saturated counterparts (*cf.* Eglinton, 1994). Since all these kerogens are predominantly of marine origin, this strongly suggests that marine algaenans are the precursors for these moieties. Additional evidence for the presence of *n*-alkyl algaenans was obtained by chemical degradation of a Monterey sample (Höld *et al.*, unpublished results). After ether bond cleavage, the residual pyrolysate has a lower relative abundance of *n*-alkenes/*n*-alkanes indicating that part of the *n*-alkenes/*n*-alkanes are ether-bound. This is consistent with the fact that predominantly even carbon numbered (mainly C_{24} and C_{30}) *n*-alkanes were released upon treatment with HI. These *n*-alkanes and *n*-alk-1-enes are probably derived from non-hydrolysable aliphatic macromolecules with linear carbon skeletons (most likely *n*-alkyl algaenans biosynthesized by marine algae) forming an ether-linked network (*e.g.* Largeau *et al.*, 1984, 1986; Gelin *et al.*, 1996b).

In the case of the FMM (Ci/FMM/16.5-21.5) kerogen pyrolysate from the Mulhouse Basin, there is a difference of at least 6‰ between the C_{10}-C_{16} *n*-alkanes and the C_{17+} *n*-alkanes, whereas no such difference was found in the other Mulhouse kerogen pyrolysate (S//452-457). This could mean that more than one biopolymer with a linear polymethylenic carbon skeleton is present in this Mulhouse kerogen (Ci/FMM/16.5-21.5) with isotopic compositions of *c.* -26‰ and *c.* -32‰, respectively. Circumstantial evidence for the presence of two linear biopolymers is the relative amount of hydrocarbons present in the pyrolysate: *n*-alkanes up to C_{16} are present in relatively higher concentrations than C_{17+} *n*-alkanes. Previously, exceptionally high abundances of free C_{15} and C_{17} *n*-alkanes were noted in the saturated hydrocarbon fraction of this sediment (Sinninghe Damsté *et al.*, 1993). The isotopic values of these two *n*-alkanes were -33.5‰ and -34.0‰, respectively, and of the C_{17+} *n*-alkanes *c.* 31‰ (Hollander *et al.*, 1993). Probably these C_{15} and C_{17} *n*-alkanes were released from the kerogen during maturation and originate from the linear biopolymer with isotopic composition of -32‰. In the saturated hydrocarbon fraction of the Mulhouse Basin (S//452-457) much lower abundances of C_{15} and C_{17} *n*-alkanes were noted (Sinninghe Damsté *et al.*, 1993). In addition, no light isotopic values were measured for these *n*-alkanes (Hollander *et al.*, 1993) and hardly any evidence was found in the off-line pyrolysate of an additional source of isotopically light

C_{13} - C_{18} *n*-alkanes (Fig. 3.7). This indicates that in the Mulhouse (S//452-457) kerogen probably only one linear biopolymer is present.

In the Kimmeridge Clay sample, the C_{21} and C_{23} *n*-alkanes have slightly heavier isotopic compositions than the other *n*-alkanes which is ascribed to an additional, possibly ether-bound, source of C_{21} and C_{23} *n*-alkanes (van Kaam-Peters *et al.*, 1997).

Isoprenoid alkanes

Free regular isoprenoid alkanes in bitumens and crude oils have several possible origins but are generally thought to be derived primarily from the phytol side chain of chlorophyll a (Volkman and Maxwell, 1986). Other origins include chlorophyll b, bacteriochlorophyll a (Gillan and Johns, 1980), tocopherols (Brassell *et al.*, 1983) and carotenoid pigments (Volkman and Maxwell, 1986). Lipids derived from Archaea, such as extreme halophiles (Kates, 1978) and methanogens (Risatti *et al.*, 1984), may also be important isoprenoid hydrocarbon contributors in ancient sedimentary environments (*e.g.* McKirdy *et al.*, 1984; ten Haven *et al.*, 1986).

Bound acyclic regular isoprenoid hydrocarbons have been identified in many kerogen pyrolysates (*e.g.* Maters *et al.*, 1977; Larter *et al.*, 1979; van Graas *et al.*, 1980). The principal isoprenoid hydrocarbons found were the C_{19} and C_{20} isoprenoids, especially prist-1-ene (Larter *et al.*, 1979), often with a C_{14} regular isoprenoid alkene being present (Larter, 1984). Goossens *et al.* (1984) showed that kerogen-bound tocopherols were likely candidates for the prist-1-ene precursor. Phytadienes in pyrolysates of suspended matter were suggested to arise from chlorophyll (van der Meent, 1980), and also S-bound phytane is a candidate for the precursor of phytenes in sulfur-rich kerogens (Gelin *et al.*, 1995). The presence of C_{11} - C_{18} isoprenoid hydrocarbons in kerogen pyrolysates is less well understood. Recently, an aliphatic biopolymer, comprised of C_{40} isoprenoid chains with a lycopane skeleton and linked through ether bridges, was identified in the *L* race of the freshwater algae *B. braunii* (PRB *L*) (Derenne *et al.*, 1990, 1992a, 1994; Gelin *et al.*, 1994). Upon pyrolysis of this algaenan C_8-C_{20} regular isoprenoid hydrocarbons (except for the C_{12} and the C_{17}), were identified in the algaenan pyrolysate. A similar algaenan may be a possible source for the isoprenoids found in the kerogen pyrolysate.

The kerogen pyrolysates investigated in this study contain pseudo homologous series of isoprenoid alkanes that have a more or less uniform isotopic composition (Fig. 3.7) indicating the presence of isoprenoidal carbon skeletons with presumably identical origins. A sulfur-bound precursor for these isoprenoid hydrocarbons is not very likely since in the Mulhouse and Vocontian Basin hardly any sulfur is present. Furthermore, multiple precursors for C_{11}-C_{18} isoprenoid hydrocarbons are unlikely because of their similar isotopic composition. Since all these kerogens are predominantly of marine origin, this suggests that marine algaenans are the precursors for these isoprenoidal macromolecules. As in the algaenan pyrolysate of PRB *L*, C_{12} and the C_{17} isoprenoid

alkanes were not present. Their absence can be explained by the fact that their formation from regular isoprenoid moieties requires the simultaneous cleavage of two carbon-carbon bonds. The isoprenoid hydrocarbon distributions differ between the kerogen pyrolysates as well as from the PRB *L* pyrolysate (Derenne *et al.*, 1990, 1994) indicating different chemical compositions for the algaenans. Probably the marine algaenans that were the precursors for these isoprenoidal macromolecules were built from isoprenoidal carbon skeletons with different chain lengths and bound by ether linkages at different positions. Additional evidence for the presence of an isoprenoid algaenan was obtained by chemical degradation of one of the Monterey samples (Höld *et al.*, unpublished results). Flash pyrolysis of the residue after ether-bond cleavage indicates a decrease of C_{11}-C_{18} isoprenoids relative to other pyrolysis products similar to the linear alkanes and alkenes upon ether-bond cleavage. These isoprenoid alkanes and alkenes are probably derived from non-hydrolysable aliphatic macromolecules with isoprenoid carbon skeletons (isoprenoid algaenans) that form an ether-linked network (*e.g.* Largeau *et al.*, 1984, 1986; Höld *et al.*, unpublished results).

For the Kimmeridge Clay pyrolysate only, one or more additional sources for the C_{11}-isoprenoid alkane may have to be invoked since this isoprenoid is significantly lighter than the rest. The isotopic composition of the isoprenoid alkenes is, in most kerogens, similar to that of the isoprenoid alkanes suggesting a common origin. Only the isotopic composition of prist-1-ene in both Monterey pyrolysates is different from its saturated counterparts and, thus, probably an additional source has to be invoked such as bound tocopherol (Goossens *et al.*, 1984). The structure and identical isotopic compositions of the two alkanes of the 2-nor isoprenoid alkane series (C_9-C_{21}), present in the Phosphoria Retort Shale sediment sample, point to a common origin.

Sources for n-alkyl vs. isoprenoid biopolymers

The small difference in the isotopic composition between isoprenoid and *n*-alkyl algaenans in some of the kerogens might suggest that they are biosynthesized by the same organism. Until now it has been assumed that a difference of *c.* 1-2 ‰ between isoprenoid and normal alkanes could be ascribed to different biosynthetic pathways, and that a larger difference would indicate different source organisms (Hayes, 1993). Recently, however, much larger differences of up to 8 ‰ between compounds with isoprenoid and *n*-alkyl chains have been measured within the same algal species (Schouten *et al.*, unpublished results). Furthermore, a new pathway for the biosynthesis of isoprenoid compounds has been found in several bacteria (Flesh and Rohmer, 1988; Rohmer *et al.*, 1993), higher plants (Rohmer *et al.*, 1996; Lichtenthaler *et al.*, 1997) and in a number of green algae (Schwender *et al.*, 1996; Lichtenthaler *et al.*, 1997), possibly resulting in large isotopic differences between isoprenoid and normal alkanes biosynthesized by similar organisms. Furthermore, it seems highly unlikely that isoprenoid and *n*-alkyl algaenans are

biosynthesized by the same organism since the co-occurrence of these types of algaenans in one organism has never been reported so far.

Thus, it is likely that isoprenoid and *n*-alkyl algaenans originate from different algal sources living in similar conditions and that the sometimes substantial isotopic differences between isoprenoids and *n*-alkanes may be due to a combination of physiological factors such as growth rate and cell size (Goericke *et al.*, 1994; Laws *et al.*, 1995) and environmental factors (Hayes, 1993). Furthermore, it is possible that during short periods of time (*e.g.* at a seasonal level) environmental conditions changed. If the algaenans were produced during different periods of time, then the isotopic compositions of the *n*-alkyl and isoprenoid algaenans reflect the different environmental conditions during which these biopolymers were biosynthesized.

$\delta^{13}C$ of the pyrolysis products vs. $\delta^{13}C_{TOC}$

In Fig. 3.7 the isotopic compositions of the *n*-alkanes and isoprenoid alkanes compared to those of the kerogen or decalcified sediment are shown. These $\Delta\ \delta^{13}C$ values represent the differences between the average isotopic composition of the *n*-alkyl algaenans (or isoprenoid algaenans) and those of the bulk TOC. The third bar indicates the weighted average $\delta^{13}C$ of algaenans compared to the bulk TOC calculated using the previously mentioned values and the i/n ratio (Table 3.1). Except for the Kimmeridge Clay, the Phosphoria Retort Shale and the Vocontian Basin the weighted $\Delta\ \delta^{13}C$ values have large negative values (between -2 and -5‰). This suggests that aliphatic biopolymers only partially contribute to the $\delta^{13}C_{TOC}$ and therefore cannot be exclusive constituents of the kerogen carbon. Accordingly, the kerogen must contain constituents relatively enriched in ^{13}C that do not yield C_{10+} aliphatic hydrocarbons as major products upon pyrolysis (e.g. lignins, polysaccharides; *cf.* Eglinton, 1994).

Furthermore, most residues after off-line pyrolysis are slightly isotopically heavier than their corresponding kerogens (Table 3.1), which reflects the generation of isotopically light pyrolysis products. The Paris Basin sample is an exception as both pyrolysis residues and aliphatic hydrocarbon products were isotopically lighter than the starting material. The liberation of unknown isotopically heavy pyrolysis products is inferred in this case and this is supported by isotopically heavier alkylbenzenes and alkylthiophenes that were found in the aromatic fraction of the off-line pyrolysate (Höld, unpublished results). Another exception is the Kimmeridge Clay Sample as the residue is isotopically lighter than the kerogen and therefore the isotopically heavier isoprenoids are probably more important constituents than the isotopically lighter *n*-alkanes.

3.6 Conclusions

Homologous series of linear hydrocarbons and isoprenoid hydrocarbons were identified in flash pyrolysates of 8 kerogen samples. In addition, a homologous series of 2-nor isoprenoid alkanes was tentatively identified in the Phosphoria Retort Shale kerogen pyrolysate. In most pyrolysates uniform stable carbon isotopic compositions were observed for the series of *n*-alkanes and isoprenoids, indicating that they are probably derived from *n*-alkyl and isoprenoid algaenans biosynthesized by marine algae. In both pyrolysates of the Mulhouse kerogens, that of the Vocontian Basin kerogen and in that of the kerogen from Kimmeridge Bay large differences were found between $\delta^{13}C$ values of isoprenoids and *n*-alkanes, indicating that the isoprenoid and linear algaenans are derived from distinct algal sources. In a number of kerogens the average isotopic compositions of the algaenans did not closely match the $\delta^{13}C_{TOC}$ and thus additional components must be considered of significance.

3.7 Acknowledgements

Dr. E. Lichtfouse and an anonymous referee are thanked for suggestions to improve the manuscript. Dr. T.I. Eglinton is thanked for provision of the Monterey TEMO25 kerogen sample. Dr. W. Pool is thanked for technical assistance and M. Dekker is acknowledged for performing GC-MS analyses. This study was supported by a PIONIER grant to JSSD from the Netherland Organization for Scientific Research (NWO). We thank Shell International Petroleum Maatschappij BV for financial support for the irm-GC-MS facility. We acknowledge R. Kloosterhuis (NIOZ) for bulk isotope analyses of the sediments and the kerogen. This is NIOZ Contribution no. 3185.

CHAPTER 4

On the origin of prist-1-ene and prist-2-ene in kerogen pyrolysates

Ingeborg M. Höld, Stefan Schouten, Sjerry J. Van der Gaast and Jaap S. Sinninghe Damsté

4.1 Abstract

The principal isoprenoid hydrocarbons in flash pyrolysates from immature kerogens are prist-1-ene and, to a lesser extent, prist-2-ene. The precise origin of these compounds is still a matter of debate. Chemical degradation experiments performed on a sulfur-rich kerogen in this study show that at least two precursors can generate pristenes upon pyrolysis of sulfur-rich kerogens: ether-bound precursors, probably tocopherols, and a sulfur-bound precursor. Prist-2-ene is likely formed by the double-bond isomerization of prist-1-ene. This isomerization of prist-1-ene into prist-2-ene depends on the amount of protons available for the formation of the intermediate carbonium ion. These protons can be derived from acidified aluminosilicates (e.g. the clay minerals montmorillonite or kaolinite) in the rock or from inorganic acids (e.g. HI, HCl). The degree of isomerization depends on the amount of protons available relative to the total organic carbon content of the sediment.

4.2 Introduction

Acyclic isoprenoid hydrocarbons have been identified in many pyrolysates of immature kerogens (e.g. Maters *et al.*, 1977; Larter *et al.*, 1979; van der Meent *et al.*, 1980; Koopmans *et al.*, 1999). The principal isoprenoid hydrocarbon is the C_{19} component, prist-1-ene (Larter, 1984). The origin of this compound, i.e. its precursors and type of linkage, is still a matter of debate (e.g. Sinninghe Damsté and de Leeuw, 1995). It is important to identify the origin of prist-1-ene in pyrolysates, since it is probably the source for a substantial part of pristane in more mature petroleum source rocks and crude oils (Goossens *et al.*, 1984). For instance, a detailed study by van Graas *et al.* (1981) of a suite of Paris Basin rock samples of increasing maturity showed a good correlation between the concurrent disappearance of the pyrolysis product prist-1-ene and the generation of pristane in the rock extract. A similar correlation was observed by Goossens *et al.* (1988) and Koopmans *et al.* (1999).

Model compound pyrolysis studies (Larter *et al.*, 1983, and references therein) indicate that prist-1-ene precursors are not ester-bound compounds, but probably C-C or C-O bound moieties that generate pristane on burial and prist-1-ene on pyrolysis. Artificial maturation experiments in combination with flash pyrolysis and chemical degradation experiments indicate that the precursor of pristane and prist-1-ene might occur in sulfur- or in oxygen-bound form (Koopmans *et al.*, 1999). Kinetic studies suggest that a single type kerogen-bound precursor is unlikely (Burnham, 1989; Tang and Stauffer, 1995).

Several studies suggest different precursors for prist-1-ene. Kerogen-bound diphytanyl ethers of archaebacteria (e.g. Chappe *et al.*, 1982) were proposed as precursors of prist-1-ene in kerogen pyrolysates. Goossens *et al.* (1984) showed that kerogen-bound tocopherols are also likely candidates for prist-1-ene precursors. Furthermore, Ishiwatari (1991) reported the formation of prist-1-ene upon pyrolysis of chlorophyll-a after preliminary heating. Recently, it was suggested that phenol-phytol condensation products (methyltrimethyltridecylchromans) bound into kerogens may also be a source of prist-1-ene upon pyrolysis (Li *et al.*, 1995), although the formation of such condensation products was questioned (Sinninghe Damsté and de Leeuw, 1995).

Besides prist-1-ene, relatively high amounts of its isomer, prist-2-ene, sometimes occur in kerogen pyrolysates. It has been suggested that during pyrolysis, prist-2-ene is formed from prist-1-ene in the presence of clay minerals (Regtop *et al.*, 1986). Clay minerals are believed to catalyze the rearrangement of steroids (Sieskind *et al.*, 1979; van Kaam-Peters *et al.*, 1998) and to isomerise alkenes (Curtis *et al.*, 1983; Regtop *et al.*, 1985). In a study by Regtop *et al.* (1986) pyrolysis of demineralised kerogen of the Condor oil shale yielded predominantly prist-1-ene whereas the presence of prist-2-ene in kerogen/kaolinite pyrolysates demonstrated that kaolinite (a clay mineral) is able to act as a catalyst for prist-1-ene isomerization. Besides prist-2-ene, small amounts of prist-5-enes and prist-6-enes were detected as well. Prist-2-ene increased in abundance with increasing proportions of kaolinite. Therefore, Regtop *et al.* (1986) proposed that the principal source of prist-2-ene in pyrolysates of the Condor oil shale is prist-1-ene and that the double bond isomerization is catalyzed by clay minerals such as kaolinite. The increasing proportion of kaolinite in the kerogen/mineral mixture was proposed to increase the opportunity for gaseous prist-1-ene to meet mineral surfaces leading to increased isomerization of prist-1-ene. Other non-clay minerals such as quartz, feldspar, calcite and pyrite gave similar, but less striking results (Regtop *et al.*, 1986).

In contrast, a different behaviour of prist-2-ene and prist-1-ene in the flash pyrolysates of chemically degraded kerogen was observed by Koopmans *et al.* (1999). Upon HI/$LiAlH_4$ treatment of the desulfurized kerogen, prist-1-ene was no longer present in the kerogen pyrolysates but the relative amount of prist-2-ene remained unchanged and

therefore different precursors were suggested. Hence, questions remain on the origin of both prist-1-ene and prist-2-ene in kerogen pyrolysates.

In this study, flash-pyrolysis was performed on extracted and decarbonated rocks and isolated kerogens. Chemical degradation techniques were used on isolated kerogens to obtain information on the precursors of prist-1-ene and prist-2-ene, to investigate how these precursors are bound to the kerogen, and the influence of clay minerals on the formation of the pristenes.

4.3 Experimental

Rock samples

The rock samples were previously described by Höld *et al.* (1998a) and are listed in Table 4.1. The clay mineral samples used in the pyrolysis experiments include kaolinite from the Source Clay Minerals Repository (Kga-1), montmorillonite from Ward's (H-25 Upton Wyoming bentonite), and a fine-grained muscovite from the Van der Marel mineral collection (sericite 1398, Villar de Puerco). These clay mineral standard samples were used as received with no pretreatment.

Table 4.1: Relative abundances of prist-1-ene/prist-2-ene (1P/2P) and 2,6,10-trimethyldec-1-ene/2,6,10-trimethyldec-2-ene (1TMD/2TMD) calculated from GC-FID peak areas.

	TOC[a)]	TOC[b)]	1P/(1P+2P)			1TMD/1TMD+2TMD		
	%	%	es[c)]	ds[c)]	ik[c)]	es[c)]	ds[c)]	ik[c)]
Monterey Formation	9.6	18	0.9	0.7	0.9	0.4	0.4	0.3
Mulhouse Basin (FMM)	1.2	1.5	0.8	0.3	0.6	0.9	0.6	0.8
Mulhouse Basin (S452)	3.0	6.5	0.7	0.4	n.d.	0.8	0.6	n.d.
Kimmeridge Clay	24	27	n.d.	0.5	1.0	n.d	0.7	1.0
Vocontian Basin	3.0	4.6	≈0	≈0	n.d.	0.5	0.5	n.d.

[a)] TOC of extracted sediment
[b)] TOC of decarbonated sediment
[c)]es=extracted sediment, ds=decalcified sediment, ik=isolated kerogen and nd=not determined

Rock extraction, decarbonation and kerogen isolation

The different sequential isolation steps are depicted schematically in Fig. 4.1. The rocks were Soxhlet extracted with dichloromethane (DCM)/methanol (MeOH) (7.5/1, v/v) for 24 h. The residue was decarbonated by treatment with 4N HCl at room temperature and ultrasonically re-extracted with water (3x), methanol (3x) and finally dichloromethane (3x). Kerogen isolation was performed by HCl/HF treatments of the

solvent-extracted residue as described previously (Eglinton, 1988). The kerogen was ultrasonically extracted with methanol and DCM, respectively.

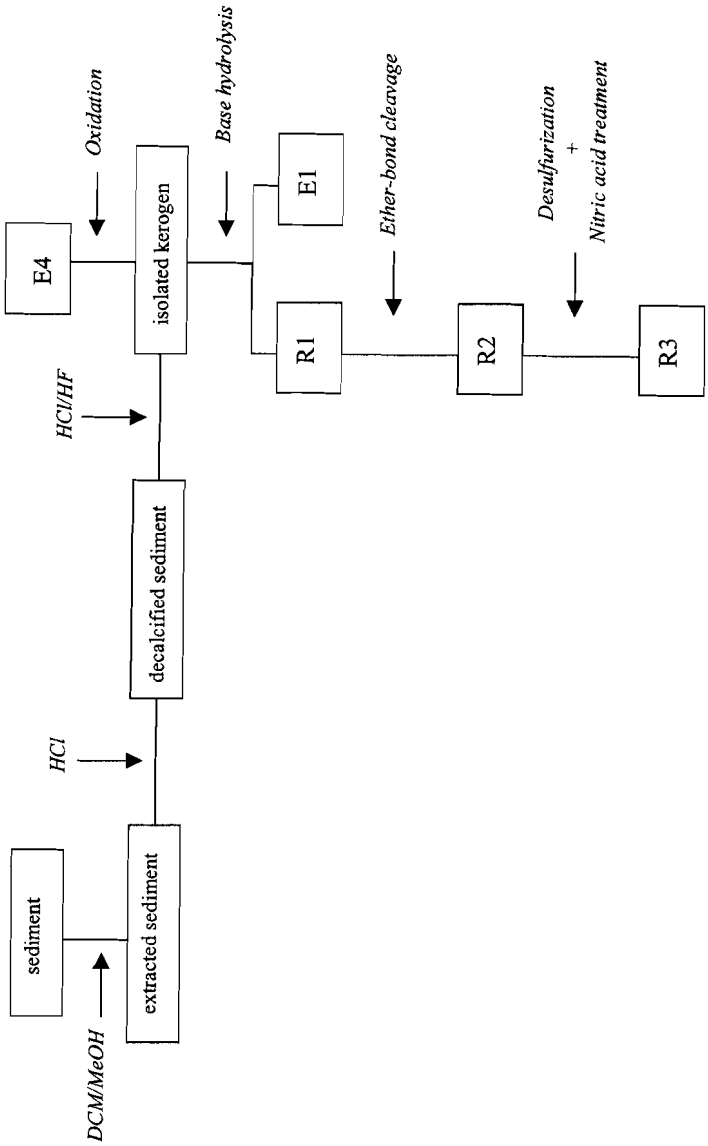

Figure 4.1 Analytical flow diagram of the chemical degradation of the Monterey kerogen (KG-1).

Sequential chemical degradation of kerogen

The different sequential chemical degradation steps are depicted schematically in Fig. 4.1. After each chemical degradation step the residue was washed with H_2O/MeOH (1:1, v/v; 3x), with MeOH (3x) and with ethyl acetate (3x). The residue was dried under nitrogen. Base hydrolysis, ether- and sulfur-bond cleavage were performed sequentially as described previously (Höld *et al.*, 1998b) to obtain and residues R_1, R_2 and R_3, respectively. Residues were analyzed by flash pyrolysis-gas chromatography-mass spectrometry (Py-GC-MS).

Firstly, an alkaline hydrolysis was performed in order to hydrolyze ester bonds within the kerogen (Goossens *et al.*, 1989). 1N KOH in methanol (MeOH) was added to 400 mg kerogen, refluxed for 1 h at 65°C under a nitrogen atmosphere and then cooled to room temperature. The pH was adjusted to 3 by adding 4 N HCl(H_2O) /MeOH (1:1,v/v). During the second step, aliphatic ethers were cleaved by treatment with HI (March, 1985). 56% HI-solution (in H_2O) was added to residue R_1, refluxed for 1 h under a nitrogen atmosphere and then cooled to room temperature. In the third step, (poly)sulfide bonds in the kerogen were cleaved by treatment with Ni_2B (Schouten *et al.*, 1993). MeOH/THF (1:1), $NiCl_2$ and $NaBH_4$ were added to residue R_2. The mixture was refluxed for 1 h under stirring and N_2 atmosphere and then cooled down to room temperature. The residue R_3 was obtained as described above. In order to remove the Ni salts present in the residue, concentrated HNO_3 was added and left to react for 12 h. The residue R_3 washed with H_2O/MeOH (1:1, v/v, 3x), with MeOH (3x) and with ethyl acetate (3x).

Py-GC, Py-GC-MS and X-ray powder diffraction (XRD)

Py-GC and Py-GC-MS were carried out as described previously (Höld *et al.*, 1998a). XRD was carried out with a Philips PW1050/25 giniometer, using CoKα radiation (40kV, 40mA) from a long fine focus tube, a graphite monochromator in the diffracted beam, and a vacuum/helium device to minimise the absorption of the X-rays by air (Van der Gaast and Vaars, 1981). The instrument was equipped with a variable divergence slit. The slit settings were: 12 mm irradiated specimen length; receiving slit, 0.1 mm; antiscatter slit, 0.5°; counting time, 2 s/0.02° 2θ. Approximately 10 mg of sample material was pressed into a 0.5 mm deep depression in a low-background sample holder (Si-wafer). The specimens were measured at 50% relative humidity. Patterns were corrected for the Lorentz and polarisation factor and for the irradiated specimen volume.

4.4 Results and discussion

General composition of flash pyrolysates of investigated sediments

Several extracted rocks, decarbonated rocks and isolated kerogens (Table 4.1) were analyzed by Py-GC and Py-GC-MS as described previously (Höld *et al.*, 1998a). The FID and TIC traces of the flash pyrolysates revealed significant differences in the composition of the pyrolysis products. Homologous series of *n*-alkanes and *n*-alkenes dominate the pyrolysates of most kerogens. Series of isoprenoid alkanes and alkenes were detected in all flash pyrolysates and consist of regular C_8-C_{20} isoprenoids, which were especially abundant in the flash pyrolysates of the Kimmeridge Clay and the Vocontian Basin samples. Three irregular isoprenoid alkanes, 2,6,10,15,19-pentamethylicosane, 2,6,15,19-tetramethylicosane and 10-ethyl-2,6,15,19-tetramethylicosane were identified in the flash pyrolysate of the kerogen of the Vocontian Basin sample (Vink *et al.*, 1998). Alkylated benzenes, naphthalenes and indenes were present in all flash pyrolysates but are abundant in the Monterey Formation and Vocontian Basin pyrolysates. Furthermore, the kerogens from the Monterey Formation are organic sulfur-rich and their flash pyrolysates contain high amounts of alkylated thiophenes, benzo[*b*]thiophenes and thiolanes. Thus, the samples investigated represent a wide range of kerogens with different compositions.

Ratio of prist-1-ene to prist-2-ene in flash pyrolysates of sediments

In most of the flash pyrolysates both prist-1-ene and prist-2-ene are present in significant amounts. The relative abundance of prist-1-ene versus prist-2-ene in the flash pyrolysates differs significantly for each rock although the reproducibility of the measurements was not determined (Table 4.1). The prist-1-ene / (prist-1-ene + prist-2-ene) (1P/(1P+2P)) ratio is not only different for different kerogens but also varies strongly between the different fractions analyzed (extracted rock, decarbonated rock and isolated kerogen). For instance, the 1P/(1P+2P) ratio in the pyrolysate of the extracted rock from the Mulhouse Basin (FMM) is > 0.5 (predominantly prist-1-ene), whereas after decarbonation using HCl, the ratio is < 0.5, and after isolation with HCl/HF, the ratio is again > 0.5 (Fig. 4.2, Table 4.1). Similar changes can be found in the relative abundance of 2,6,10-trimethylundec-1-ene compared to 2,6,10-trimethylundec-2-ene (Fig. 4.2; Table 4.1).

In order to find out what causes these changes in the 1P/(1P+2P) ratio, isolated kerogen from the Mulhouse Basin sample (FMM), which has abundant prist-1-ene in its flash pyrolysate (Fig. 4.2f), was mixed in a 1 to 3 ratio (w/w) with the residue of the decarbonated rock from the Mulhouse Basin after off-line pyrolysis. Flash pyrolysis of this residue indicated that no thermally releasable organic material was present and that it was basically composed of inorganic minerals. The flash pyrolysate of the mixture of the off-line pyrolysis residue and the kerogen showed a much lower 1P/(1P+2P) ratio

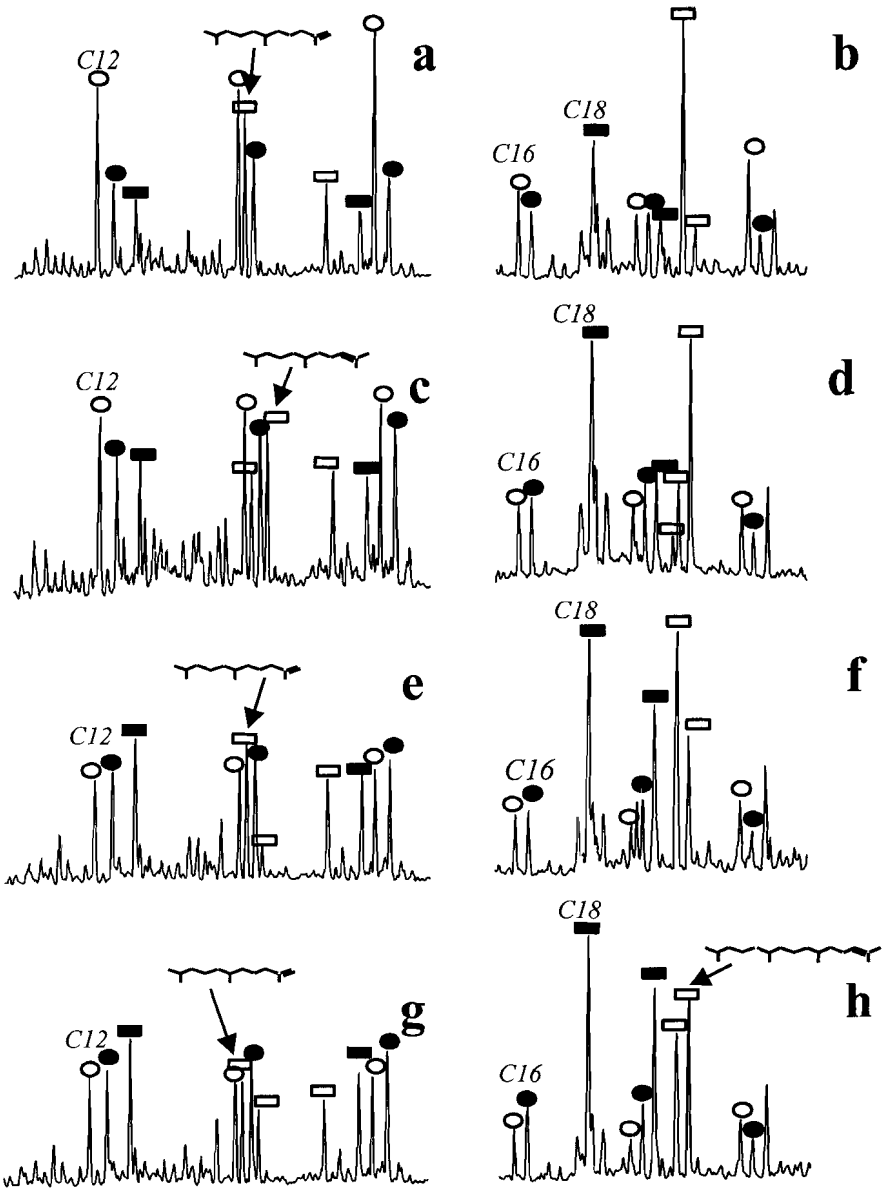

Figure 4.2 Partial FID traces of the flash pyrolysates (Curie temperature 610 °C) of (**a** and **b**) extracted sediment, (**c** and **d**) decalcified sediment, (**e** and **f**) isolated kerogen and (**g** and **h**) isolated kerogen/off-line pyrolysis residue mixture from the Mulhouse (FMM) Basin. Filled and open circles indicate the homologous series of *n*-alkanes and *n*-alk-1-enes, respectively with the number of carbon atoms indicated. Filled and open rectangles indicate pseudo homologous series of isoprenoid *(i-)* alkanes and *i*-alk-1-enes, respectively. Their number of carbon atoms is indicated with italic numbers.

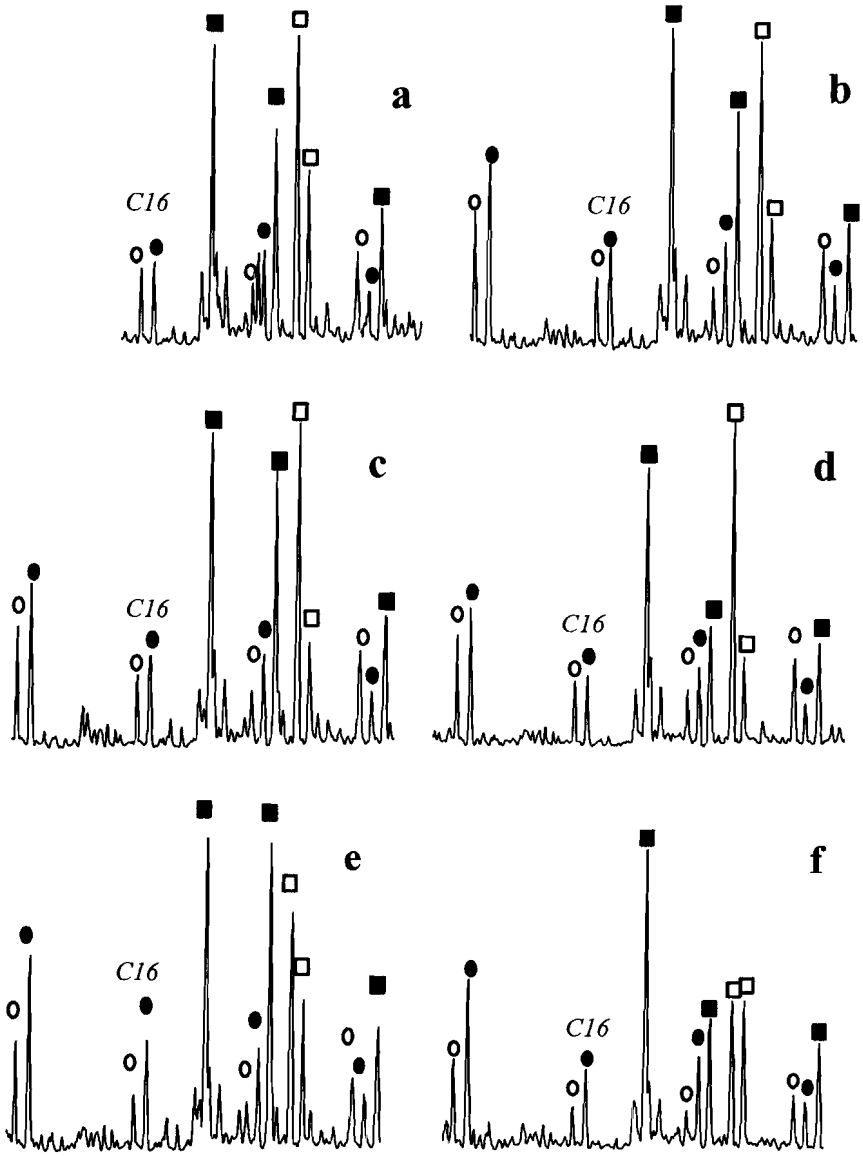

Figure 4.3 Partial FID traces of the Mulhouse (FMM) pyrolysates (Curie temperature 610 °C) of (**a**) isolated kerogen, (**b**) isolated kerogen/serite mixture, (**c**) isolated kerogen/kaolinite mixture, (**d**) isolated kerogen/kaolinite mixture (activated by HCl), (**e**) isolated kerogen/montmorillonite mixture and (**f**) isolated kerogen/montmorillonite mixture (activated by HCl). Filled and open circles indicate the homologous series of *n*-alkanes and *n*-alk-1-enes, respectively with the number of carbon atoms indicated. Filled and open rectangles indicate pseudo homologous series of isoprenoid *(i-)* alkanes and *i*-alk-1-enes, respectively. Their number of carbon atoms is indicated with italic numbers.

compared to the isolated kerogen (Fig. 4.2h). Similar but smaller changes were found in the relative abundance of 2,6,10-trimethylundec-1-ene compared to 2,6,10-trimethylundec-2-ene (Figs. 4.2e and 4.2g). This experiment indicates that the inorganic matrix of the rock has a catalytic activity that results in the formation of prist-2-ene (cf. Regtop *et al.*, 1986).

Influence of clay minerals on the 1P/(1P+2P) ratio in rocks

Isolated kerogen from the Mulhouse Basin sample (FMM) which contains abundant prist-1-ene in its flash pyrolysate (Fig. 4.2f), was mixed in a 1:3 ratio (w/w) with three different clay minerals: sericite, kaolinite and montmorillonite, in order to find out which clay minerals cause these changes in prist-1-ene and prist-2-ene concentrations during flash pyrolysis. These clay minerals are representatives of the three major clay mineral groups. The flash pyrolysate of the mixture of sericite and kerogen showed almost no decrease in the 1P/(1P+2P) ratio compared to that of the pyrolysate of the isolated kerogen (Fig. 4.3b, Table 4.2). A slight decrease in the 1P/(1P+2P) ratio was detected in the case of kaolinite (Fig. 4.3c, Table 4.2). However, a significant decrease in the 1P/(1P+2P) ratio was detected in the montmorillonite experiment (Fig. 4.3e, Table 4.2). Similar changes were found in the relative abundance of 2,6,10-trimethylundec-1-ene compared to 2,6,10-trimethylundec-2-ene. However, none of the kerogen/clay mineral mixtures yielded a 1P/(1P+2P) ratio lower than 0.5 as was found upon flash-pyrolysis of the decarbonated Mulhouse rock (Table 4.2) suggesting that an additional catalyst or factor must operate in the decarbonated samples.

Table 4.2: Ratio of 1P/(1P+2P) in the flash pyrolysate (400°C) of the Mulhouse (FMM) kerogen calculated form GC-FID peak areas.

	1P/(1P+2P)
es[1)]	0.8
ds[1)]	0.3
ik[1)]	0.6
ik:sericite = 1:3	0.7
ik:sericite = 1:3 (HCl)	0.8
ik:kaolinite = 1:3	0.7
ik:kaolinite = 1:3 (HCl)	0.7
ik:montmorillonite = 1:3	0.6
ik:montmorillonite = 1:3 (HCl)	0.5

[1)]es=extracted sediment, ds=decarbonated sediment and ik=isolated kerogen

To investigate the influence of decarbonation of rocks on the 1P/(1P+2P) ratio, the kerogen/clay mineral mixtures were treated with 4N HCl and washed with water thereafter. The flash pyrolysates of the HCl-treated kerogen/sericite and kerogen/kaolinite

mixtures showed only small differences in the 1P/(1P+2P) ratios compared to the untreated mixtures (Fig. 4.3d, Table 4.2). However, the ratio in the pyrolysate of the HCl treated kerogen/montmorillonite mixture decreased substantially compared to the untreated mixture (Figs. 4.3e and f, Table 4.2). This indicates that HCl treatment of the montmorillonite increases its catalytic properties and relatively more prist-1-ene isomerizes to prist-2-ene. Furthermore, the relative amount of pristane is decreasing substantially upon HCl treatment of the clayminerals (Figs 4.3d and f).

Interestingly, the use of acidified clay minerals as catalysts was already disclosed in German patents in 1923. Most of these clay catalysts were prepared by the acid treatment of montmorillonite and halloysite (Rupert *et al.*, 1987). Acidic aluminosilicates (e.g. montmorillonite) can cause migration of the double bond in olefins and thus cause isomerization of the double bond in prist-1-ene to form prist-2-ene (Rupert *et al.*, 1987). This reaction probably proceeds *via* a carbonium ion intermediate, which arises by transfer of a proton from the catalyst surface to the reactant (prist-1-ene; Rupert *et al.*, 1987). Hydrogen clay minerals have acid strengths corresponding to sulfuric acid solutions between 71 and 90 wt% H_2SO_4 (Rupert *et al.*, 1987). Alumina is thought to be the source of the acidic nature of the surface. Isomorphous substitution of Al^{3+} for Si^{4+} in tetrahedral coordination in an aluminosilicate causes a net negative charge. A charge-balancing proton associated with this tetrahedral aluminium corresponds to a Brønsted, or protonic acid site (*e.g.* Rupert *et al.*, 1987). It is postulated that removal of one of a pair of octahedral aluminium ions from montmorillonite, for example, removes two hydroxyl groups and leaves the remaining aluminium in four-fold coordination. This tetrahedral aluminium, with its charge-balancing proton, forms an additional Brønsted, or protonic acid site, increasing the catalytic activity of the clay minerals (*e.g.* Rupert *et al.*, 1987). Acid treatment of hydrogen clays would therefore be expected to enhance the effect of these materials in promoting double bond isomerization of prist-1-ene to form prist-2-ene. In order to minimize this extra catalytic effect rocks must therefore be washed thoroughly after acid treatment.

Besides the acidic strength of clay minerals the ratio of clay/TOC is an additional factor that determines the degree of isomerization of prist-1-ene to prist-2-ene. In a previous study it was shown that the diasterane/sterane ratios in samples from the Kimmeridge Clay and the Toarcian shale Formations strongly depend upon the ratio of clay to organic matter (van Kaam-Peters *et al.*, 1998). A similar phenomenon might occur for the isomerization of prist-1-ene. TOC values, clay/carbonate content and 1P/(1P+2P) ratios in the pyrolysates were determined from thirteen samples of the Kimmeridge Clay and are shown in Table 4.3 (van Kaam-Peters *et al.*, 1998). No correlation between clay mineral concentration and 1P/(1P+2P) ratio is observed. However, samples with high clay/TOC ratios have relatively low 1P/(1P+2P) ratios and vice versa (Table 4.3, Fig 4.4).

These results support an origin of most prist-2-ene in pyrolysates from clay-catalyzed isomerization of prist-1-ene, as proposed by Regtop *et al.* (1986).

Table 4.3: Data of the Kimmeridge Clay Formation (XRD and flash pyrolysis).

	TOC[a)]	Carbonate	1P/(1P+2P)[b)]	Clay[c)]	Clay/TOC
	%	%		%	
KC1	7.0	85	0.9	3.4	0.5
KC2	6.2	10	0.4	70	11
KC3	10.7	71	0.9	11	1.0
KC4	18.2	0	0.7	57	3.1
KC5	2.1	86	0.5	10	4.5
KC6	4.8	22	0.3	53	11
KC7	52.1	17	0.9	3.1	0.06
KC8	3.7	25	0.3	56	15
KC9	10.8	25	0.4	47	4.4
KC10	0.6	76	0.01	21	33
KC11	24.1	10	0.7	43	1.8
KC12	4.5	93	1.0	0.3	0.06
KC13	7.4	30	0.4	44	5.9

[a]in the extraced sediment
[b]in the decalcified sediment
[c]100 – (carbonate + quartz +pyrite + (1.5 x TOC))

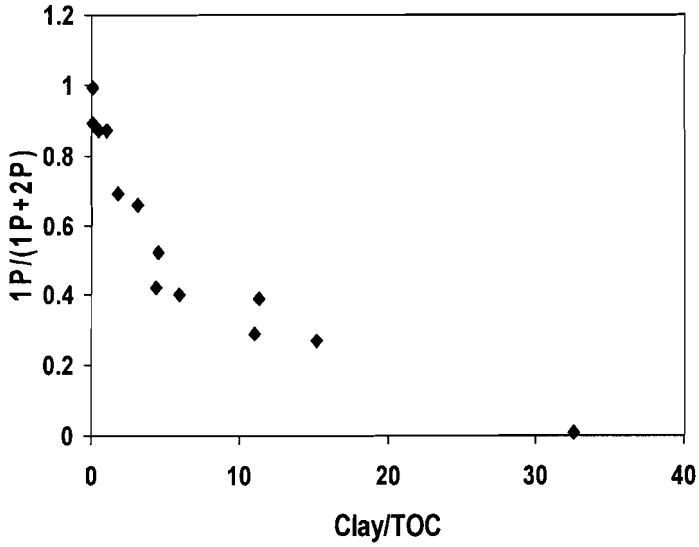

Figure 4.4 The 1P/(1P+2P) ratio in samples from the Kimmeridge Clay Formation as a function of clay / TOC.

The percentage of prist-2-ene seems to correlate with the relative amount of both the montmorillonite/smectite and kaolinite, determined by XRD-analysis. This indicates that montmorillonite/smectite may be an important isomerization catalyst in addition to kaolinite, that was mentioned by Regtop *et al.* (1986). This is consistent with the sericite/kaolinite/montmorillonite experiments described above and the fact that the acid strength of H-montmorillonite is even stronger than that of H-kaolinite (Rupert *et al.*. 1987). In a sample from the Monterey Formation where kaolinite is not present (Isaacs *et al.*, personal communication) prist-2-ene occurs in the flash pyrolysate, indicating again that kaolinite cannot be the main catalyst (Table 4.1). However, kaolinite may still act in a number of sediments as the prime catalyst. For instance, XRD-analysis indicated the presence of clay minerals in two decarbonated Mulhouse rocks (FMM and S452) and a decarbonated Vocontian Basin rock. In the S452 Mulhouse and in the Vocontian Basin rock montmorillonite was present in much higher abundance than kaolinite. However, in the FMM Mulhouse rock montmorillonite is much less abundant and kaolinite is more abundant compared to the other two rocks. All three rocks have a relatively high amount of prist-2-ene in their pyrolysates. Since in the FMM Mulhouse rock little montmorillonite was present, kaolinite probably was the main catalyst, indicating that probably both montmorillonite and kaolinite can act as the isomerization catalyst.

Sequential chemical degradation experiments

It is clear from the above results that prist-2-ene can be formed by isomerization of prist-1-ene, which contrasts with Höld *et al.* (1998b) and Koopmans *et al.* (1999), who proposed different precursors for prist-1-ene and prist-2-ene. How prist-1-ene is formed and from what precursor remains uncertain, although it is generally presumed that tocopherol is the main precursor of prist-1-ene (Goossens *et al.*, 1984, 1988).

In an attempt to resolve this issue, we performed flash pyrolysis on an isolated Monterey kerogen (KG-1) after saponification. The pyrolysate still contains prist-1-ene, small amounts of prist-2-ene and one of their alleged precursors, α– or γ– tocopherol (Figs. 4.5a and b; Goossens *et al.*, 1984). Upon HI/$LiAlH_4$ treatment (which cleaves ether-bonds) of saponified Monterey kerogen, prist-1-ene and 2,6,10-trimethylundec-1-ene as well as α– and γ– tocopherol nearly disappeared from the residue pyrolysate, while prist-2-ene and 2,6,10-trimethylundec-2-ene significantly increased (Fig. 4.5c; Höld *et al.*. 1998b). Since bound tocopherols can thermally generate prist-1-ene *via* a Retro-Diels Alder reaction (Goossens *et al.*, 1984), ether-bound tocopherols are a likely major source of prist-1-ene in kerogen pyrolysates, at least in the Monterey Formation. However, tocopherols were not among the products released after HI treatment of the Monterey kerogen, possibly because the HI treatment effects the ether bond in the tocopherol as well. Intriguingly, upon RuO_4 oxidation of a related Monterey kerogen (KG-2) released

three isoprenoid compounds (Fig 4.6). These three isoprenoid compounds are also generated by oxidation of 2-methyl-2-(4,8,12-trimethyldecyl)chroman whereas only 6,10,14-trimethylpentadecan-2-one is generated upon oxidation of phytol. These results provide additional evidence for the presence of bound chromans/tocopherols in the Monterey kerogen. Chappe *et al.*, (1982) suggested kerogen-bound diphytanyl ethers as precursors for prist-1-ene and Koopmans *et al.* (1999) suggested that pristane could be thermally generated from ester-bound diphytanyl glyceryl ethers. Furthermore, they suggested that phytane, identified in the extract upon ether-bond cleavage, could originate from these ester-bound diphytanyl glyceryl ethers. Phytane was released upon HI treatment of the Monterey kerogen. However, no diphytanyl glyceryl ethers were released upon saponification, suggesting that no ester-bound diphytanyl glyceryl ethers occur in this Monterey kerogen.

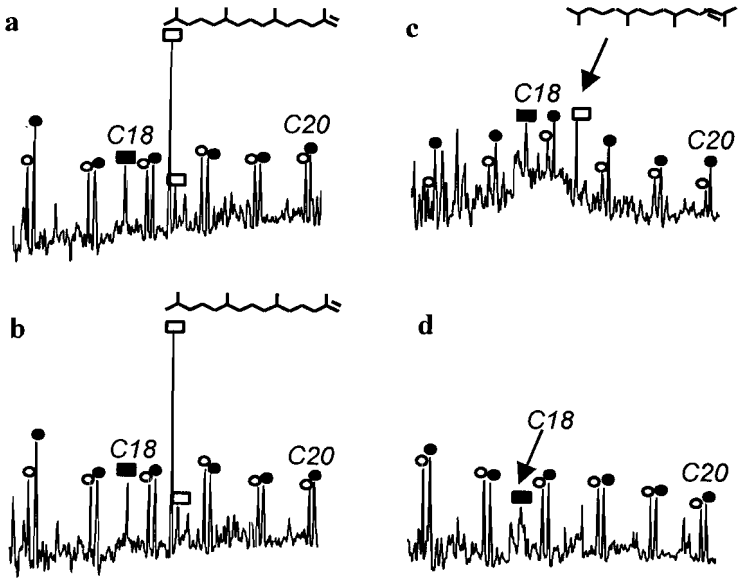

Figure 4.5 Partial FID trace of the Monterey pyrolysate (Curie temperature 610 °C) of (**a**) the isolated kerogen, (**b**) the residue R_1 after alkaline hydrolysis, (**c**) the residue R_2 after ether-bond cleavage, (**d**) the residue R_3 after desulfurization. Filled and open circles indicate the homologous series of *n*-alkanes and *n*-alk-1-enes, respectively. Their number of carbon atoms is indicated with italic numbers. Filled and open squares indicate pseudo homologous series of isoprenoid alkanes and alk-1-enes, respectively.

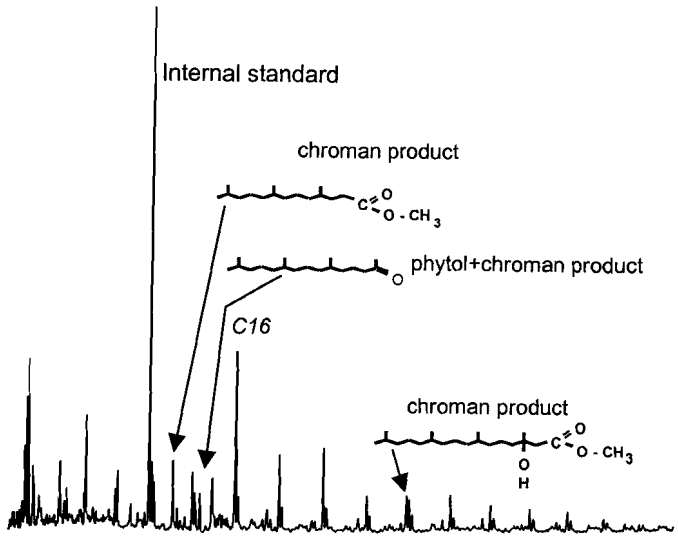

Figure 4.6 FID trace of the extract released upon RuO_4 oxidation of a Monterey kerogen (KG-2). Stars indicate linear monocarboxylic acids. Triangles indicate linear dicarboxylic acids. Their number of carbon atoms is indicated with italic numbers.

As described above, HI/$LiAlH_4$ treatment resulted in the disappearance of the O-bound precursor of prist-1-ene from the residue pyrolysate. However, an unknown precursor was still present because prist-2-ene was generated upon pyrolysis, since clay minerals were no longer present, one might expect primarily prist-1-ene rather than the observed prist-2-ene. The same phenomena were observed in samples from the Vena del Gesso (Gelin *et al.*, personal communication) and the Green River Formation (Koopmans *et al.*, 1999), large amounts of prist-2-ene compared to prist-1-ene occurred in the pyrolysate of the residue after HI treatment of the kerogen. A likely explanation for this phenomenon is that an isomerization reaction takes place *via* the transfer of protons originating from incompletely removed HI, thereby generating prist-2-ene. A similar observation was made upon isolation of the Mulhouse kerogen with HCl/HF, where transfer of protons from incompletely removed acid probably caused a relatively low 1P/(1P+2P) ratio (Tables 4.1-4.2). This latter isomerization effect is probably smaller compared to the isomerization effect due to HI treatment, since HI is a much stronger acid than HCl and HF and may be more difficult to remove. After desulphurization of the kerogen with Ni_2B no compounds with a pristane carbon skeleton were observed in the pyrolysate (Fig. 4.5d). This indicates that the unknown precursor was probably removed and may have been bound by S- or S- and O-linkages.

The chemical degradation experiments in this study therefore indicate the presence of at least two different pristene precursors in sulfur-rich kerogens, an ether-bound precursor (probably tocopherol) and an unknown sulfur- or ether- and sulfur-bound precursor. However, in S-poor kerogens, tocopherols may be the predominant precursors. This is supported by the fact that the Pristane Formation Index, based upon the release of pristane from kerogen-bound tocopherols, seems to work with most kerogens (Goossens *et al.,* 1988).

4.5 Conclusions

1) The double bond isomerization of prist-1-ene to form prist-2-ene during pyrolysis depends on the amount of protons available for the formation of the intermediate carbonium ion which can originate from untreated aluminosilicates (e.g. montmorillonite, kaolinite), the acid used in decarbonation (HCl), or degradation (HI).
2) The extent of isomerization depends on the amount of clay minerals versus TOC and whether the clay minerals are activated by a proton donor (e.g. HCl).
3) The clay minerals that can act as isomerization catalysts are primarily montmorillonite and to a lesser extent kaolinite.
4) At least two precursors in the sulfur-rich kerogens investigated that can generate pristenes during pyrolysis: an ether-bound precursor, probably tocopherols, and an unknown sulfur-bound precursor. In other (sulfur-poor) kerogens, tocopherols are probably the only precursors for pristenes.

4.6 Acknowledgements

Dr. W. Pool is thanked for technical assistance and M. Dekker is acknowledged for performing GC-MS analyses. This study was supported by a PIONIER grant to JSSD from the Netherland Organization for Scientific Research (NWO). This is NIOZ Contribution 3388.

CHAPTER 5

Evidence for sequestered non-aromatic carotenoids in kerogens

Ingeborg M. Höld, Stefan Schouten, Walter A. Hartgers and Jaap S. Sinninghe Damsté

5.1 Abstract

In this study several compounds possessing a 1,1,3,-trimethylcyclohexyl moiety (**I-IX**) were tentatively identified in flash pyrolysates of kerogens (e.g. the Green River, the Monterey Formation). The same products were found in the flash pyrolysate of the sodium salt of retinoic acid (**X**), a compound thought to mimic the pyrolysis behaviour of kerogen-bound carotenoids. This indicates that non-aromatic cyclic carotenoids such as β-carotene are present in sedimentary macromolecular aggregates. Selective chemical degradation was performed on two kerogens. The results suggest that ether-bound non-aromatic cyclic carotenoids possessing a 1,1,3-trimethylcyclohex-2-ene moiety are present in these kerogens and are probably the precursors of these compounds. Relatively high amounts of specific methylated benzenes (*e.g.* 1,2,3-trimethylbenzene) were also identified in these kerogen pyrolysates. Possibly these compounds are derived from aromatised products of non-aromatic cyclic carotenoids as formed during diagenesis.

5.2 Introduction

Carotenoids are widely distributed in nature since they are biosynthesized by almost all photosynthetic organisms (e.g. algae, photosynthetic bacteria, higher plants; Ratledge and Wilkinson, 1988). Several intact carotenoids have been identified in ancient sediments (e.g. Keely et al., 1995; Sinninghe Damsté and Koopmans, 1997, and references therein). However, these findings have been regarded as exceptions, since carotenoids are considered to have a low survival potential due to the presence of multiple double bonds, which would make them prone to diagenetic reactions (Brassell, 1993). Recently, however, it has become clear that the potential for preservation of carotenoid skeletons is actually larger than anticipated. It has been well documented that naturally occurring carotenoids can be stabilized through cyclization and aromatization reactions upon diagenesis (*e.g.* Koopmans *et al.*, 1996). Furthermore, under certain circumstances the conjugated double bonds can actually enhance the survival potential of carotenoid skeletons in the geosphere by facilitating the formation of intermolecular linkages and

thus incorporation in macromolecular aggregates (Sinninghe Damsté and Koopmans, 1997).

Specific examples of this phenomenon are diaromatic carotenoids derived from photosynthetic green sulfur bacteria. It was shown that the occurrence of substantial amounts of 1,2,3,4-tetramethylbenzene and 2-ethyl-1,3,4-trimethylbenzene in kerogen pyrolysates is indicative for a significant contribution of diaromatic carotenoids to the kerogen (e.g. Hartgers et al., 1994a). However, there are only few indications that non-aromatic carotenoids may be sequestered in kerogens. Hartgers *et al.* (1994b) reported a relatively high abundance of 1,2,3-trimethylbenzene in several kerogen pyrolysates and proposed this to be indicative of the presence of bound non-aromatic carotenoids [*e.g.* β-carotene (**XI**)], which have undergone aromatization either upon pyrolysis or during diagenesis. However, it remains unclear if this compound is indeed derived from pyrolysis of bound non-aromatic carotenoids and how these carotenoids are bound in kerogens.

In this study we report the presence of specific pyrolysis products exclusively derived from non-aromatic cyclic carotenoids possessing a 1,1,3-trimethyl-2-alkylcyclohex-2-ene moiety in a number of kerogens. In addition, selective chemical degradation was performed on two kerogens (Green River, Monterey) in order to investigate the mode of binding of non-aromatic cyclic carotenoids in these macromolecular aggregates.

5.3 Experimental

Samples

A sediment sample (KG-1) was taken from a fresh outcrop of the middle Miocene carbonaceous marls of the Monterey Formation at Naples Beach (USA; Isaacs et al., 1992). The sample has a TOC content of 9.6 wt.%. Elemental analysis of the isolated kerogen indicated that it is an immature Type II-S kerogen with an atomic H/C ratio of 1.27, an atomic O/C ratio of 0.15, and an atomic S_{org}/C ratio of 0.05. An organic matter-rich (15.2 wt.% TOC) dolomitic marlstone from the Green River Formation (USA, Late Eocene) was used in this study. Elemental analysis of the isolated kerogen indicated it was an immature (R_0 = 0.44%) Type I kerogen. Descriptions of the other samples (Table 5.1) can be found in Hartgers et al. (1994b).

Table 5.1 Retention indices and presence of **I-IX** in a number of kerogen pyrolysates.

	(I)	**(II)**	**(III)**	**(IV)**	**(V)**	**(VI)**	**(VII)**	**(VIII)**	**(IX)**
MW	122	122	124	136	136	138	174	172	176
Retention Index (RI)	820	831	849	971	974	978	1322	1317	1383
Presence in kerogen pyrolysates									
Monterey (TEMO25)	√	√	√	√	√	√	√	√	n.d
Monterey (KG-1)	√	√	√	√	√	√	√	n.d	√
Green River	√	√	√	-	√	√	√	√	-
Jurf et Darwish	n.d	n.d	n.d	√	√	n.d	n.d	n.d	n.d
Peru Margin	√	√	√	√	√	√	√	√	n.d
Georgina Basin	n.d	n.d	n.d	-	√	n.d	n.d	n.d	n.d
Vena del Gesso	√	√	-	-	√	-	-	-	n.d
Mulhouse Basin	n.d	n.d	n.d	-	-	n.d	n.d	n.d	n.d
Posidonian Shale	n.d	n.d	n.d	-	-	n.d	n.d	n.d	n.d
Paris Basin	n.d	n.d	n.d	-	-	n.d	n.d	n.d	n.d
Vocontian Basin	n.d	n.d	n.d	-	-	n.d	n.d	n.d	n.d
Walcott Chuar Group	n.d	n.d	n.d	-	-	n.d	n.d	n.d	n.d

√=present, n.d.= not determined, - not detected

Extraction and kerogen isolation

The powdered samples were Soxhlet extracted with dichloromethane/methanol (DCM/MeOH; 7.5:1, v/v) for 32 h. Carbonates were removed by treatment with 4N HCl at room temperature and ultrasonically extracted with water (3x), MeOH (3x) and finally DCM (3x). Kerogen isolation was performed by HCl/HF treatments of the solvent-extracted sediment (Eglinton, 1988). The isolated kerogen was ultrasonically extracted with MeOH, DCM/MeOH (1:1) and DCM.

Sequential chemical degradation

The different sequential chemical degradation steps (alkaline hydrolysis, ether-bond cleavage) were performed as described by Höld et al. (1998). After every chemical degradation step the residue was washed three times with H_2O/MeOH (1:1, v/v), three times with MeOH and three times with ethyl acetate. The residue was dried under nitrogen.

Gas chromatography (GC), gas chromatography-mass spectrometry (GC-MS), flash pyrolysis-gas chromatography (Py-GC) and flash pyrolysis-GC-mass spectrometry (Py-GC-MS)

GC, GC-MS, Py-GC and Py-GC-MS were carried out as described previously (Höld et al., 1998).

5.4 Results and discussion

Cyclohexenes and related products

In a number of kerogens pyrolysates products are encountered with structures that suggest that they may be derived from non-aromatic cyclic carotenoids. Specifically, 1,1,3-trimethylcyclohexadienes (**I-II**), 1,1,3-trimethylcyclohex-2-ene (**III**), smaller amounts of its pseudohomologues 1,1,2,3-tetramethylcyclohexadiene (**IV-V**), 1,1,2,3-tetramethylcyclohex-2-ene (**VI**), and ionene (**VII**) and related compounds **VIII** and **IX**, identified based on comparison of mass spectral data with that of the literature, were identified as significant components in numbers of kerogen pyrolysates (Fig. 5.1, Table 5.1). Compounds **I-VI** can be generated upon α- and β-cleavage of macromolecularly-bound partially hydrogenated β-carotene. Ionene (**VII**), previously identified in the aromatic hydrocarbon fraction from a Green River shale sediment (Koopmans et al., 1997) and upon thermal degradation of β-carotene (Day and Erdman, 1963), and compound **VIII** and **IX** may be generated *via* cleavage followed by cyclization and aromatization (Fig. 5.2). Interestingly, several of these compounds (**III, VI, VII**) are also the main constituents in the flash pyrolysate of the sodium salt of retinoic acid (**X,** Fig

5.3). The pyrolysis of sodium salts of specific organic compounds are thought to reflect the pyrolysis behaviour of such moieties when bound in macromolecular material (Hartgers et al., 1995). Retinoic acid (**X**) and β-carotene (**XI**) have similar chemical structures with respect to conjugated double bonds and the cyclohexyl ring. This is a strong indication that macromolecularly-bound, partially hydrogenated β-carotene is the precursor of the pyrolysis products **I-IX** and thus present in the studied kerogens.

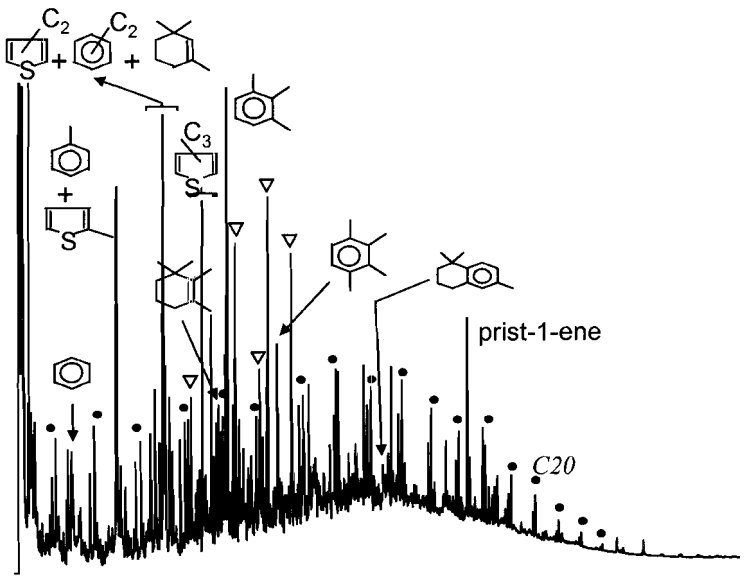

Figure 5.1 Total Ion Current (TIC) traces of the flash pyrolysates (Curie temperature 610 °C) of the kerogen of the Monterey Formation (TEMO25). Closed circles indicate the homologous series of *n*-alkanes and *n*-alk-1-enes, with the number of carbon atoms indicated. Open triangles indicate alkylpyrroles.

Alkylbenzenes

Hartgers et al. (1994b) proposed that a relatively high abundance of 1,2,3-trimethylbenzene and 1,3-/1,4-dimethylbenzene in kerogen pyrolysates indicates the presence of non-aromatic carotenoids such as β-carotene. Indeed, the alkylbenzene distribution patterns of the pyrolysates of the kerogens containing relatively high amounts of cyclohexenes (Monterey and Green River) have relatively abundant 1,2,3-trimethylbenzene and 1,3-/1,4-dimethyl benzene (Fig. 5.4). There are two distinct possibilities for the formation of the benzene isomers from macromolecularly-bound β-carotene derivatives.

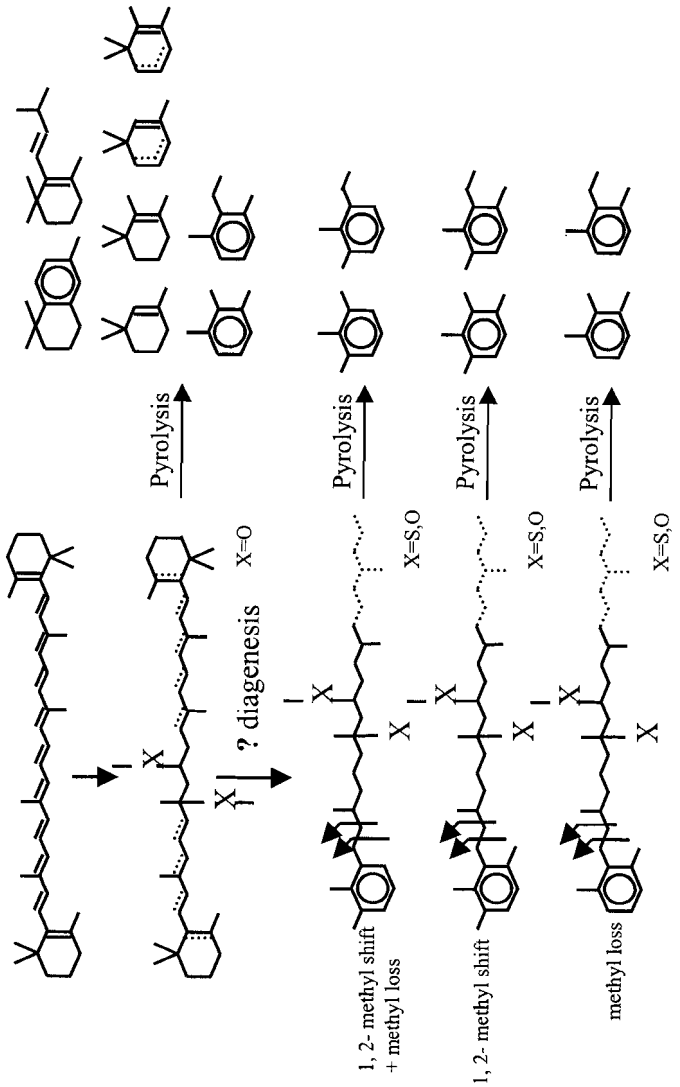

Figure 5.2 Diagenetic pathway of β-carotene and the reaction mechanisms that take place during pyrolysis of its incorparated derivatives.

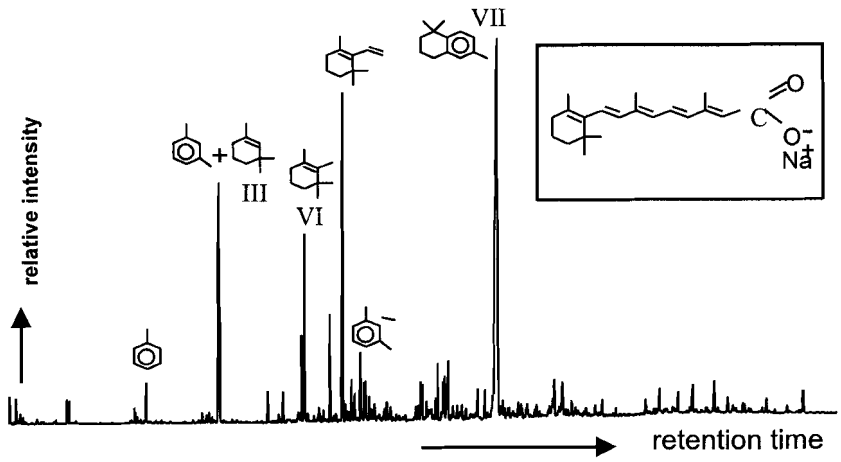

Figure 5.3 FID trace of the flash pyrolysates (Curie temperature 610 °C) of sodium salt of retinoic acid.

Firstly, the specific alkylbenzenes may be formed from kerogen-bound partially hydrogenated β-carotene. Pyrolysis of, for example, macromolecularly bound β-carotene (**X**) may yield 1,2,3-trimethylbenzene (Fig. 5.2). However, 1,2,3-trimethylbenzene is only a minor product (relative to the cyclohexenes) in the flash pyrolysate of the sodium salt of retenoic acid, which indicates that this aromatisation process is not so important (Fig. 5.3).

Alternatively, upon diagenesis, macromolecularly bound β-carotene aromatizes and undergoes a rearrangement of methyl groups involving elimination of one methyl group and/or a 1,2-shift of a geminal methyl group, yielding macromolecularly bound alkyl-dimethyl and/or alkyl-trimethyl substituted aromatic moieties (Fig. 5.2; cf. Koopmans et al., 1997; Sinninghe Damsté et al. 1997). Analysis of the C_4 and C_5 alkylated benzene clusters in the kerogen pyrolysate provides a tool to discriminate between three different resulting substitution patterns of the formed aromatic moiety (cf. Hartgers et al., 1994b). Pyrolysis of the kerogen-bound 1,2-dimethyl-3-alkylbenzene and 1,3-dimethyl-2-alkylbenzene moieties will yield, upon β-cleavage, 1,2,3-trimethylbenzene, and upon γ-cleavage, 1,2-dimethyl-3-ethylbenzene or 1,3-dimethyl-2-

ethylbenzene, respectively (Fig. 5.2). Pyrolysis of the kerogen-bound 1,2,4-trimethyl-3-alkylbenzene moiety will yield, upon β-cleavage, 1,2,3,4-tetramethylbenzene, and upon γ-cleavage, 1,2,4-trimethyl-3-ethylbenzene (Fig. 5.2). The predominant dimethylethylbenzene in the Monterey and Green River kerogen pyrolysates is 1,3-dimethyl-2-ethylbenzene (Fig. 5.4). Since 1,2-dimethyl-3-ethylbenzene and 1,2,4-trimethyl-3-alkylbenzene are not abundantly present in these pyrolysates (Hartgers et al., 1994), the 1,2-methyl shift during diagenesis does not seem to take place on a large scale in the Monterey and Green River kerogens.

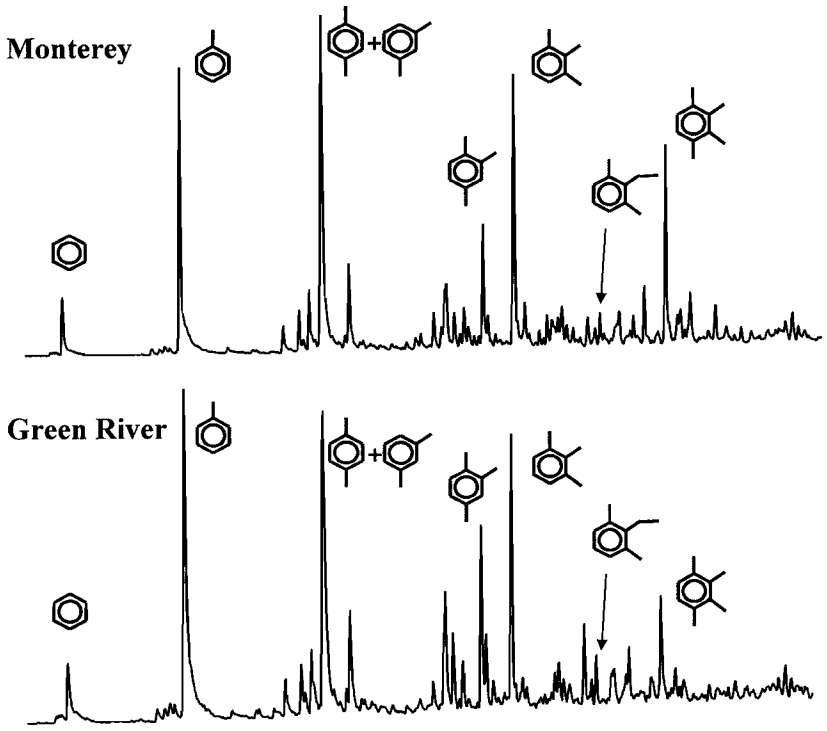

Figure 5.4 Mass chromatogram of the alkylbenzenes (*m/z 78+91+92+105+106+119+ 120+133+134)* of (**a**) the Monterey kerogen and (**b**) the Green River kerogen.

Mode of binding

In order to establish the mode of binding of the non-aromatic carotenoids, chemical degradation was performed on the Monterey and Green River kerogens. Compounds **I-VIII** are still present after base hydrolysis, but have completely disappeared from

pyrolysates of both kerogens after subsequent ether-bond cleavage, using $HI/LiAlH_4$. Furthermore, 1,3-/1,4-dimethylbenzene, 1,2,3-trimethylbenzene, 1,3-dimethyl-2-ethylbenzene and 1,2,3,4-teramethylbenzene are less predominant in the residue pyrolysates of both kerogens. This indicates that part of their precursors, i.e. β-carotenes and their aromatised diagenetic products, occur ether-bound in the kerogen. As was mentioned in the introduction, the polyene system of carotenoids has been shown to be prone to reactions leading to sequestration, specifically natural vulcanisation. However, this polyene system makes it also relatively easy to oxidize carotenoids via radical reactions (in fact, one of the biological functions of carotenoids is the scavenging of radicals). Possibly, upon the presence of a sufficiently high oxygen concentration in the water column or the sediment, oxidation of β-carotenes may result in the formation of ether-bonds which crosslink the molecules to form macromolecular aggregates. Indeed, Jenisch et al. (1999) recently noted a similar phenomenon for other lipids like fatty acids.

Interestingly, there is no indication for the presence of a sulfur bound precursor of these polymethylated cyclohexenes since all their precursors were removed from the pyrolysate after ether-bond cleavage. A possible explanation for this phenomenon could be that acid (HI) used for ether-bond cleavage was not completely removed from the residue (Höld *et al.*, 1999), resulting in an increase of double bound migration and/or shifting of methyl groups. This would yield different products upon pyrolysis such as enhanced formation of trimethylated benzenes. Another explanation may be that non-aromatic carotenoids bound by sulfur give, upon pyrolysis, different pyrolysis products (alkylbenzenes vs. cyclohexenes) compared to those bound by oxygen, although this seems highly unlikely.

5.5 Conclusions

Our results show that kerogens may contain ether–bound partially hydrogenated β-carotene. These moieties are probably the precursors of a number of specific methylated cyclohexenes and cyclohexadienes (**I-VIII**). Possibly, diagenetic products of these contain ether–bound non-aromatic cyclic carotenoids are the precursors of a number of methylated benzenes (1,2,3-trimethylbenzene and 1,3-dimethyl-2-ethylbenzene) in kerogen pyrolysates. This indicates that during early diagenesis β-carotene can react with oxygen to form ether bound moieties (Fig. 5.2), which can escape microbial degradation. In this way carotenoids, once thought to be very labile compounds not able to survive early diagenesis, may be preserved over millions of years in macromolecular aggregates such as kerogens.

5.6 Acknowledgements

Dr. C.M. Isaacs is thanked for provision of the Monterey KG-1 sample. Dr. W. Pool is thanked for technical assistance and M. Dekker is acknowledged for performing GC-MS analyses. This study was supported by a PIONIER grant to JSSD from the Netherlands Organization for Scientific Research (NWO). This is NIOZ Contribution no. 3413.

Appendix

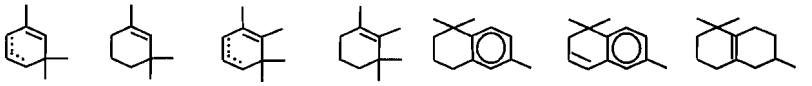

(I-II) (III) (IV-V) (VI) (VII) (VIII) (IX)

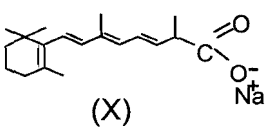

(X)

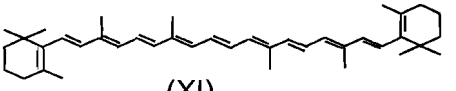

(XI)

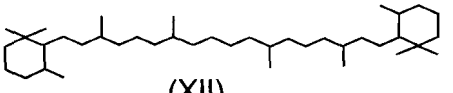

(XII)

CHAPTER 6

Origin of free and bound mid-chain methyl alkanes in oils, bitumens and kerogens of the marine, Infracambrian Huqf Formation (Oman)

Ingeborg M. Höld, Stefan Schouten, Joyce Jellema and Jaap S. Sinninghe Damsté

6.1 Abstract

The Huqf oil from Oman and other time-equivalent oils are characterized by relatively large contents of mid-chain branched monomethyl alkanes. The Huqf oil, the saturated hydrocarbon fractions, the desulfurized polar fractions of the bitumens and the kerogen pyrolysates of three potential source rocks from the Huqf Formation (Oman) were analyzed in order to resolve the origin of these mid-chain branched monomethyl alkanes. Using off-line pyrolysis and chemical degradation in combination with compound specific carbon isotope analysis, it was assessed that the mid-chain branched monomethyl alkanes are not rearrangement products but are derived from a biological source, probably from lipids with C_{28+} carbon skeletons and methyl branching at the 12- or 13-position. These compounds were incorporated in the kerogen through reactions of sulfur with functional groups at different positions in the precursor lipid(s).

6.2 Introduction

Mid-chain branched monomethyl alkanes have been reported in sediments and crude oils ranging in age from modern to Precambrian (e.g. Hoering, 1976; Hoering, 1981; de Leeuw et al., 1985; Jackson et al., 1986; Klomp, 1986; Fowler and Douglas, 1987; Summons, 1987; Summons et al., 1988a; Summons et al., 1988b; Grantham et al., 1988; Robinson and Eglinton, 1990; Shiea et al., 1990; McKirdy and Imbuss, 1992; Kenig et al., 1995). Several origins have been suggested for monomethyl alkanes present in oils and sediments (e.g. Shiea et al., 1990). (i) Direct biological contributions (Makushina et al., 1978; Fowler and Douglas, 1987). (ii) Diagenetic products formed by the transformation of functionalized lipid precursors such as carboxylic acids (Summons, 1987; Summons et al., 1988b; Thiel et al., 1999). Mid-chain methylation of *n*-alkyl lipids may have been a strategy for controlling the membrane fluidity of organisms before the development of an oxic biosphere and the evolution of the now dominant oxygen-dependent desaturation pathways in the biosynthesis of fluidity regulating membrane lipids (Dowling et al., 1986; Summons, 1987). This may explain why mid-chain branched monomethyl alkanes occur

predominantly in Proterozoic and early Paleozoic rocks and oils. (iii) Products produced from a limited range of isomers upon long-term equilibration (Hoering, 1981; Klomp, 1986), or (iv) products of the acid-catalyzed (e.g. clays) thermal cracking of alkenes (Kissin, 1986).

The "Huqf oils" from Oman have been associated with the Infracambrian Huqf source rocks (Grantham et al., 1988) and contain relatively large amounts of mid-chain branched monomethyl alkanes ('X' compounds; Klomp, 1986). The oils are characterized by the following properties: (i) sulfur rich, (ii) pristane/phytane ratios <1.0, (iii) a strong predominance of C_{29} steranes, (iv) a relatively low content of rearranged steranes and (v) relatively light stable carbon isotope values of ca. -36‰ (Grantham, 1986 and 1988). The same geochemical features are encountered in a tar from a well in Pakistan (Grantham et al., 1988), in oils from the Eastern Siberian Platform (Fowler and Douglas, 1987; Summons and Powell, 1992), the East European Platform (Bazhenova and Arefiev, 1998) and in oils from India (Peters et al., 1995), all from the same age-period. The Pakistan and South Oman salt basin were in close proximity, and were possibly continuous, during the Infra-Cambrian (Gorin et al., 1982). The highly negative stable carbon isotope values in these samples are among the most negative values known for crude oils. Sharkey and Berry (1985) hypothesized that the negative carbon isotope values in Precambrian stromatolites and kerogens may be related to the fact that the active transport system for dissolved inorganic carbon (DIC), which results in less discrimination against ^{13}C, had not evolved at that time. Alternatively, it has been hypothesized that during the Cambrian elevated atmospheric CO_2 levels resulted in higher fractionation during photosynthesis (Summons and Powell, 1992). From the above it is clear that the origin of the mid-chain branched alkanes and the cause of the low ^{13}C values are still matters of debate. In an attempt to unravel the origin of the mid-chain methyl alkanes, three Huqf source rocks were analyzed for the presence of free and sulfur-bound biomarkers. Furthermore, the Huqf oil, the bitumen and the pyrolysis products of the three kerogens as well as stable carbon isotopic compositions of individual compounds were studied.

6.3 Experimental

Samples

The Huqf Group is the oldest known sedimentary sequence overlying crystalline basement in the Sultanate of Oman (Gorin et al., 1982) and is subdivided into five formations corresponding to an alternation of clastic (Abu Mahara and Shuram Formations) and carbonate rocks (Khufai and Buah Formations) deposited in essentially shallow marine to supratidal (or fluviatile) environments and terminated by an evaporatic sequence (Ara Formation; Gorin et al., 1982). Regional correlations suggest that the predominantly carbonate-evaporatic facies of the Huqf Group was widely distributed in late Precambrian-Early Cambrian time. The Huqf basin is

tentatively considered part of a belt of evaporitic basins and intervening carbonate platforms, which stretched across the Indian subcontinent through South Yemen, Oman and Saudi Arabia into the gulf states and Iran (Gorin et al., 1982). The distribution of the oil accumulations above the dissolution edge of the Ara salt is a prime indication that the hydrocarbons originate from beneath or within the salt (Aley and Nash, 1984). Good source rocks for oil occur in South Oman in several formations of the Huqf group. The three investigated representative rock samples (Huqf-1, Huqf-2 and Huqf-3; Table 6.1) originate from the Huqf Group and were supplied by Shell International Petroleum Maatschappij B.V.

Table 6.1: Geochemical background and stable carbon isotopic compositions.

Sample	Location	Age	Type	TOC[a] (%)	TOC[b] (%)	$\delta^{13}C^{c}$ (‰)	$\delta^{13}C^{d}$ (‰)	Py yield (%)
Huqf-1	Huqf Group, Oman	Infracambrian	decalc. sed.	6.3	6.9	-37.7	-38.1	17
Huqf-2	Huqf Group, Oman	Infracambrian	decalc. sed.	1.0	1.2	-38.1	-37.7	17
Huqf-3	Huqf Group, Oman	Infracambrian	decalc. sed.	1.8	2.1	-37.1	-37.2	14

[a] Total Organic Carbon (TOC) of the extracted sediment
[b] TOC of the decalcified and extracted sediment
[c] Isotopic composition of the decalcified and extracted sediment
[d] Isotopic composition of the residue after off-line pyrolysis

Extraction and separation.

A Huqf crude oil was fractionated into a saturated hydrocarbon, an aromatic hydrocarbon-I, an aromatic hydrocarbon-II and a polar fraction by column chromatography as previously described (Sinninghe Damsté et al., 1994). The first three fractions were analyzed by gas chromatography (GC), gas chromatography-mass spectrometry (GC-MS) and Isotope ratio monitoring-GC/C/MS (irm-GC/C/MS). The polar fraction was desulfurized and subsequently analyzed by GC and GC-MS.

The powdered rocks were Soxhlet extracted, the asphaltenes were removed from the bitumen and the residual maltene fractions were then separated into apolar and polar fractions by column chromatography as described previously (Schouten et al., 1999). The apolar fraction was separated by argentious thin layer chromatography (TLC) into four fractions (van Kaam-Peters et al., 1995). All four fractions (A1 - A4) were analyzed by GC, GC-MS and irm-GC/C/MS. The relative amounts of the fractions obtained are listed in Table 6.2.

Desulfurization

Aliquots of the polar and the asphaltene fractions of the oil were desulfurized using Raney Ni as described previously (Sinninghe Damsté et al., 1994). Aliquots of the polar and the asphaltene fractions of the sediment extracts were desulfurized using Raney Ni and Nickel boride, respectively. Before desulfurization an internal standard [2,3-dimethyl-5-(1,1-dideuterohexadecyl)thiophene] was added to both the polar and the asphaltene fractions. Ca. 15 mg of each polar fraction was desulfurized and subsequently

hydrogenated as described elsewhere (Sinninghe Damsté et al., 1990). The apolar fractions were analyzed using GC and GC-MS. In case of desulfurization with Ni_2B (Schouten et al., 1993), 0.6 g $NaBH_4$ and 0.6 g $NiCl_2$ were added to ca. 10 mg asphaltenes dissolved in 11 ml of a tetrahydrofuran:MeOH mixture (1:1, v/v). After 1.5 h of refluxing under a nitrogen blanket, the desulfurization products were obtained in a similar manner as with the Raney Ni procedure. The relative amounts of the fractions obtained are listed in Table 6.2.

Table 6.2: Yields of bitumen fractions for the three rocks.

	Huqf-1	Huqf-2	Huqf-3
asphaltenes (%[a])	25	6	26
maltenes (%[a])	72	89	66
Desulfurized asphaltenes (%[a])	1.2	1.0	0.8
fraction A1 (%[b])	7.2	26	0.5
fraction A2 (%[b])	7.2	11	2
fraction A3 (%[b])	3.3	6.7	0.4
fraction A4 (%[b])	3.3	4.7	1.3
polar fraction (%[b])	21	30	47
Desulfurized polars (%[b])	4.9	10.3	10.4

[a] percentage of the total extract [b] percentage of the maltenes

Decalcification and kerogen isolation

The residue after extraction was decalcified by treatment with 4N HCl at room temperature and ultrasonically reextracted with water (3x), methanol (3x) and finally dichloromethane (3x). Kerogen isolation was performed by HCl/HF treatments of the solvent-extracted rock as described previously (Eglinton, 1988). The kerogen was subsequently ultrasonically extracted with methanol and DCM.

Off-line pyrolysis and separation of pyrolysis products

Decarbonated rocks or isolated kerogens were off-line pyrolysed in an oven at 400°C for 1 h under a nitrogen flow. The pyrolysis products were collected in two traps filled with hexane/dichloromethane (7/1, v/v). The second trap was cooled with acetone/CO_2(s). The pyrolysis products of the two traps were combined to yield the total pyrolysate which was separated, as described previously (Höld et al., 1998a), into a polar, an aromatic, a saturated and an unsaturated hydrocarbon fraction. The latter was subsequently hydrogenated. The pyrolysis yields were determined from the TOC values and the weight of the samples before and after pyrolysis. The aromatic, the saturated and the hydrogenated unsaturated hydrocarbon fractions were analyzed by GC, GC-MS and irm-GC-MS.

Sequential chemical degradation of the Huqf-2 kerogen

The different sequential chemical degradation steps are schematically depicted in Fig. 6.1. After each chemical degradation step the residue was washed three times with H_2O/MeOH (1:1, v/v), three times with MeOH and three times with ethyl acetate. The residue was dried under nitrogen. Base hydrolysis, ether- and sulfur-bond cleavage was performed subsequently as described previously (Höld et al., 1998b) and residues R_1, R_2 and R_3 were obtained, respectively.

Gas chromatography (GC)

GC analysis was performed using a Carlo Erba 5300 HRGC, a HP6890 or a HP5890 instrument, all equipped with on-column injectors. A fused silica capillary column (25 m x 0.32 mm) coated with CP Sil-5 (film thickness 0.12 μm) was used with Helium as carrier gas. Compounds analyzed on the Carlo Erba 5300 HRGC and HP 6890 were detected by a flame ionization detector (FID). Compounds analyzed on the HP 5890 were detected simultaneously by FID and sulfur-selective flame photometric detectors (FPD), using a stream-splitter at the end of the column (split ratio FID:FPD=1:2). The extracts (dissolved in hexane or ethylacetate) were injected at 70°C and the oven was programmed to 130°C at 20°/min and subsequently at 4°/min to 320°C where it was held for 20 min. The off-line pyrolysis products (in hexane) were injected at 35°C. After 5 minutes at 35°C, the oven was heated to 310°C at 4°C/min and was held at 310°C for 10 min.

Gas chromatography-mass spectrometry (GC-MS)

GC-MS was carried out on a HP5890 gas chromatograph connected to a VG-Autospec Ultima mass spectrometer operated at 70 eV with a mass range *m/z* 40-800 and a cycle time of 1.8 s (resolution 1000). The gas chromatograph was equipped with a fused silica capillary column (25 m x 0.32 mm) coated with CP Sil-5 (film thickness 0.12 μm) using helium as carrier gas. The extracts were injected at 60°C and subsequently the oven was programmed to 130°C at 20°/min and at 4°/min to 320°C where it was held for 20 min. The off-line pyrolysis products were injected at 35°C. After 5 minutes at 35°C, the oven was heated to 310°C at 4°C/min and held at 310°C for 10 minutes.

Flash pyrolysis-gas chromatography (Py-GC), flash pyrolysis-GC-mass spectrometry (Py-GC-MS) and irm-GC-MS.

Py-GC, Py-GC-MS and irm-GC-MS were carried out as described previously (Höld et al., 1998a).

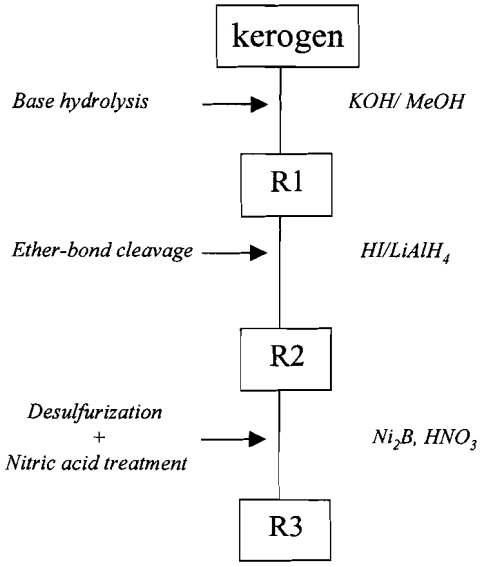

Figure 6.1 Analytical flow diagram

Quantification

Several compounds were quantified by using an internal standard and peak areas obtained by the integration of mass chromatograms. To obtain these, integration data mass chromatograms of *m/z* 57 were used for phytane, *n*-C_{24} alkanes and mid chain-methyl C_{24} alkanes, mass chromatograms of *m/z* 191 were used for C_{30} hopanes, dinorhopane and C_{23} tricyclic terpanes and mass chromatograms of *m/z* 217 were used for C_{29} ααα steranes and pregnanes. No correction was made for the difference in the ion yields of the used fragment ions.

Bulk stable carbon isotopic analyses

TOC and stable carbon isotopic compositions for the whole rocks and kerogens were determined by automated on-line combustion (Carlo Erba CN analyzer 1502 series) followed by conventional isotope ratio-mass spectrometry (Fisons Optima; Fry et al., 1992).

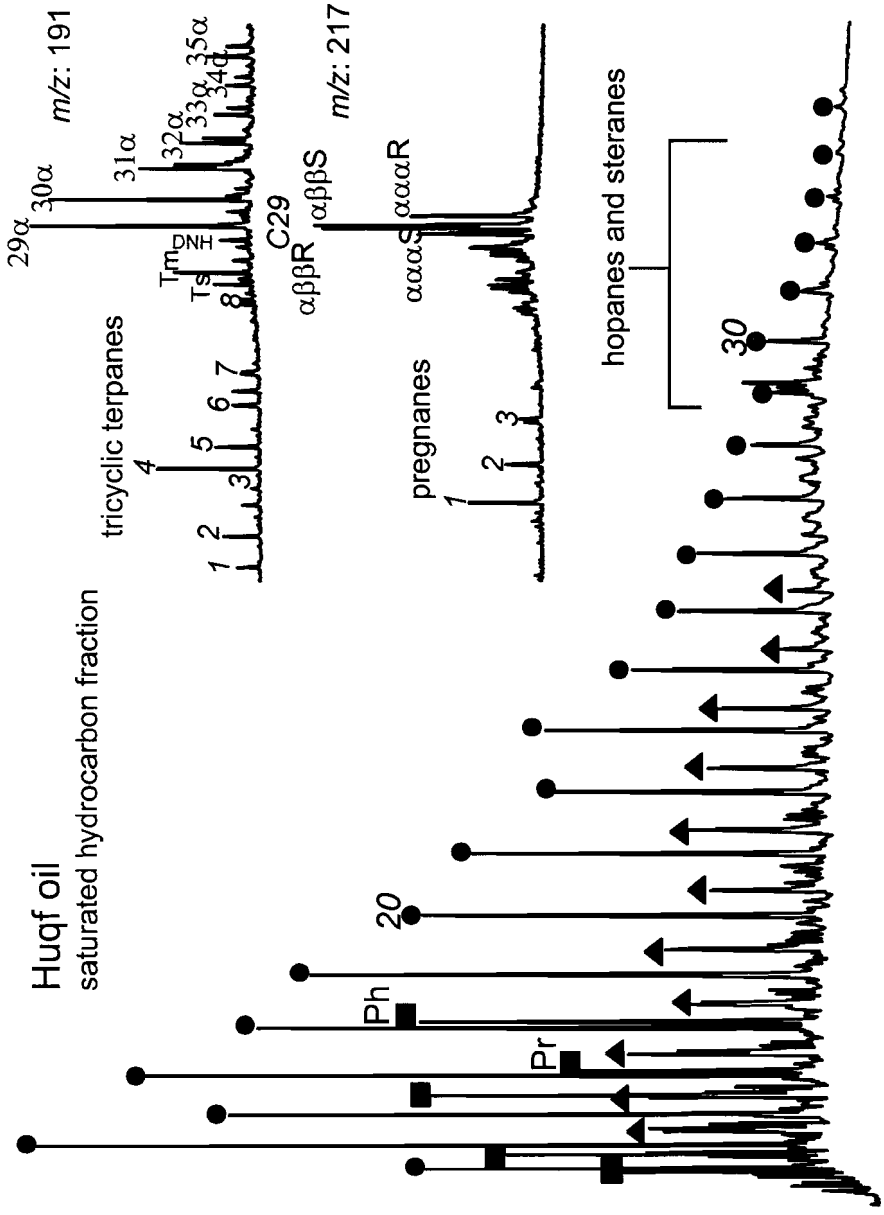

Figure 6.2 Total Ion Current (TIC) traces of the saturated hydrocarbon fraction of the Huqf oil and partial mass chromatograms of *m/z* 191 and *m/z* 217. Numbers refer to compounds listed in Tables 4 and 5. Filled circles indicate the homologous series of *n*-alkanes. Their number of carbon atoms is indicated with italic numbers. Filled squares indicate a pseudo homologous series of isoprenoid *(i-)* alkanes. Filled triangles indicate the series of mid-chain methyl alkanes (see Table 3).

Table 6.3: The major fragments in the mass spectra of the methyl alkane series

Alkanes	*m/z 42* 2-me	*m/z 56* 3-me	*m/z 70* 4-me	*m/z 84* 5-me	*m/z 98* 6-me	*m/z 112* 7-me	*m/z 126* 8-me	*m/z 140* 9-me	*m/z 154* 10-me	*m/z 168* 11-me	*m/z 182* 12-me	*m/z 196* 13-me
C_{14}	X											
C_{15}	X	X										
C_{16}		X	X									
C_{17}			X	X								
C_{18}				X	X							
C_{19}					X	X						
C_{20}						X	X					
C_{21}							X	X				
C_{22}								X	X			
C_{23}									X	X		
C_{24}										X	X	
C_{25}											X	
C_{26}											X	X
C_{27}											X	X
C_{28}											X	X

6.4 Results

Huqf crude oil

Upon separation of the Huqf oil into an asphaltene and a maltene fractions no asphaltenes were recovered. The maltene fraction was fractionated into saturated hydrocarbon, low-molecular-weight aromatic hydrocarbon fraction, high-molecular-weight aromatic hydrocarbon fraction and polar fractions (Sinninghe Damsté et al., 1994). The saturated hydrocarbon fraction (Fig. 6.2) is dominated by homologous series of *n*-alkanes (C_{14}-C_{35}), isoprenoid alkanes (C_{15}-C_{20}) and mid-chain methyl alkanes (C_{15}-C_{30}) with maxima around C_{17}. Klomp (1986) suggested that the major fragments in the mass spectra of the latter compounds, previously described as X-peaks, indicated that they were dimethyl alkanes. However, calculated Kovats indices for dimethyl alkanes (Kissin, 1986) are substantially lower than those observed for the X-peaks. Furthermore, Fowler and Douglas (1987) showed that the fragments observed in the mass spectra of these compounds can not reflect the dimethyl alkanes suggested by Klomp (1986), since the dominant fragmentation can be explained by one mid-chain methyl group. The predominant branching position of the methyl alkanes can be determined by mass spectrometry. The mass spectrum of a mid-chain methyl alkane contains a relatively high even mass fragment originating from the carbon-carbon bond cleavage adjacent to the branching position. Therefore, based on relative retention times and mass spectral data, these X-peaks represent monomethyl alkanes. The predominant branching position of the mid-chain methyl alkanes in the Huqf oil changes with carbon number (Table 6.3), in agreement with data reported by Fowler and Douglas (1987) for an Eastern Siberian oil. In addition to the acyclic compounds, *n*-alkylbenzenes (C_{14}-C_{23}), pregnanes (C_{21}-C_{23}), steranes (C_{27}-C_{29}) with a strong predominance of C_{29} steranes, tricyclic terpanes (C_{20}-C_{29}) and C_{29}-C_{35} 17α,21β(H)-hopanes were identified (Fig. 6.2; Tables 6.4 and 6.5).

GC-FID/FPD analyses indicated that the low-molecular-weight aromatic hydrocarbon fractions contain hardly any organic sulfur compounds (Sinninghe Damsté et al., 1994) and are dominated by 2-phenylalkanes and C_2-C_3 alkylated naphthalenes. Flash pyrolysis GC-FID/FPD analyses of the high-molecular-weight aromatic hydrocarbon fraction revealed only low amounts of dibenzothiophenes, alkylated derivatives of dibenzothiophenes and probably tri- and tetra-aromatic hydrocarbons (Sinninghe Damsté et al., 1994).

Flash pyrolysis GC-FID/FPD analyses of the polar fraction revealed that it is dominated by *n*-alkanes and *n*-alk-1-enes. Furthermore, homologous series of 2-alkyl-5-methylthiolanes, 2-alkyl-5-ethylthiolanes and both *cis* and *trans* 2,5-dialkylthiolanes are present. Raney Nickel desulfurization of the polar fraction yielded a small amount (7 wt. % of the polar fraction) of saturated hydrocarbons. The major hydrocarbons are *n*-alkanes (C_{15}-C_{42}), phytane, mid-chain methyl alkanes (C_{16}-C_{30}) and *n*-alkylcyclohexanes (Sinninghe Damsté et al., 1994).

Table 6.4. Triterpanes and hopanes identified in the Huqf oil, the saturated hydrocarbon fraction and desulfurized polar fraction of the bitumens and in the kerogen pyrolysates

peak[a]	component
1	C_{20} 13β, 14α(H) tricyclic terpane
2	C_{21} 13β, 14α(H) tricyclic terpane
3	C_{22} 13β, 14α(H) tricyclic terpane
4	C_{23} 13β, 14α(H) tricyclic terpane
5	C_{24} 13β, 14α(H) tricyclic terpane
6	C_{25} 13β, 14α(H) tricyclic terpane
7	C_{26} 13β, 14α(H) tricyclic terpane
8	C_{28} 13β, 14α(H) tricyclic terpane
T_s	18α -22,29,30-trisnorhopane
T_m	17α -22,29,30-trisnorhopane
29α	17α, 21β(H) norhopane
30α	17α, 21β(H) hopane
31α	17α, 21β(H) homohopane 22S and R
32α	17α, 21β(H) bishomohopane 22S and R
33α	17α, 21β(H) trishomohopane 22S and R
34α	17α, 21β(H) tetrahomohopane 22S and R
35α	17α, 21β(H) pentahomohopane 22S and R

[a]numbers refer to Figs. 2,3,4 and 7 (m/z 191 chromatogram)

Aliphatic hydrocarbon fractions of rock bitumens

All aliphatic hydrocarbon fractions of the rock bitumens contain series of *n*-alkanes (C_{15}-C_{36}), mid-chain methyl alkanes ranging from C_{16} to C_{33}, acyclic isoprenoid hydrocarbons (C_{18}-C_{21} and C_{23}), alkylcyclohexanes (C_{15}-C_{27}), steranes (C_{21}-C_{29}) dominated by C_{29} steranes, tricyclic terpanes (C_{20}-C_{29}) and C_{29}-C_{35} 17α,21ß(H)-hopanes (Fig. 6.3; Tables 6.4, 6.5 and 6.6). The hopane distributions are characterised by the predominance of the C_{29} 17α,21ß(H)-norhopane over the C_{30} 17α,21ß(H)-hopane. All three rock samples are thermally mature as shown by the the 22S/(22S + 22R) C_{32} bishomohopane ratio of 0.57 and 20S/(20S+20R) sterane ratio ≈ 0.5 (Peters and Moldowan, 1993).

Some differences between the samples can be noted (Fig. 6.3): (i) In the Huqf-2 bitumen, long-chain *n*-alkanes predominate, maximising at C_{26}, whereas in the other two samples shorter *n*-alkanes are relatively more important. (ii) The Huqf-3 bitumen contain relatively higher amounts of C_{21} and C_{23} regular isoprenoids compared to the Huqf-1 and Huqf-2 samples (iii) In the Huqf-2 bitumen the short-chain steranes (pregnane, 20-methylpregnane, 20-ethylpregnane) are relatively less abundant and in the Huqf-1 bitumen the short-chain steranes are relatively more abundant compared to the C_{29} 20R and 20S 5α,14α,17α(H)- and 5α,14α,17ß(H)-steranes. (iv) In the Huqf-2 bitumen the tricyclic terpanes are less abundant relative to the hopanes. The carbon number distributions of the tricyclic terpanes and hopanes are remarkably similar except with respect to the 28,30-dinorhopane (DNH) which is absent in the Huqf-2 sample but is clearly present in the Huqf-1 and Huqf-3 samples. (v) The concentrations of the *n*-alkanes and mid-chain methyl alkanes are a factor 10-50 higher in the Huqf-2 bitumen than in the other two bitumens (Table 6.6).

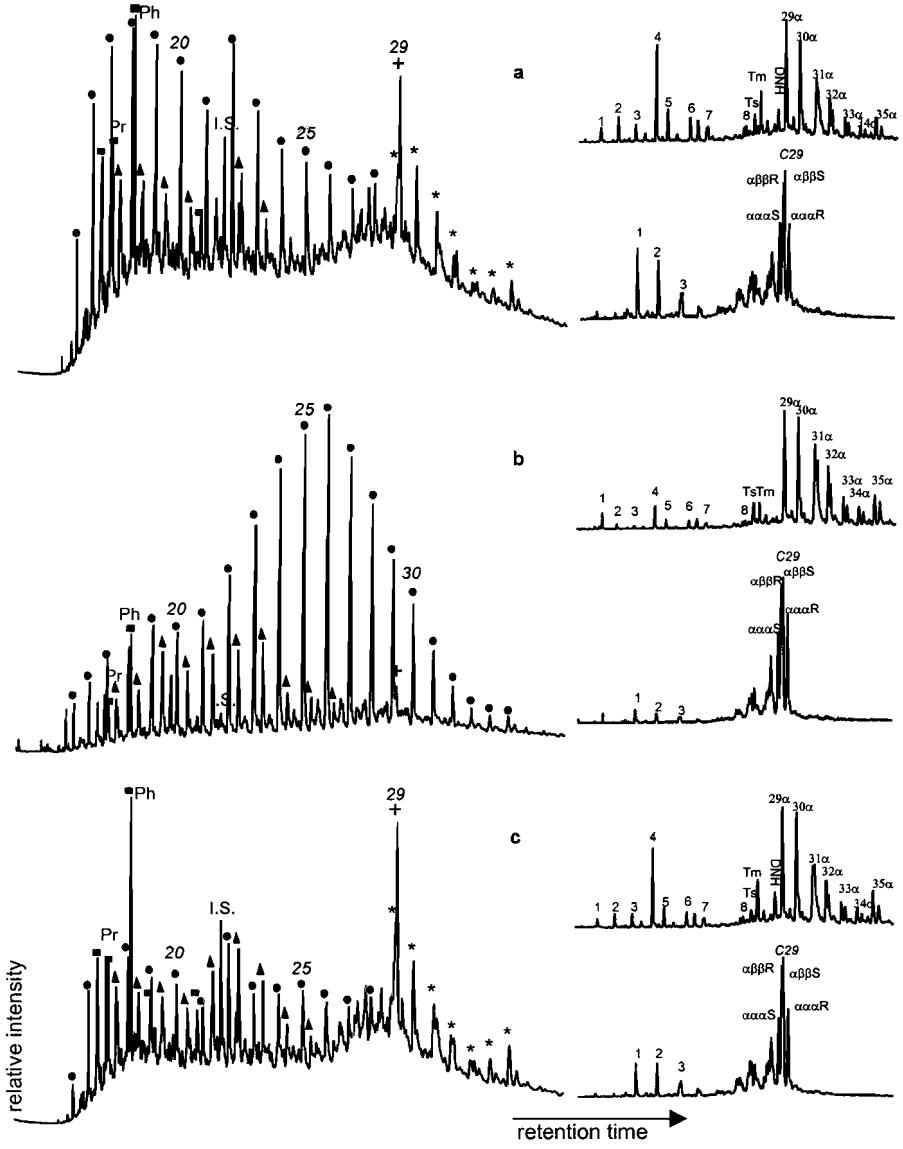

Figure 6.3 Total Ion Current (TIC) traces and partial mass chromatograms of *m/z* 191 and *m/z* 217 of the saturated hydrocarbon fractions of (**a**) the Huqf1, (**b**) the Huqf2 and (**c**) the Huqf3 bitumens. Numbers refer to compounds listed in Tables 4 and 5. Filled circles indicate the homologous series of *n*-alkanes. Their number of carbon atoms is indicated with italic numbers. Filled squares indicate pseudo homologous series of isoprenoid *(i-)* alkanes. Filled triangles indicate a series of mid-chain methyl alkanes. Stars indicate a series of hopanes. The cross indicates the C_{29} sterane. Internal Standard (I.S.): 6,6-d_2-2-methylhenicosane.

Aromatic hydrocarbon fractions of the rock bitumens

The aromatic hydrocarbon fractions are composed of extremely complex mixtures of components. Three groups of biomarkers were identified in the A2 fractions: alkylbenzenes and alkylmethylbenzenes (C_{11}-C_{27}), C-ring monoaromatic steroids (C_{21}-C_{29}) dominated by C_{29} members and C_{32}-C_{35} benzohopanes. No alkylthiophenes were detected in these fractions. The distributions of the alkylbenzenes and C-ring monoaromatic steroids in the different samples are quite similar, whilst the distribution of the benzohopanes shows some variation. However, this may be due to the presence of some benzohopanes in the A3-fraction. The A3 fractions also contain extremely complicated mixtures of compounds. The only large difference between the samples is the abundance of C_1-C_5 alkylated dibenzothiophenes in the Huqf-2 sample, whereas these components are relatively low in the other A3 fractions. Hardly any compounds could be detected in the A4 fractions. Only the Huqf-2 sample contained small amounts of cyclic sulphides, such as thiolanes and thianes.

Table 6.5. Pregnanes and steranes identified in the Huqf oil, the saturated hydrocarbon fraction and desulfurized polar fraction of the bitumens and in the kerogen pyrolysates

peak[a]	component
1	pregnane
2	20-methylpregnane
3	20-ethylpregnane
C_{29} ααα**S**	5α, 14α, 17α(H) 24-ethyl-cholestane 20S
C_{29} αββ**R**	5α, 14β, 17β(H) 24-ethyl-cholestane 20R
C_{29} αββ**S**	5α, 14β, 17β(H) 24-ethyl-cholestane 20S
C_{29} ααα**R**	5α, 14α, 17α(H) 24-ethyl-cholestane 20R

[a]numbers refer to Figs. 2,3,4 and 7 (m/z 217 chromatogram)

Desulfurized polar and asphaltene fractions of the rock bitumens

Substantial amounts of hydrocarbons were released by desulfurization with Raney Ni of the polar fractions of the bitumens. Similar suites of components were released upon desulfurization as those present in the hydrocarbon fractions (Fig. 6.4, Table 6.6). However, in the desulfurized polar fraction of the Huqf-2 bitumen the higher carbon number *n*-alkanes are relatively less abundant than in the saturated hydrocarbon fraction. The relative abundance of the other compound classes varies as well. For example, the relative abundance of the C_{23} tricyclic terpane as revealed by the *m/z* 191 mass chromatogram is much higher than in the saturated hydrocarbon fractions. It is apparent that the concentrations of S-bound *n*-alkyl and mid-chain methyl alkyl moieties are a factor 10-50 higher in the Huqf-2 bitumen than those in the Huqf-1 and Huqf-3 bitumens (Table 6.6).

Table 6.6: Concentrations (μg/g TOC) of selected biomarkers in the saturated hydrocarbon-, desulfurized polar- , desulfurized asphaltene and off-line pyrolysis fractions.

	Huqf-1				Huqf-2				Huqf-3			
	off-line pyrolysate	desulfurized asphaltenes	desulfurized polars	A1-fraction	off-line pyrolysate	desulfurized asphaltenes	desulfurized polars	A1-fraction	off-line pyrolysate	desulfurized asphaltenes	desulfurized polars	A1-fraction
C_{30} hopane	13	0.1	---[a]	2.0	5	0.6	---[a]	2.4	7	0.1	0.1	8.7
C_{29} ααα R sterane	---[b]	---[a]	---[a]	0.8	2	0.2	0.1	1.0	2	0.1	0.1	4.6
C_{23} tricyclic Terpane	22	0.1	0.1	1.9	1	0.1	---[a]	0.4	4	0.1	0.4	5.0
Dinorhopane	---[b]	---[a]	---[a]	0.5	---[b]	---[a]	---[a]	---[a]	---[b]	---[a]	---[a]	2.8
Pregnane	---[b]	---[a]	---[a]	0.5	4	---[a]	---[a]	0.1	4	---[a]	---[a]	1.5
Phytane	---[b]	0.1	0.2	5.4	22	5.4	3.6	96	---[b]	0.3	1.5	33
n-C_{24} alkane	87	0.1	0.2	12	122	6.7	7.3	340	164	0.4	0.8	9.7
C_{24} midchain Methylalkane	---[b]	---[a]	---[a]	2.5	99	6.6	5.0	110	49	---[a]	0.7	12

[a] <0.1μg/g TOC
[b] <1μg/g TOC

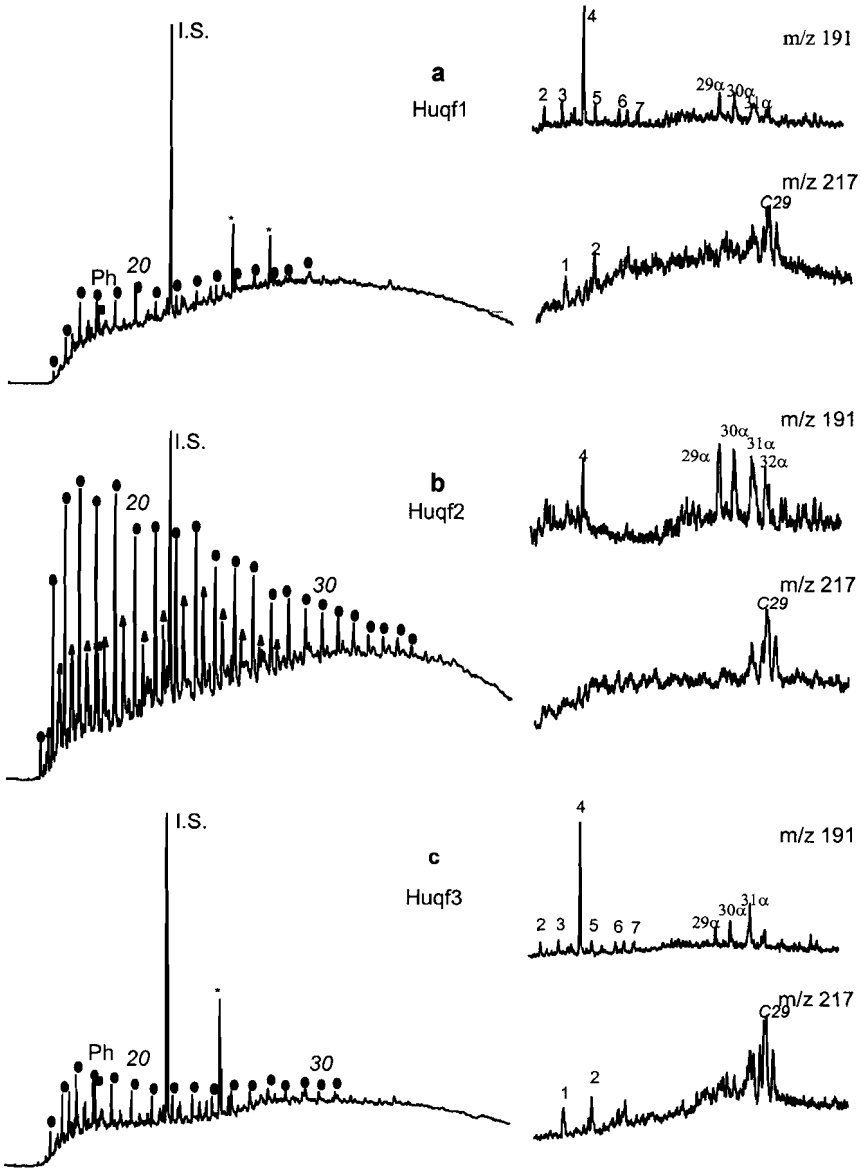

Figure 6.4 Total Ion Current (TIC) traces and summed mass chromatograms of *m/z* 191 and *m/z* 217 of the desulfurized polar fractions of (**a**) the Huqf1, (**b**) the Huqf2 and (**c**) the Huqf3 sediment. Numbers refer to compounds listed in Tables 4 and 5. Filled circles indicate the homologous series of *n*-alkanes. Their number of carbon atoms is indicated with italic numbers. Filled squares indicate pseudo homologous series of isoprenoid *(i-)* alkanes. Filled triangles indicate the series of mid-chain methyl alkanes. Stars indicate comtamination. Internal Standards (I.S.): 6,6-d_2-2-methylhenicosane.

Concentrations of isoprenoid alkanes, *n*-alkanes and mid-chain methyl alkanes in fractions from the desulfurized asphaltene fraction of the Huqf-2 sample are also much higher than those in the other two samples (Table 6.6). The distributions of the released hydrocarbons are in general similar to those present in the saturated hydrocarbon fraction with one exception. The distribution of the *n*-alkanes in the desulfurized asphaltene fraction of the Huqf-2 sample, like in the desulfurized polar fraction, shows that the higher carbon number *n*-alkanes are relatively less abundant than those in the saturated hydrocarbon fraction.

Flash pyrolysis

The three decalcified rocks (Table 6.1) and one isolated kerogen (Huqf-2) were subjected to py-GC-MS. The TIC traces reveal significant differences in the compositions of the flash pyrolysates (Fig. 6.5). Homologous series of *n*-alkanes and *n*-alk-1-enes dominate the pyrolysates of all three decalcified rocks, with a maximum at C_{10}. Alkylbenzenes and low amounts of alkylthiophenes and alkylnaphthalenes are present in all three samples as well as traces of 22,29,30-trinorhop-17(21)-ene, 17α-22,29,30-trinorhopane, 30-norhop-17(21)-ene, 17α,21β-30-norhopane and steranes (C_{21}-C_{23}, C_{29}). Low amounts of a series of isoprenoid alkanes (C_9-C_{20}) and isoprenoid alkenes (C_{14}-C_{16}) are also present in all three samples and very low amounts of mid-chain methyl alkanes (C_{14}-C_{29}, maximizing around C_{24}) and mid-chain methyl alkenes (C_{18}-C_{24}) were detected in the flash pyrolysate of the decalcified Huqf-1 and Huqf-3 rocks. Relatively high amounts of these latter compounds were detected in the flash pyrolysate of the decalcified Huqf-2 rock but after kerogen isolation the mid-chain methyl alkanes were less abundantly present in the kerogen flash-pyrolysate (Fig. 6.6). Part of these iso-alkanes may thus have been encapsulated in the mineral matrix. Circumstantial evidence for this comes from the observation that upon py-GC-MS of the Huqf-2 sample at 358°C, a temperature where only evaporation takes place (Sinninghe Damsté et al., 1994), a series of *n*-alkanes is released from the well extracted decalcified rock, maximizing at C_{15}, as well as a series of mid-chain alkanes (C_{14}-C_{29}). No compounds were released upon py-GC-MS at 358°C from the decalcified rock of the Huqf-1 and Huqf-3 samples and the isolated kerogen of the Huqf-2 sample.

Off-line pyrolysis

To enable detailed structural studies and the determination of ^{13}C contents of individual pyrolysis products, off-line pyrolysis at 400°C was performed on all three samples. The pyrolysis yields varied between 14-17% (Table 6.1). Saturated and unsaturated hydrocarbon fractions were obtained from the off-line pyrolysates by column chromatography.

The summed mass chromatograms of *m/z* 182+196 of the saturated hydrocarbon fractions of the off-line pyrolysates reveal differences in their general composition (Fig. 6.7). In the Huqf-2 sample the abundance of mid-chain methyl

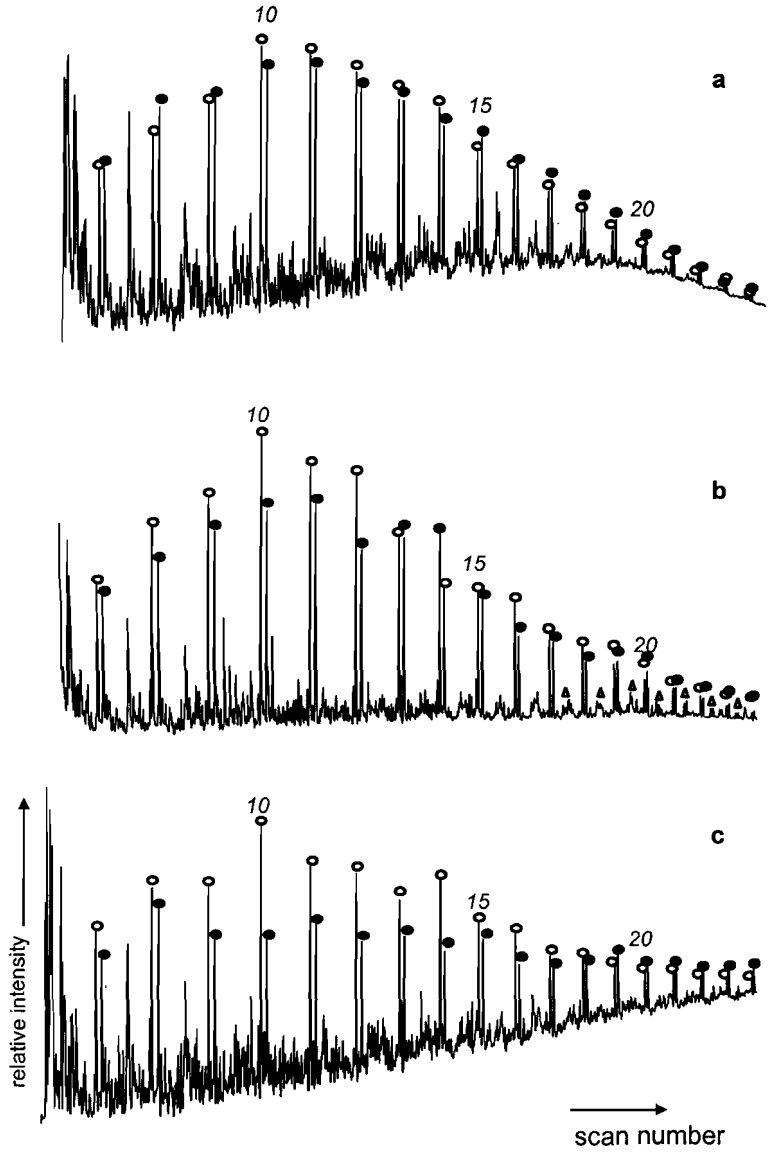

Figure 6.5 Total Ion Current (TIC) traces of the flash pyrolysates (Curie temperature 610 °C) of the (**a**) Huqf-1., (**b**) the Huqf-2 and (**c**) the Huqf-3 kerogen. Filled and open circles indicate the homologous series of *n*-alkanes and *n*-alk-1-enes, respectively. Their number of carbon atoms is indicated with italic numbers.

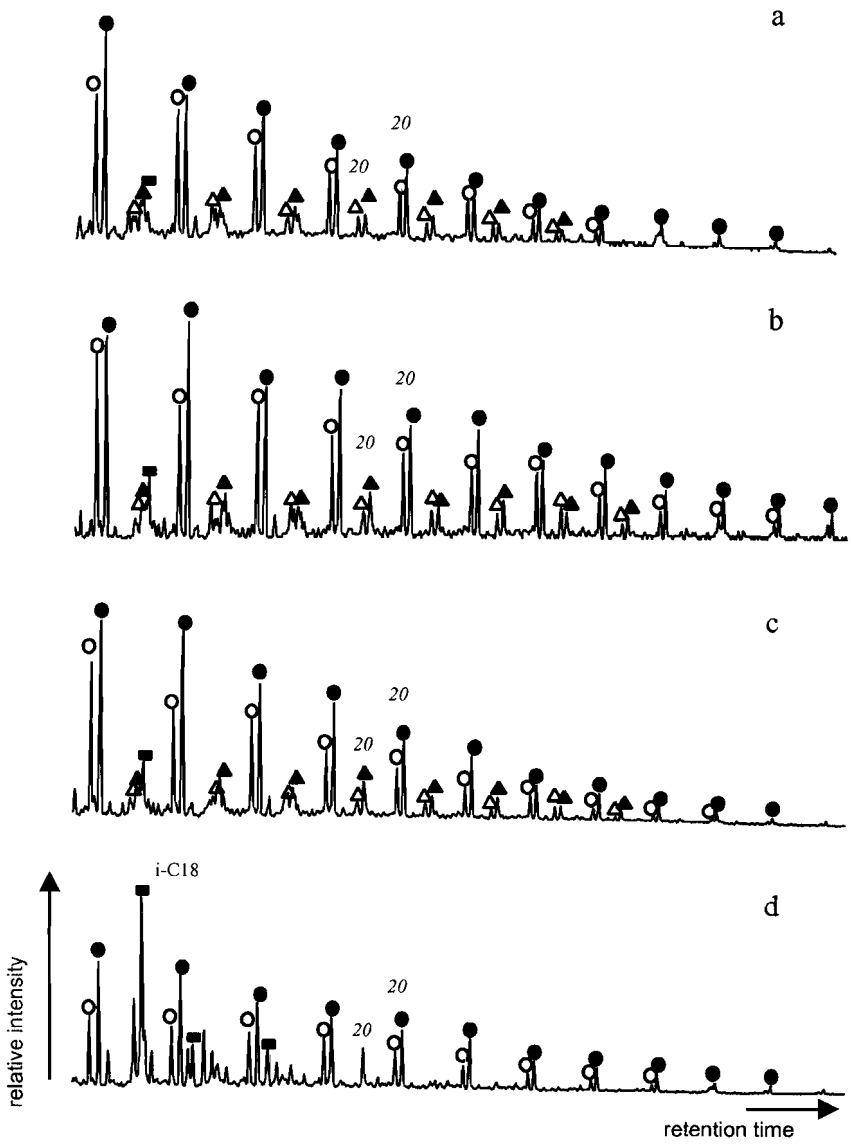

Figure 6.6 Total Ion Current (TIC) traces of the flash pyrolysates (Curie point temperature 610 °C of (**a**) the isolated Huqf-2 kerogen and the residue after (**b**) base-hydrolysis, (**c**) ether-bond cleavage and (**d**) desulfurization and nitric acid treatment. Filled and open circles indicate the homologous series of *n*-alkanes and *n*-alk-1-enes, respectively. Their number of carbon atoms is indicated with italic numbers. Filled and open triangles indicate the homologous series of mid-chain methyl alkanes and alk-1-enes, respectively.

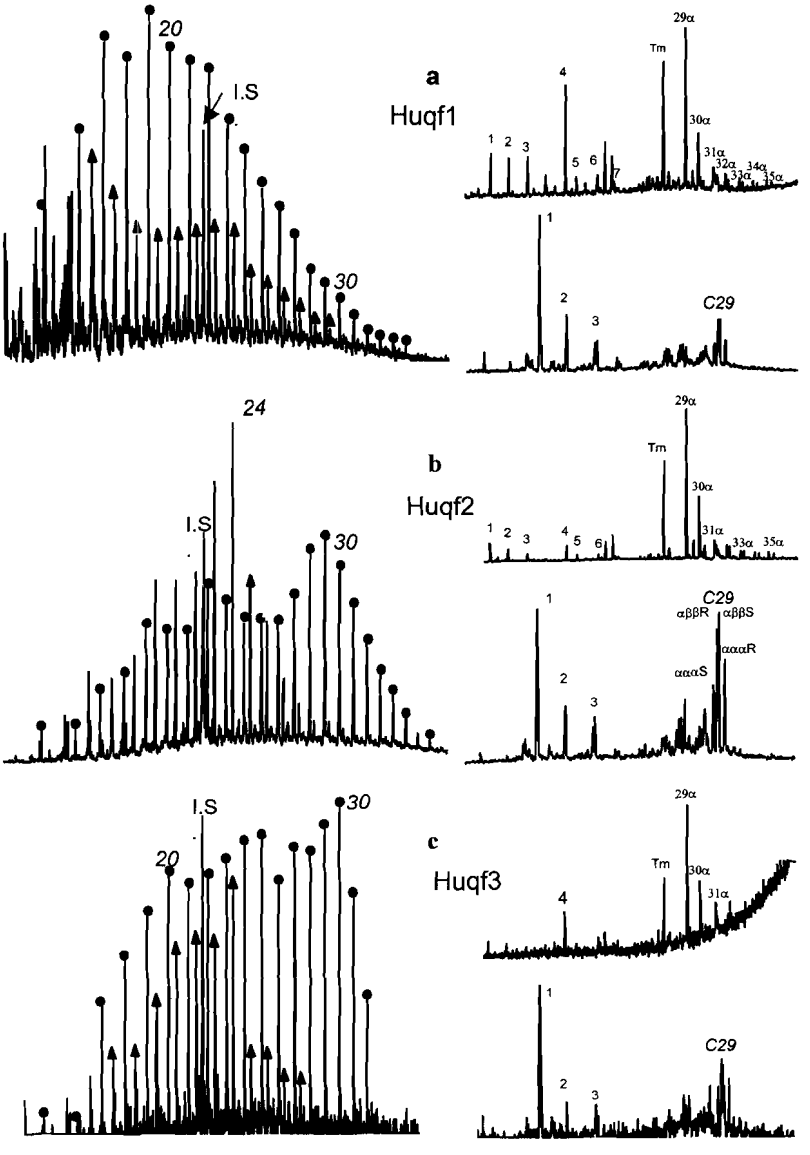

Figure 6.7 Summed mass chromatogram of *m/z* 182+196, *m/z* 191 and *m/z* 217 of the saturated alkane fraction obtained from the Huqf-2 kerogen. Filled circles indicate the homologous series of *n*-alkanes. Their number of carbon atoms is indicated with italic numbers. Filled squares indicate pseudo homologous series of isoprenoid *(i-)* alkanes. Filled triangles indicate the series of mid-chain methyl alkanes. Internal Standard (I.S.): 6,6-d_2-2-methylhenicosane.

alkanes is relatively high in contrast to that in the Huqf-1 and Huqf-3 samples where these methyl alkanes are much lower, in agreement with the flash pyrolysis results (Figs. 6.5 and 6.7, Table 6.5). However, in the summed mass chromatograms of *m/z* 182+196 (Fig. 6.7) these methyl alkanes can be identified in all three samples. Homologous series of *n*-alkanes dominate the saturated hydrocarbon fraction of all three kerogen pyrolysates, decreasing in abundance from C_8 till C_{36}. Furthermore, isoprenoid alkanes (C_{13}-C_{20}), steranes (C_{21}-C_{29}), tricyclic terpanes (C_{20}-C_{29}) and C_{27}-C_{35} 17α,21β(H)-hopanes were identified in the off-line pyrolysates (Fig. 6.7). In the Huqf-2 pyrolysate the pregnanes (C_{21}-C_{23}) are as abundant as the C_{29} 20R and 20S 5α,14α,17α(H)- and 5α,14ß,17ß(H)-steranes. In the Huqf-1 and Huqf-3 pyrolysates these short-chain steranes are more abundant relative to the C_{29} 20R and 20S 5α,14α,17α(H)- and 5α,14ß,17ß(H)-steranes.

The FID traces of the unsaturated hydrocarbon fractions of the kerogen pyrolysates are dominated by a homologous series of *n*-alk-1-enes. Furthermore, isoprenoid alkenes (C_{14}-C_{19}) and, in the Huqf-2 sample, mid-chain methyl alkenes were identified in the kerogen pyrolysates. To prove this latter assignment, the alkene fraction was hydrogenated and indeed mid-chain methyl alkanes were formed. The presence of both mid-chain methyl alkanes and mid-chain methyl alkenes suggests that these compounds were bound to the kerogen and were released upon pyrolysis.

Chemical degradation

To find out how the methyl alkane skeletons are bound in the Huqf-2 kerogen, chemical degradation was performed on the isolated kerogen. The applied chemical degradation steps are shown in Fig. 6.1.

GC-MS analysis of the flash pyrolysates of the residues R_1 and R_2 left after base hydrolysis and after base hydrolysis and ether bond cleavage, respectively, revealed similar components as present in the pyrolysates of the initial kerogens. There were few changes in relative abundances of the different compound classes. Only the *n*-alkanes and *n*-alkenes are slightly less abundant compared to the isoprenoid alkanes and alkenes (cf. Figs. 6.6 and 6.8). GC/MS analysis of the flash pyrolysate of final residue R_3, obtained after desulfurization (and nitric acid treatment to remove the Ni_2B reagent) of the residue R_2, showed major changes in relative abundance of the different compound classes. Normal alkanes and alkenes are significantly less dominant compared to other compounds and the mid-chain methyl alkanes and alkenes have disappeared completely from the pyrolysate of this residue. However, no compounds could be identified in the extract released upon desulfurization that, if S-bound in the kerogen, could have generated mid-chain methyl alkanes upon pyrolysis, possibly because these compounds were not GC-amenable. Furthermore, it is striking that the thiophenes are relatively more abundant when compared with several other compound classes. However, they did not increase relative to the isoprenoids. It has been previously noted that upon desulfurization not all thiophenes disappeared from the flash pyrolysate (Höld et al., 1998b) probably because the reagent cannot completely

access the solid substrate. The relative abundance of the thiophenes in the pyrolysate after desulfurization will increase if, upon desulfurization, it is more difficult to release these thiophenes in the kerogen compared to other compounds; for example because the former are linked tighter (with several S-bonds) into the kerogen.

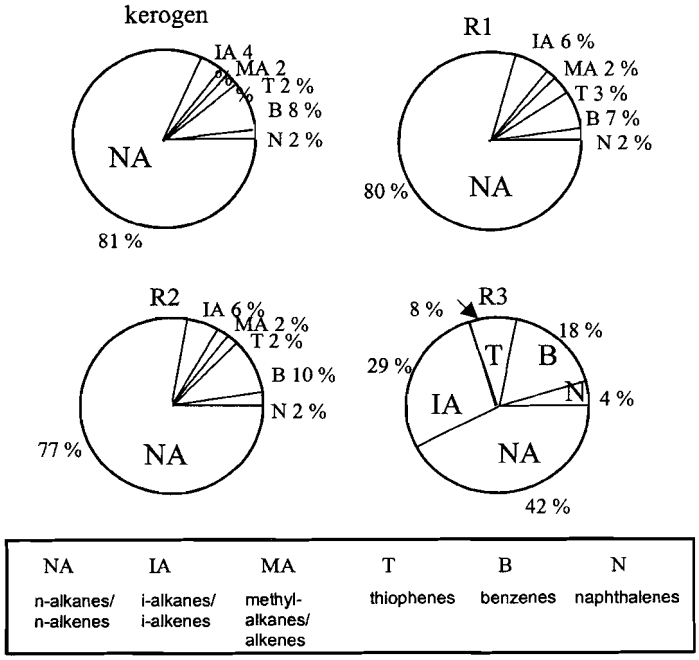

Figure 6.8 Relative abundances of the different component classes in the pyrolysate of the initial kerogen and residues after sequential chemical degradation.

Stable carbon isotope analysis

The *n*-alkane series in the saturated hydrocarbon fraction of the Huqf crude oil has a uniform isotopic composition of -36.3±0.2 ‰ (Fig. 6.9a). The $\delta^{13}C$ values of the mid-chain methyl alkanes are -36.8±0.4 ‰ and are thus slightly depleted relative to the average value of the *n*-alkanes.

The *n*-alkanes in the saturated hydrocarbon fraction of the Huqf-2 bitumen have $\delta^{13}C$ values starting at -36.9 ‰ for C_{19} and steadily increasing until -29.5 ‰ for C_{29} (Fig. 6.9b). The mid-chain methyl alkanes have $\delta^{13}C$ values of ca. -37 ‰. The *n*-alkanes in the saturated hydrocarbon fractions of the Huqf-1 and Huqf-3 bitumen have $\delta^{13}C$ values of ca. -35 ‰.

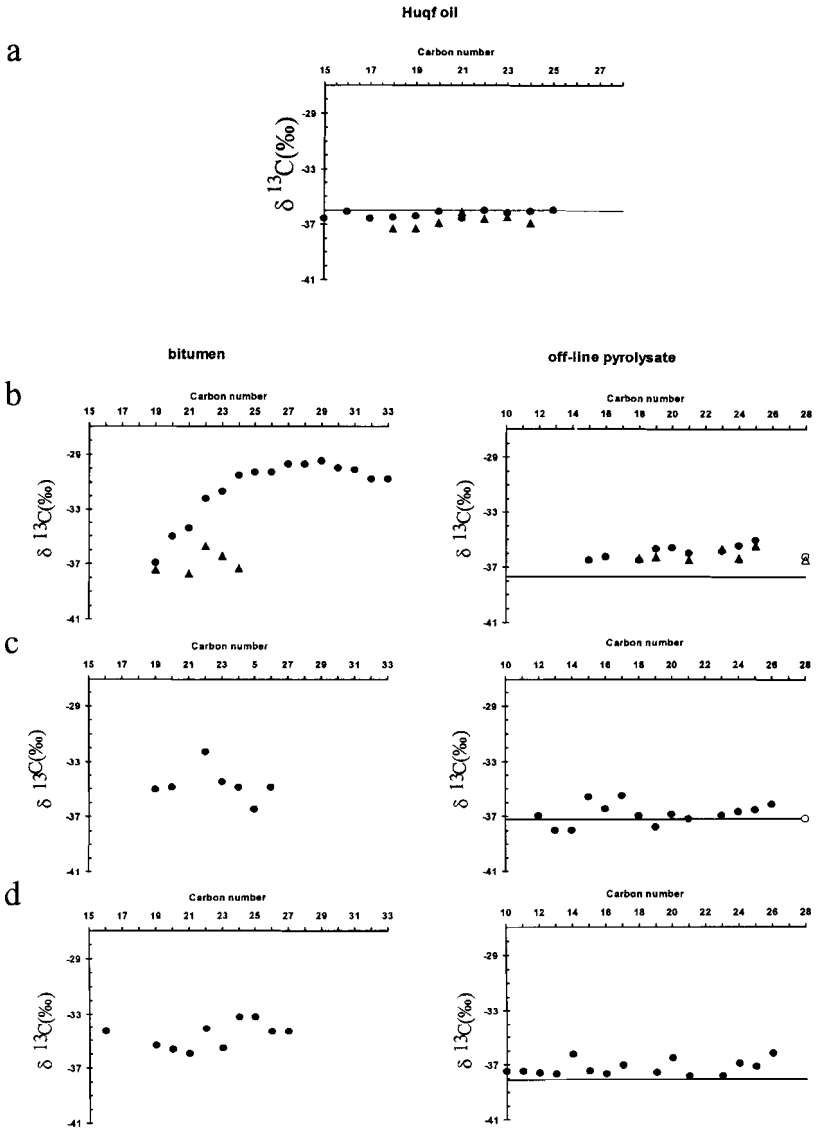

Figure 6.9 Plot of $\delta^{13}C$ values (‰) as a function of carbon number for aliphatic hydrocarbon pyrolysis products from (**a**) the Huqf oil, (**b**) the Huqf-2, (**c**) the Huqf-3 and (**d**) the Huqf-1. Filled circles and triangles indicate the homologous series of *n*-alkanes and mid-chain methyl alkanes, respectively. Open circles indicate the average *n*-alkene value and open triangles indicate the average mid-chain methyl alkene value. The straight line indicates the bulk TOC value.

Results of bulk isotopic analysis of the rocks before and after off-line pyrolysis (Table 6.1) in combination with the relatively high yields suggest that in all three samples the residual organic matter is isotopically identical to the starting material, indicating that the released organic matter is probably isotopically representative of the kerogen.

The *n*-alkanes in the Huqf-1, Huqf-2 and Huqf-3 off-line pyrolysates have $\delta^{13}C$ values of -35.9±0.5 ‰, -37.3±0.5 ‰ and -36.9±0.8 ‰, respectively. The *n*-alkenes in the off-line pyrolysate of the Huqf-2 and Huqf-3 samples (analyzed after hydrogenation) have $\delta^{13}C$ values of -36.3±0.3 ‰ and -37.2±0.4 ‰, respectively, identical to the $\delta^{13}C$ values of their saturated counterparts. The mid-chain methyl alkanes and methyl alkanes in the off-line pyrolysate of the Huqf-2 have an average isotopic composition of -36.3±0.5 ‰ and -36.5±0.2 ‰, respectively, which is c. 1.0 ‰ lighter than the average value of the *n*-alkanes though this difference is within analytical uncertainty.

6.5 Discussion

The predominant branching position of the methyl alkanes (Table 6.3) changes with carbon number but the distribution is the same in the Huqf oil, the saturated hydrocarbon fraction and desulfurized polar fraction of the bitumens and in the pyrolysates of the Huqf-2 kerogen and its residues after base hydrolysis and HI treatment. Mid-chain methyl alkenes were also identified in the pyrolysates, indicating that the corresponding alkyl-moieties were linked to the kerogen. The location of the double bond could provide an indication of the position at which the precursor moiety was linked to the kerogen. However, it is difficult to identify the exact location of the double bond in the mid-chain methyl alkenes by their mass spectra, since the mass spectra of the different unsaturated isomers are expected to be very similar. Since the mid-chain methyl alkane moieties are released from the Huqf-2 bitumen and kerogen upon desulfurization, they occur probably sulfur- (or possibly sulfur- and ether-)bound in the kerogen and in other macromolecular fractions. The similar $\delta^{13}C$ values of the mid-chain methyl alkanes (and, if present, alkenes) in the Huqf oil, in the saturated hydrocarbon fraction of the bitumens and in the pyrolysates of the Huqf-2 kerogen suggest one or similar precursors. The precursor of the mid-chain alkanes and alkenes are probably sulfur- (and possibly sulfur- and ether-) bound lipids with a methyl group at the C-12 or C-13 position.

The most logical position(s) for the S-bond(s) [and possibly O-bond(s)] is at the variable end of the chain and since the chain length of the methyl alkanes in oil, bitumens and pyrolysates has a maximum around C_{24}, the predominant positions of the S-bonds are probably at the 24-position and higher (Fig. 6.10). This is a result of the reaction of reduced inorganic sulfur species with the original functional groups (e.g.

double bonds, alcohol groups) at the 24- and higher positions in the precursor(s). Upon both catagenesis and pyrolysis of these S- (and possibly O-) bound precursors, 12- and 13-methyl alkanes (predominantly C_{24}) are generated. A similar phenomenon is noticed for C_{30-35} homohopanoids in sediments and crude oils. These homohopanes are presumably formed via initial sulfurization of C_{35}-hopanepolyol derivatives and subsequent desulfurization/side-chain cleavage during the early stages of thermal maturation yielding the lower homologues (Sinninghe Damsté et al., 1995; Köster et al., 1997). The higher the carbon number of the released homohopane, the more S-bonds must have been broken before side-chain cleavage to release it and the lower its relative abundance is. Thus, similar to the homohopanoids, the precursor for the mid-chain methyl alkanes may have had a polar head group (possibly also a sugar unit) and a (C_{24}?) hydrocarbon tail. Sulfurization of the polar units present in these hypothetical lipids could then bind them into the kerogen. Upon cleavage of one carbon bond located directly next to the carbon-sulfur bond the predominant C_{24} mid-chain methyl alkane could be released. Additional sulfur bond cleavage before side-chain cleavage would release longer chain mid-chain methyl alkanes. Interestingly, C_{35}-hopanepolyols or derivatives thereof serve as membrane rigidifiers in prokaryotes (Rohmer et al., 1992), which would reinforce the suggestion that mid-chain methylation may have been a strategy for controlling the membrane fluidity (Dowling et al., 1986; Summons, 1987).

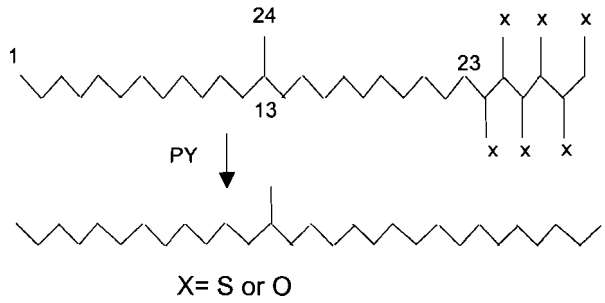

Figure 6.10 Proposed mechanism of pyrolysis for the formation of the mid-chain methyl alkanes and alkenes.

Based on the ideas of Makushina et al. (1978), Fowler and Douglas (1987) discussed cyclopropyl acids as possible precursor for the mid-chain methyl alkanes found in oils from the Siberian Platform (cf. Table 3). These cyclopropyl acids are common in bacteria (Goldfine, 1972; Hofmann et al., 1952; Jacques and Hunt, 1980), in some protozoa (Meyer and Holz, 1966) and have been encountered in algal mats

(Cardoso et al., 1978; Gibbons, 1978) and in recent lake sediments (Cranwell, 1973). The precursor of the most abundant branched alkanes in these Precambrian Siberian oils, 11- and 12-methyltricosanes, was suggested to be 12,13-methylene tetracosanoic acid. Through opening of the cyclopropyl ring and decarboxylation, the branched alkanes were assumed to be formed from this precursor. It should be noted, however, that such long-chain methylene fatty acids have not yet been reported as biochemicals so far.

Mid-chain methyl branching does occur in the fatty acids of extant bacteria, in sponges, which have bacterial symbionts (e.g. Thiel et al., 1999), in cyanobacterial hydrocarbons (Gelpi et al., 1970) and these branched lipids are observed in modern microbial mats dominated by cyanobacteria (e.g. Boon and de Leeuw, 1987; Robinson and Eglinton, 1990; Shiea et al., 1990). Mid-chain branched alkanes in bitumens and oils may thus be derived from biosynthetic hydrocarbons (cyanobacteria) or from carboxylic acids after decarboxylation (bacteria). However, the isomer distributions of the methyl alkanes for both oil and bitumens reported in this study differ significantly from the distributions found in cyanobacteria. Thiel et al. (1999) did observe complex patterns of mid-chain branched alkanes in a fossil sponge-microbially derived, micritic carbonate crust. These authors suggested complex suites of mid-chain branched alkanoic acids as potential biological precursors for the complex branched alkane patterns found in ancient rocks. Such compounds were found in recent marine demosponges and are most likely derived from their specific, bacterial symbionts. In the samples from the Huqf Formation, the functionality of the precursor is not located at the end of the molecule but probably at the 24-position. In addition, the chain length of the methyl alkanes found in the Huqf oil and in bitumens and kerogen pyrolysates of the Huqf-2 rock (C_{14}-C_{28}, maximizing at C_{24} in bitumen and pyrolysate) differs from the chain lengths found by Thiel et al. (1999) in the sponges samples (C_{14}-C_{25}, maximizing at C_{16} and C_{18}). Therefore, it is unlikely that these mid-chain branched alkanoic acids are the precursors for the branched alkane patterns found in the samples from the Huqf Formation.

The stable carbon isotopic composition of the mid-chain methyl alkanes are relatively depleted in ^{13}C compared to most modern-day membrane lipids suggesting no significant limitation in inorganic carbon uptake. However, since it is unclear what the isotopic fractionation patterns were of the parent organism it is difficult to speculate on the cause of the depleted values.

6.6 Conclusions

In this study it is shown that mid-chain methyl alkanes in sediments from the Huqf-formation are bound into the kerogen and that they are released into the bitumen during maturation. The isomer distribution of the series of mid-chain methyl alkanes is the same in the Infra-Cambrian Huqf oil, the bitumens and in the pyrolysates of the

Huqf-2 kerogen. The precursor for the mid-chain methyl alkanes may have been C_{30} lipids with a C_6 (sugar?) unit as a polar head group and a C_{24} hydrocarbon tail. Sulfurization during early diagenesis of the polar units present in these lipids could then bind these lipids into the kerogen. These lipids might have been present in biological membranes during the Precambrian for controlling their fluidity and may be associated with the dramatic evolutionary changes occurring at this time.

6.7 Acknowledgement

Dr. M.E.L. Kohnen is thanked for providing the oil and rock samples. Dr. W. Pool is thanked for technical assistance and M. Dekker is acknowledged for performing GC-MS analyses. This study was supported by a PIONIER grant to JSSD from the Netherland Organization for Scientific Research (NWO). We thank Shell International Petroleum Maatschappij BV for financial support for the irm-GC-MS facility. We acknowledge R. Kloosterhuis (NIOZ) for bulk carbon isotope analyses of the rocks. This is NIOZ Contribution 3380.

CHAPTER 7

Occurrence of ester-bound cyclic mono- and diterpenoids in marine kerogens

Ingeborg M. Höld, Niels J. Brussee, Stefam Schouten, Jaap S. Sinninghe Damsté

7.1 Abstract

The presence of kerogen-bound cyclic monoterpenoids (α-terpineol, borneol and fenchylalcohol) has been established in Tertiary, Cambrian and Late Proterozoic kerogens and of cyclic diterpenoids in a Cambrian marine kerogen through flash pyrolysis and alkaline hydrolysis. The unsaturated and aromatic terpenoids in the kerogen pyrolysate are formed from rearrangement reactions of the ester bound precursors followed by aromatisation. Their presence in sediments predating the evolution of higher plants would indicate that these cyclic monoterpenoids can not be used as terrestrial markers. However, there are serious doubts if these terpenoids are indigenous to these marine kerogens.

7.2 Introduction

Terpenoids are so-called secondary metabolites which are mostly unique to certain species and have usually no proven effect on the organisms itself but only on predators or competitors. Monoterpenoids are known as components of fragrant oils which can be obtained from the leaves, flowers and fruits of many higher plants and occur as acyclic, monocyclic (*p*-menthane skeleton, **I**) and bicyclic (*e.g.* camphane (**II**) and fenchane (**III**) skeleton) components. Six dienes possessing the *p*-menthane skeleton occur in nature, i.e. α-terpinene (**IV**), γ-terpinene (**V**), terpinolene (**VI**), limonene (**VII**), α-phellandrene (**VIII**) and β-phellandrene (**IX**). All these six dienes can readily isomerize in the presence of acids (Whittaker, 1972). Cyclic diterpenoid acids, alcohols and hydrocarbons are also predominant constituents of higher plant resins and supportive tissue, especially in conifers. The major skeletal structures types that are found are the abietanes (**X**), pimaranes (**XI**), kauranes (**XII**), podocarpanes (**XIII**) and labdanes (**XIV**); other skeletal types are usually only present in small amounts.

In contrast to terrestrial organisms, which biosynthesize predominantly non-halogenated acyclic and cyclic terpenoids, marine organisms are known to

biosynthesize halogenated terpenoids. Red seaweeds and sea hares of the genus *Aplysia* contain oils rich in acyclic and cyclic halogenated monoterpenes (Naylor *et al.*, 1983). Nearly all of the marine monoterpenoids observed to date are halogenated. This may not be surprising considering that sea water contains high concentrations of chloride and bromide ions, whereas similar concentrations of halide ions are not found in the terrestrial environment. Non-halogenated cyclic monoterpenoids in marine organisms have so far only been reported as components of some Chlorophyta, Phaeophyta and Rhodophyta (Katayama, 1955, 1962).

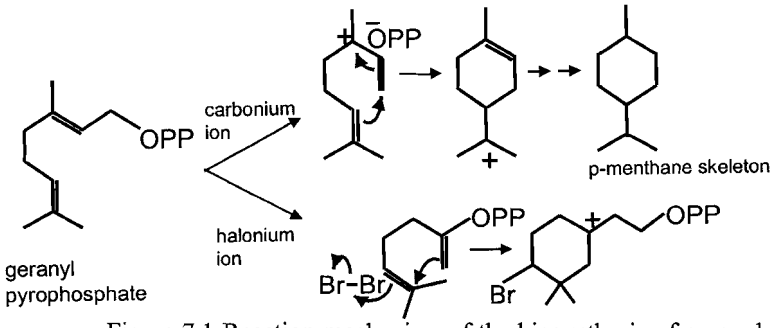

Figure 7.1 Reaction mechanism of the biosynthesis of geranyl pyrophosphate and the two pathways generating halogenated and non-halogenated cyclic monoterpenoids, respectively.

Cyclic monoterpenoids are biosynthesized from geranyl pyrophosphate. This process can occur through two different pathways generating different groups of cyclic monoterpenoids (Fig. 7.1). One of the pathways uses carbonium ion induced cyclization generating non-halogenated cyclic monoterpenoids with *p*-menthane (**I**), fenchane (**II**) and camphane (**III**) carbon skeletons, the other uses a halonium ion induced cyclization and generates predominantly halogenated cyclic monoterpenoids (Naylor *et al.*, 1983; Zheng *et al.*, 1994). The acyclic diterpenoid geranylgeraniol pyrophosphate is the biosynthetic precursor for cyclic diterpenoids. A large number of the terrestrial diterpenoids (*e.g.* abietanes (**X**) and pimaranes (**XI**)) are derived by a proton-induced cyclization of all-*trans*-geranylgeraniol pyrophosphate (Fig. 7.2; Fenical, 1978). In contrast, only two groups of marine diterpenoids, the bromolabdanes (**XV**) and the sponge-derived isoagathic acid (**XVI**) are formed through this cyclization mechanism (Fenical, 1978).

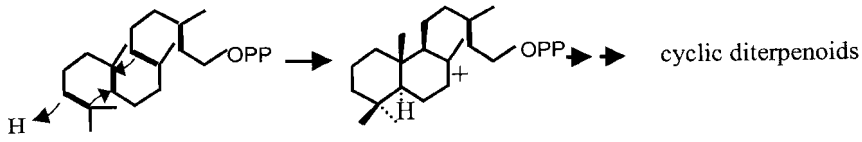

Figure 7.2 Reaction mechanism of the biosynthesis of cyclic diterpenoids from geranylgeraniol pyrophosphate.

Ioppolo-Armanios *et al.* (1994) have reported the identification and occurrence of isopropylmethylphenols, including thymol and carvacrol, in crude oils. These monoterpenoids were suggested to originate from higher plants. Diterpenoidal hydrocarbons and monocarboxylic acids have been found in the geosphere in fossil resins and ambers (*e.g.* Langenheim, 1969; Simoneit, 1977; Mills *et al.*, 1984; Simoneit *et al.*, 1986), coals (*e.g.* Hagemann and Hollerbach, 1980; Grimalt *et al.*, 1988; Li *et al.*, 1990; Heppenheimer *et al.*, 1992) and sediments (*e.g.* Simoneit, 1977; LaFlamme and Hites, 1978; Barnes and Barnes, 1983; Simoneit *et al.*, 1986; Otto *et al.*, 1997) and are considered to be molecular indicators for terrestrial sources from resinous plants as they were considered not to be produced by marine biota (Simoneit, 1977).

In this study the presence of ester-bound monoterpenoids has been established in Tertiary, Cambrian and Late Proterozoic marine kerogens and the presence of ester-bound diterpenoids with abietane (**X**) and pimarane (**XI**) skeletons has been established in a Cambrian marine kerogen. However, subsequent experiments indicate that it is questionable whether these terpenoids are indigenous to these marine kerogens.

7.3 Experimental

Samples

The KG-1 sediment sample was taken from a fresh outcrop of the middle Miocene carbonaceous marl member of the Monterey Formation at Naples Beach and has a TOC content of 9.6 % (USA; Isaacs *et al.*, 1992). The Huqf sediment sample originates from the Precambrian-Cambrian Huqf Group in Oman and has a TOC content of 1.0 % (Gorin *et al.*, 1982). The Late-Proterozoic Walcott Chuar sediment sample originates from the Grand Canyon in Arizona and has a TOC of 1-2 % (USA; Summons *et al.*, 1988a).

Kerogen isolation

Kerogen isolation was performed by HCl/HF treatments of the solvent-extracted sediment as described elsewhere (Eglinton, 1988). The isolated kerogen was ultrasonically extracted with MeOH, DCM/MeOH (1:1) and DCM.

Base hydrolysis

Base hydrolysis was performed in order to cleave ester bonds present in the kerogen (Goossens *et al.*, 1989). 30 ml 1N KOH in methanol was added to 400 mg kerogen. The mixture was refluxed for 1 h and then cooled to room temperature. The pH was adjusted to 3 by adding 4 N HCl in methanol (1:1). The residue was extracted with H_2O/MeOH (1:1, v/v, 3x), with MeOH (3x) and ethyl acetate (3x) and dried

pH was adjusted to 3 by adding 4 N HCl in methanol (1:1). The residue was extracted with H_2O/MeOH (1:1, v/v, 3x), with MeOH (3x) and ethyl acetate (3x) and dried under nitrogen. The combined extracts were and washed with H_2O saturated with NaCl (3x) and with H_2O (2x). The extract was dried with Na_2SO_4 and the ethyl acetate was distilled of. The extract was derivatised by treatment with CH_2N_2 and BSTFA/pyridine to methylate and silylate (TMS) fatty acids and alcohols, respectively. Extract and residue were analyzed by GC-MS or flash pyrolysis-GC-MS, respectively.

Gas chromatography (GC)

GC was performed on a Hewlett Packard 6890 instrument equipped with on-column injectors. A fused silica capillary column (25 m x 0.32 mm) coated with CP Sil-5 (film thickness 0.12 μm) was used with helium as carrier gas. Compounds analyzed were detected by a flame ionization detector (FID). The fractions (in hexane) were injected at 35°C. After 5 minutes at 35°C, the oven was heated to 310°C at 4°C/min and was held at 310°C for 10 min.

Gas chromatography-mass spectrometry (GC-MS)

GC-MS was carried out as in (van Kaam-Peters *et al.*, 1997a) except that fractions were injected at 35°C. After 5 minutes at 35°C the oven was heated to 310°C at 4°C/min and was held at 310°C for 10 minutes.

Flash pyrolysis-gas chromatography (Py-GC) and mass spectrometry (Py-GC-MS)

Py-GC and py-GC-MS analysis were carried out as in (Höld *et al.*, 1998a). The temperature was programmed from 0°C (5 min), to 300°C (10 min) at a rate of 3°C/min.

Isotope ratio monitoring-GC-MS (irmGC-MS)

These analyses were carried out as described in (van Kaam-Peters *et al.*, 1997a) except that fractions were injected on a 60 m column at 35°C. After 5 min at 35°C the oven was programmed to 310 °C at 4°C/min and was held at 310°C for 10 min. The stable carbon isotopic compositions of components were determined from separately integrated ion currents of masses 44, 45 and 46 (Merrit *et al.*, 1994). Values were calibrated against those of deuterated *n*-alkane isotopic standards (co-injection with the sample) as well as an external CO_2 reference gas. The standard error in the mean of the deuterated standards was ≤ 0.1 and the standard error in a single observation of the deuterated standards was ≤ 0.6. Isotopic compositions are reported relative to the Pee Dee Belemnite (PDB) standard and $\delta^{13}C$ values are averaged from duplicate or triplicate measurements.

7.4 Results

Identification and $\delta^{13}C$ values of monoterpenoids

Flash pyrolysis of the isolated kerogen from the Miocene Monterey Formation revealed the presence of several compounds with a molecular ion *m/z* 136 ($C_{10}H_{14}$, Fig. 7.3a). Six of these compounds were unambiguously identified by coelution with authentic standards as α-terpinene (**IV**), γ-terpinene (**V**), terpinolene (**VI**), limonene (**VII**) tricyclene (**XVII**), camphene (**XVIII**), whilst one was tentatively identified by massspectrometry as cyclofenchene (**XIX**, Table 7.1). Two compounds with a molecular weight of 136 and possessing a 1,3,3-trimethylcyclohexyl moiety present in the flash-pyrolysate of the isolated kerogen are discussed elsewhere and are not related to the cyclic monoterpenoids discussed here (Höld et al., 2000). Interestingly, the pyrolysate also contained relatively high amounts of 1-methyl-4-isopropylbenzene (**XX**, Fig. 7.4a) which has a *p*-menthane (**I**) skeleton as well (cf. Hartgers, 1994a).

Table 7.1: Retention indices and MS data of the monoterpenoids.

monoterpenoid	RI	MS data
α-terpinene (**IV**)	1003	136(44), 121 (100), 105(18), 93(88)
γ-terpinene (**V**)	1041	136(29), 121(25), 105(10), 93(100)
terpinolene (**VI**)	1071	136(67), 121(92), 105(19), 93(100)
limonene (**VII**)	1015	136(14), 121 (16), 93(56), 107(15), 68(100)
tricyclene (**XVII**)	906	136(14), 121 (21), 105(6), 93(100)
camphene (**XVIII**)	929	136(13), 121 (67), 107(30), 93(100)
cyclofenchene (**XIX**)	919	136(8), 121(13), 107(7), 93(100)

To decipher the origin of these pyrolysis products, base hydrolysis was performed in order to hydrolyse ester bonds present in the kerogen. Most monoterpenoids (**IV-IX, XVII-XX**) were not present anymore in the pyrolysate of the kerogen residue after hydrolysis, indicating that the precursors of these molecules were probably linked to the kerogen by ester bonds. The extract obtained after base hydrolysis of the kerogen (Fig. 7.5a) contained five monoterpenoid alcohols ($C_{10}H_{14}O$) of which three could be identified as their TMS derivative by coinjection with authentic standards as fenchylalcohol (**XXI**), borneol (**XXII**) and α-terpineol (**XXIII**). One of the remaining two monoterpenoid alcohols could be tentatively identified as bornyl acetate (Fig. 7.5a). Possibly, traces of acetic acid present in the ethyl acetate used in the extraction reacted with alcohol groups since other alkyl and aryl acetates could also be identified in the extracts.

Flash pyrolysates of the kerogen of the Cambrian Huqf Formation and the Late Proterozoic Walcott Chuar also contained α-terpinene (**I**), tricyclene (**II**), camphene (**III**), limonene (**IV**), γ-terpinene (**V**) and cyclofenchene (**VII**) (Fig. 7.3b-c). The pyrolysates also contained relatively high amounts of 1-methyl-4-isopropylbenzene

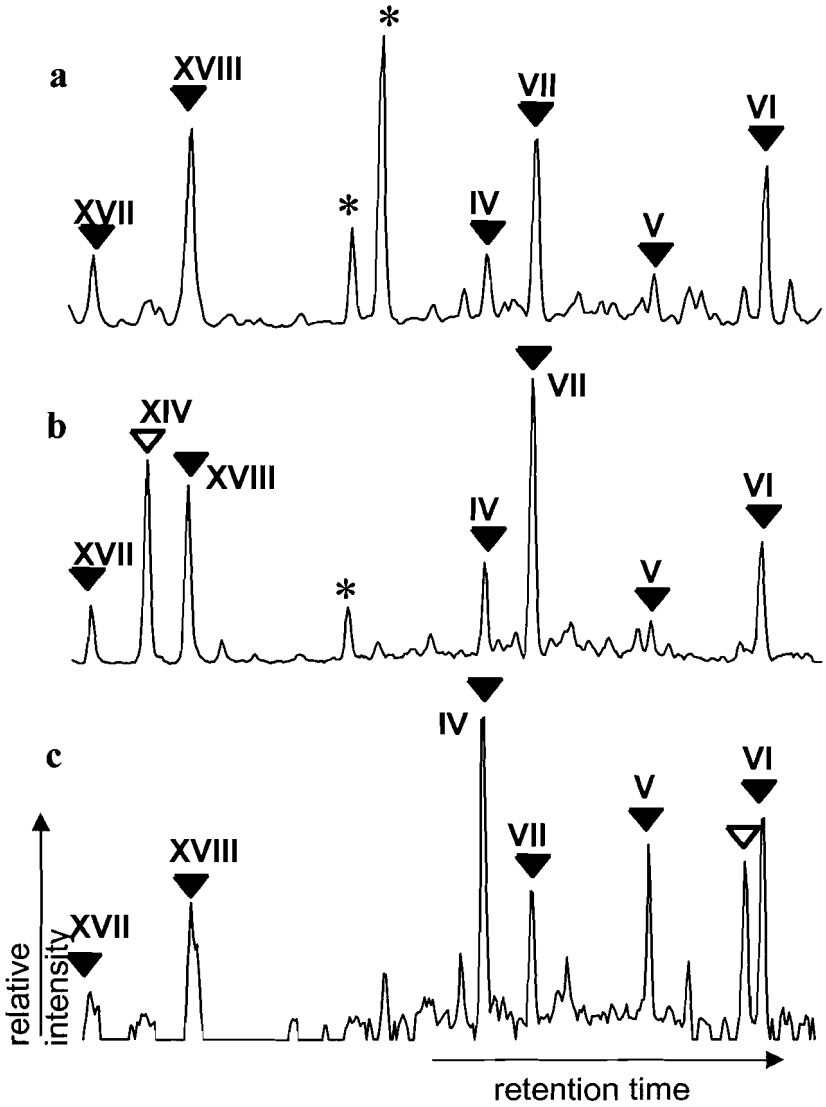

Figure 7.3 Summed mass chromatogram of *m/z* 136 of the monoterpenoids in the flash pyrolysate of (**a**) the Monterey, (**b**) the Huqf and (**c**) the Walcott Chuar Formations. Filled triangles indicate the compounds that were identified using authentic standards. Open triangles indicate the compounds that were tentatively or not yet identified. Stars indicate the compounds that are not related to the monoterpenoids discussed here.

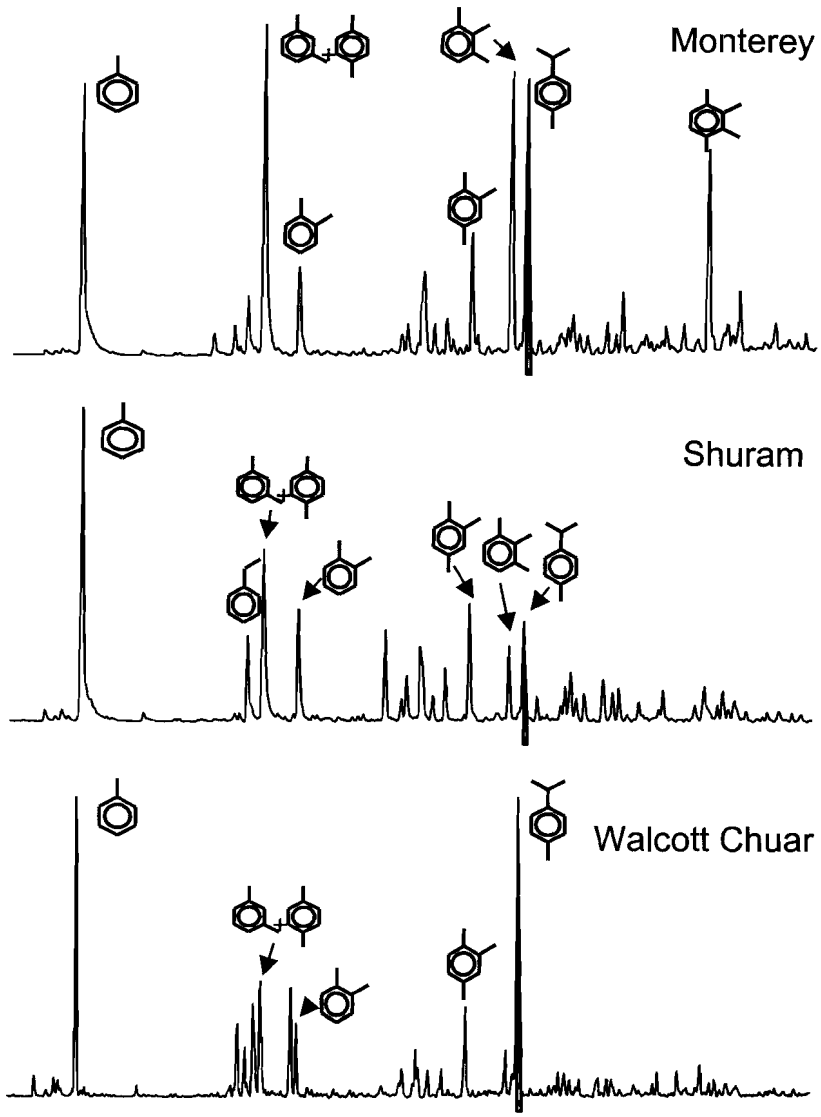

Figure 7.4 Summed mass chromatogram of *m/z* 91+92+105+106+ 119+120+133+134 of the alkylbenzenes (Hartgers *et al.*, 1992) in the flash pyrolysate of the kerogen of (**a**) the Monterey Formation (KG-1), (**b**) the Huqf and (**c**) the Walcott Chuar.

(**VIII**, Fig. 7.4b-c). The extract obtained after base hydrolysis of the Huqf kerogen (Fig. 7.5b) contained three monoterpenoid alcohols (as their TMS derivatives) of which two could be identified by coinjection with authentic standards as being borneol (**XXII**) and α-terpineol (**XXIII**). The stable carbon isotopic compositions of α-terpineol (**XXIII**) and fenchylalcohol (**XXI**) in the Huqf extract are ca. -34‰. The stable carbon isotopic compositions of α-terpineol (**XXIII**), fenchylalcohol (**XXI**) and borneol (**XXII**) in the Monterey extract are also ca. -34‰. No stable carbon isotopic compositions could be measured of borneol (**XXII**) in the Huqf extract because of its low concentration.

Unfortunately, when the kerogen isolation from the same Huqf sediment was repeated the above results could not be reproduced suggesting that the monoterpenoids are possibly not indigenous to this marine kerogen.

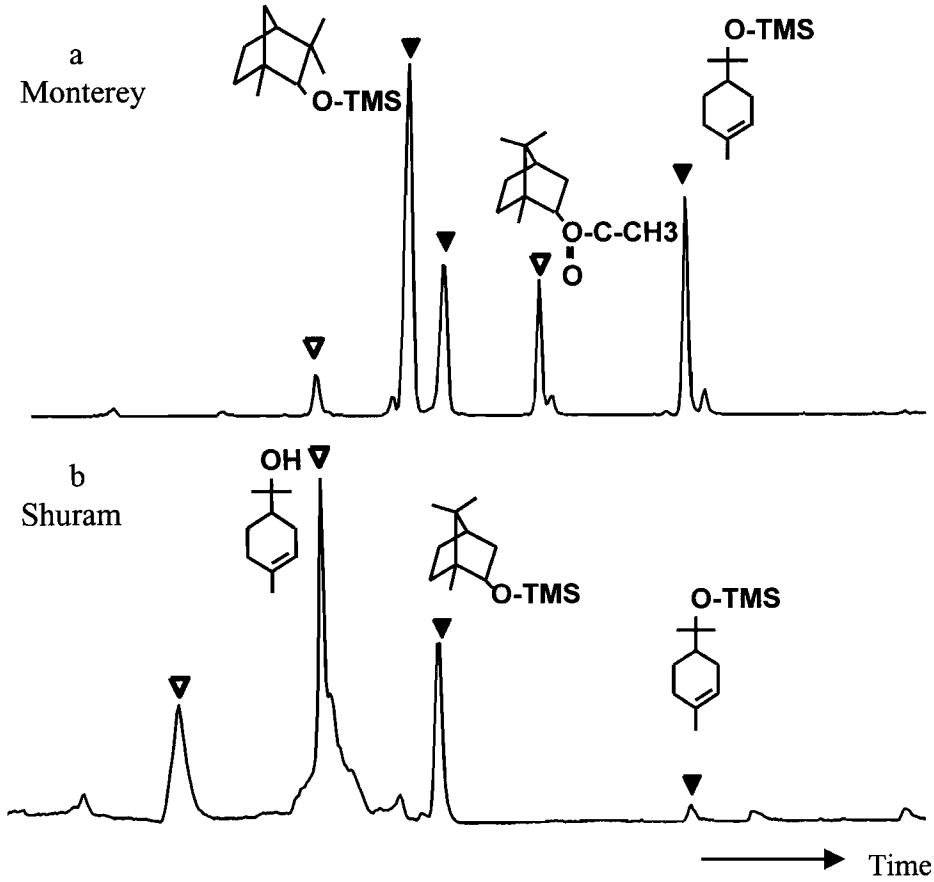

Figure 7.5 Summed mass chromatogram of *m/z* 136 of the released fraction after base hydrolysis of (**a**) the Monterey Formation (KG-1) and (**b**) the Huqf Formation. Filled triangles indicate the compounds that were identified using authentic standards. Open triangles indicate the compounds that were tentatively or not yet identified.

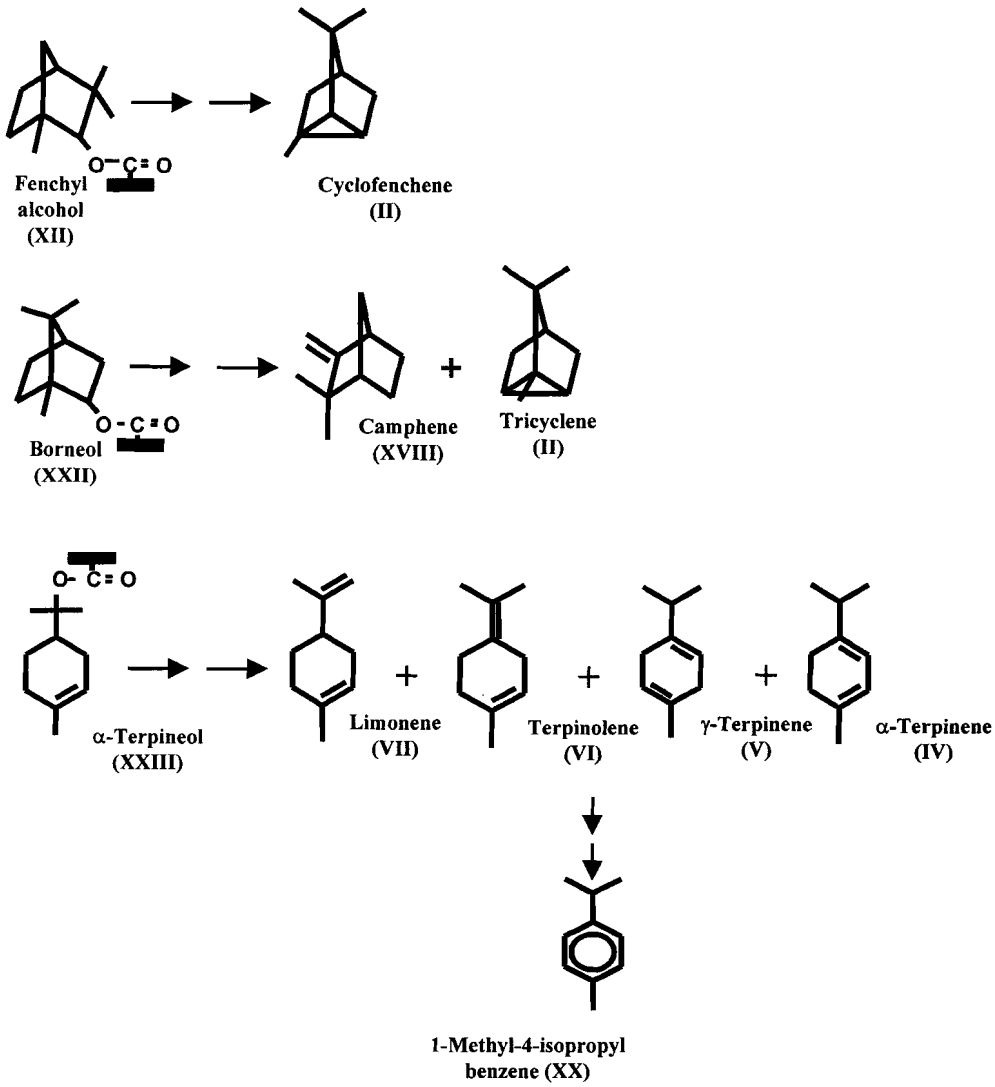

Figure 7.6 The rearrangement and aromatisation reactions of the ester bound monoterpenoids upon pyrolysis.

Identification of diterpenoids

Flash pyrolysis of the isolated kerogen from the Huqf Formation revealed the presence of diterpenoids (Fig. 7.6, Table 7.2). The mass spectra of the diterpenoids are shown in Fig. 7.7. Part of the diterpenoids could be identified by comparing their mass spectra with mass spectra reported in the literature (Table 7.2), the other diterpenoids were tentatively identified. The presence of methyl esters in the kerogen pyrolysate is not readily explained.

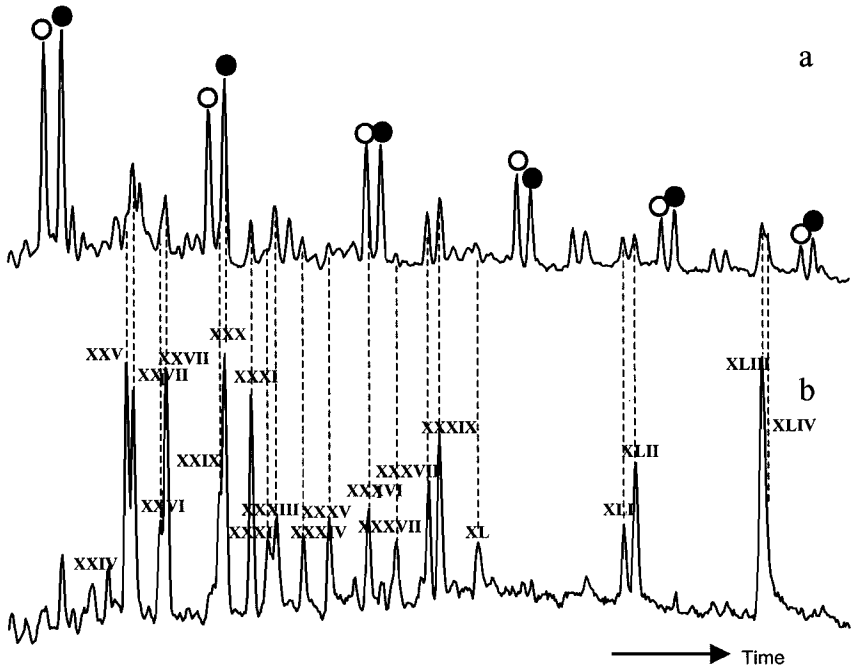

Figure 7.7 (**a**) Total Ion Current (TIC) trace and (**b**) summed mass chromatogram of *m/z* 159+183+185+195+197+199+211+219+221+223+234+236+237+238+239+240+241+252+254+285+299+300+312+314 of the flash pyrolysate (Curie temperature 610 °C) of the kerogen of the Huqf Formation. Filled and open circles indicate the homologous series of *n*-alkanes and *n*-alk-1-enes, respectively with the number of carbon atoms indicated.

To decipher the origin of these pyrolysis products, base hydrolysis was performed in order to hydrolyse the ester bonds present in the kerogen. Pyrolysis-GC-MS of the kerogen residue after hydrolysis indicated that no diterpenoids were present anymore, indicating that the precursors of these molecules were probably linked to the kerogen by ester bonds. The extract obtained after base hydrolysis of the kerogen (Fig. 7.8) and derivatization contained several diterpenoids that could be tentatively identified by mass spectra as the methyl esters of unsaturated hydroabietic acid (**XLI**), hydroabietic acid (**XLII-XLIII**), pimaric acid (**XLIV-XLV**), isopimaric acid (**XLVI**) and abietic acid (**XLVII**). The predominance of the abietanes over the pimaranes in the Huqf Fm. is not surprising since under thermal or other diagenetic conditions the pimarane skeleton converts to the abietane skeleton (Simoneit, 1977). The absence of diterpenoids with a pimarane carbon skeleton in the kerogen pyrolysate is probably due to their lower concentration.

Unfortunately, when the kerogen isolation from the same Huqf sediment was repeated the above results could not be reproduced suggesting that the diterpenoids are possibly not indigenous to this marine kerogen.

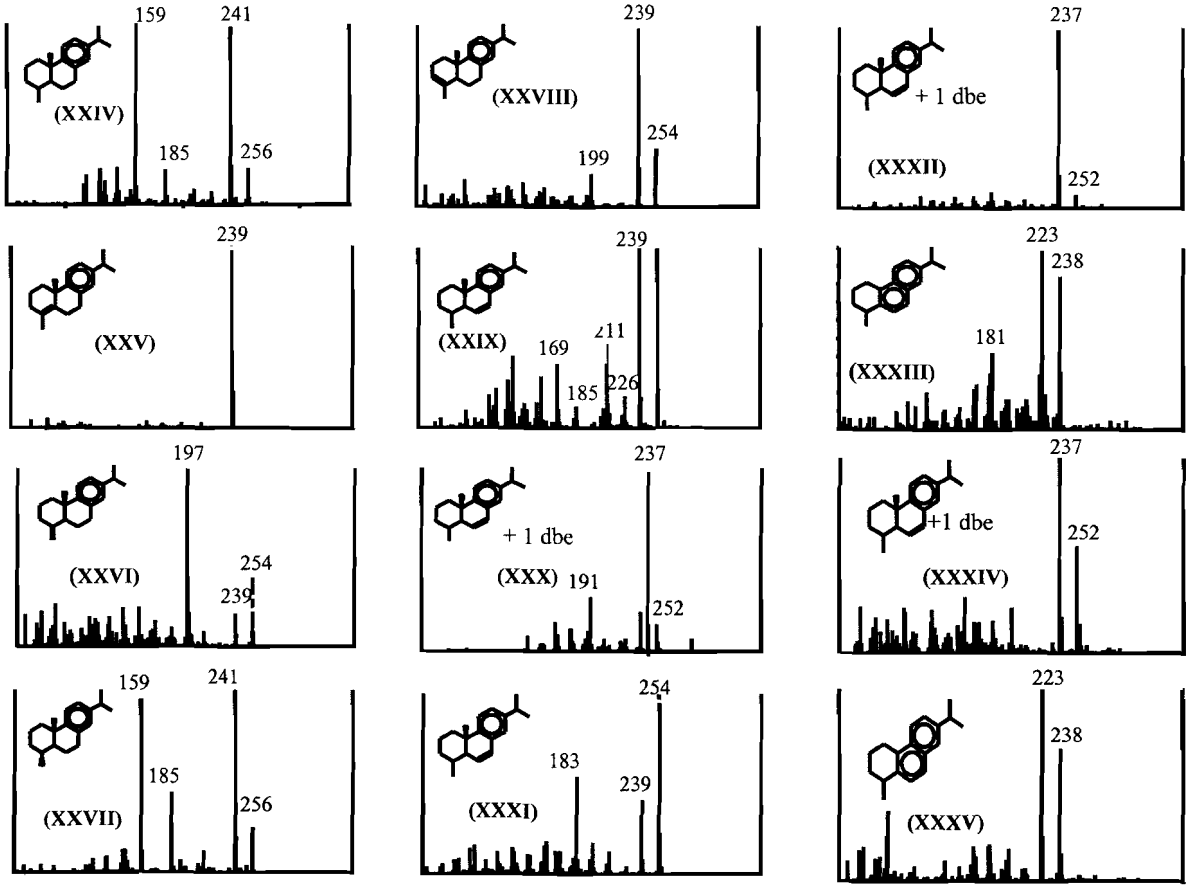
159
241
(XXIV)
185
256
239
(XXV)
197
(XXVI)
254
239
159
241
(XXVII)
185
256
239
(XXVIII)
199
254
239
(XXIX)
169
211
185
226
237
+ 1 dbe
(XXX)
191
252
254
(XXXI)
183
239
237
+ 1 dbe
(XXXII)
252
223
238
(XXXIII)
181
237
+1 dbe
(XXXIV)
252
223
238
(XXXV)

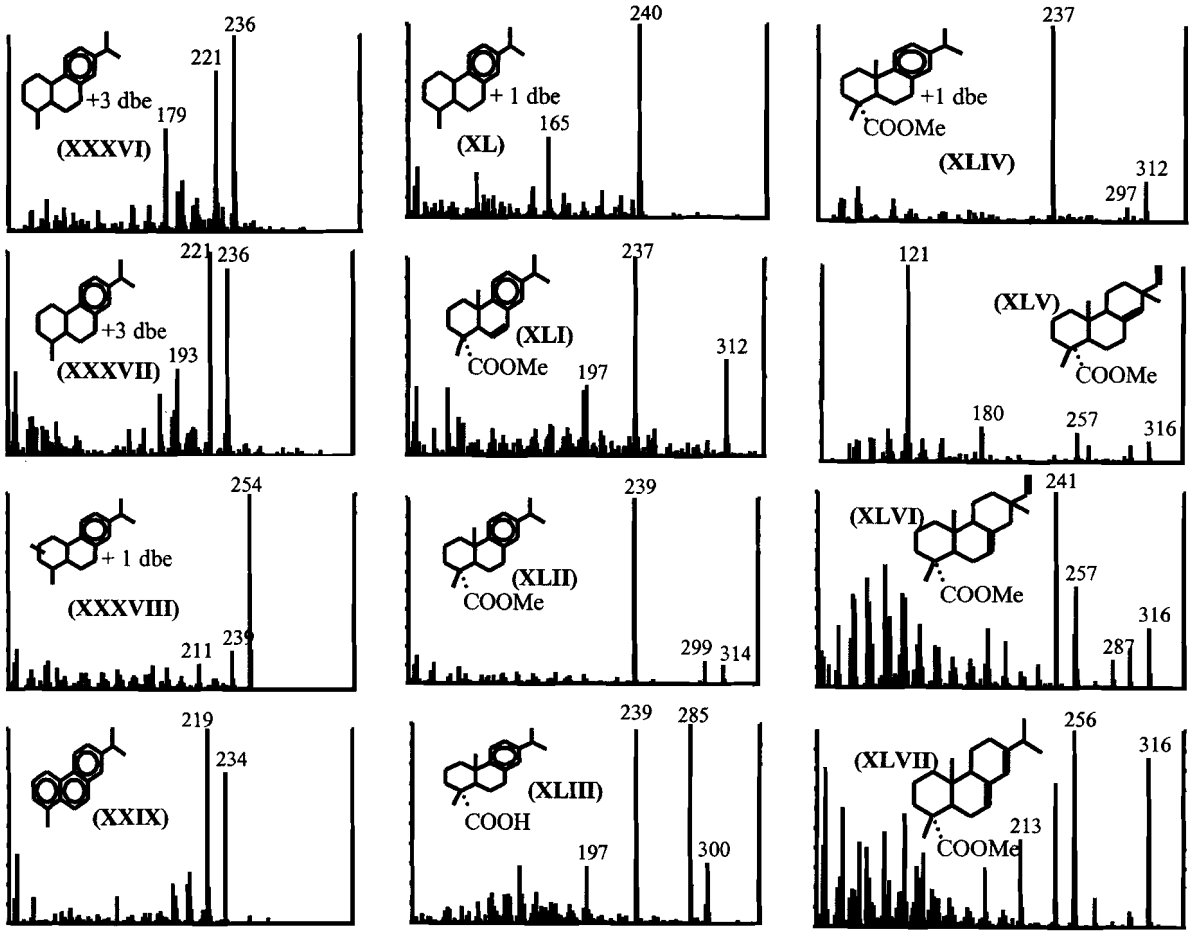

Figure 7.8 Mass spectra of tricyclic diterpenoids present in the flashpyrolysate of the Huqf kerogen (**XXIV-XLIV**) and released from the kerogen upon base hydrolysis (**XLI-XLVII**). Dbe = double bond equivalent.

7.5 Discussion

The results indicate that monoterpenoids and diterpenoids in these kerogen pyrolysates are formed from rearrangement reactions of ester bound precursors in some cases followed by aromatisation (Fig. 7.9). To the best of our knowledge this is the first time that these cyclic monoterpenoids have been identified in sediments. Similar cyclic diterpanes with abietane skeletons have been reported previously in the Precambrian Zhangjiakou chert (Wu et al., 1986; Wang et al., 1995).

Non-halogenated cyclic monoterpenoids with *p*-menthane-, camphane- and fenchane- skeletons have up till now been reported in most higher plant species and in aerosols in the proximity of forests (Johns, 1986). However, since vascular plants appeared only since the Silurian (400 Ma, Banks, 1975) and two samples are much older than 400 Ma, and contain predominantly marine organic matter, we have to invoke an algal or bacterial origin or we have to invoke a non-indigenous source for these compounds. Only Katayama (1955, 1962) identified non-halogenated cyclic monoterpenoids with a *p*-menthane carbon skeleton in some Chlorophyta, Phaeophyta and Rhodophyta.

Table 7.2: Diterpenoids found in the kerogen-pyrolysate or released after basic hydrolysis of the kerogen.

	name	formula	Mw	RI	MS Identification
XXIV	19-norabieta-8,11,13-triene	$C_{19}H_{28}$	256	1929	Simoneit, 1977; Wakeham *et al.*, 1980
XXV	19-norabieta-4(5),8,11,13-tetraene	$C_{19}H_{26}$	254	1940	Philp, 1985
XXVI	19-norabieta-4(18),8,11,13-tetraene	$C_{19}H_{26}$	254	1944	Simoneit, 1975
XXVII	18-norabieta-8,11,13-triene	$C_{19}H_{28}$	256	1961	Simoneit, 1977; Wakeham *et al.*, 1980
XXVIII	19-norabieta-3,8,11,13-tetraene	$C_{19}H_{26}$	254	1964	Philp, 1985
XXIX		$C_{19}H_{26}$	254	1997	
XXX		$C_{19}H_{24}$	252	2000	
XXXI		$C_{19}H_{26}$	254	2017	
XXXII		$C_{19}H_{24}$	252	2027	
XXXIII	1,2,3,4-tetrahydroretene	$C_{18}H_{22}$	238	2033	Simoneit, 1975; Wakeham *et al.*, 1980
XXXIV		$C_{19}H_{24}$	252	2050	
XXXV	1,2,3,4-tetrahydroretene	$C_{18}H_{22}$	238	2067	Simoneit, 1975; Wakeham *et al.*, 1980
XXXVI		$C_{18}H_{20}$	236	2092	
XXXVII		$C_{18}H_{20}$	236	2110	
XXXVII I		$C_{19}H_{26}$	254	2132	
XXXIX	retene	$C_{18}H_{18}$	234	2139	Simoneit 1977; Wakeham *et al.*, 1980
XL		$C_{18}H_{26}$	240	2164	
XLI		$C_{21}H_{28}O_2$	312	2265	McLafferty and Stauffer, 1989
XLII	methyl dehydroabietate	$C_{21}H_{30}O_2$	314	2273	Simoneit, 1977
XLIII	dehydroabietate	$C_{20}H_{28}O_2$	300	2363	McLafferty and Stauffer, 1989
XLIV		$C_{21}H_{28}O_2$	312	2364	
XLV	methyl pimarate	$C_{21}H_{32}O_2$	316		McLafferty and Stauffer, 1989
XLVI	methyl isopimarate	$C_{21}H_{32}O_2$	316		
XLVII	methyl abietate	$C_{21}H_{32}O_2$	316		

Both the monoterpenoids and diterpenoids identified in these sediments were ester-bound to the kerogen. Possibly the monoterpenoid and diterpenoid alcohols may occur ester-bound in marine biota and such structures may have become part of the kerogen. Alternatively, the alcohol groups of their precursors may have reacted after deposition with acid-groups in the kerogen matrix. This reaction could have occurred during the formation of kerogen, or upon acid treatment during kerogen isolation. The latter hypothesis implies that the precursors of these mono and diterpenoids were contaminants introduced during the isolation procedure. Additional circumstantial evidence for this is that the bulk stable carbon isotopic compositions of the Huqf extract and the Monterey extract differ ca. 14‰, but that the monoterpenoids in the Huqf extract and in the Monterey extract are isotopically relatively the same. Furthermore, when the kerogen isolation was repeated the results could not be reproduced. However, it must be noted that the isolations of these three kerogens were performed in two different laboratories, making it unlikely that exactly the same contaminants were introduced. Thus it is uncertain if the terpenoids identified in these sediments are indigenous to the kerogens and it seems more likely that they are laboratory artifacts. Confirmation of an indigenous origin would indicate that cyclic monoterpenoids and diterpenoids can no longer be used as terrestrial markers.

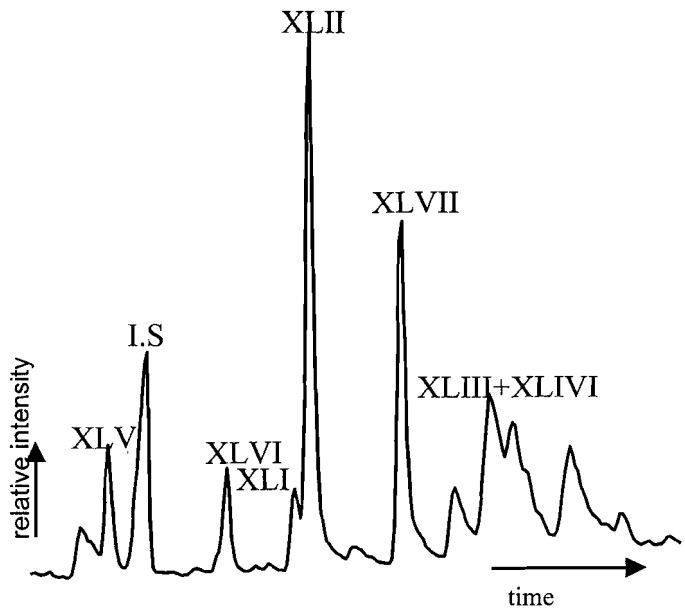

Figure 7.9 Summed mass chromatogram of *m/z* 121+237+239+241+ 253+256+285+298+300+302+312+314+316+328 of the fraction released from the Huqf kerogen after base hydrolysis.

7.6 Acknowledgements

Dr. R.E. Summons and Dr. M.E.L. Kohnen are thanked for provision of the Walcott Chuar kerogen and Huqf sediment, respectively. Dr. W. Pool is thanked for technical assistance and M. Dekker is acknowledged for performing GC-MS analyses. This study was supported by a PIONIER grant to JSSD from the Netherlands Organization for Scientific Research (NWO). This is NIOZ Contribution no. 3280.

Appendix

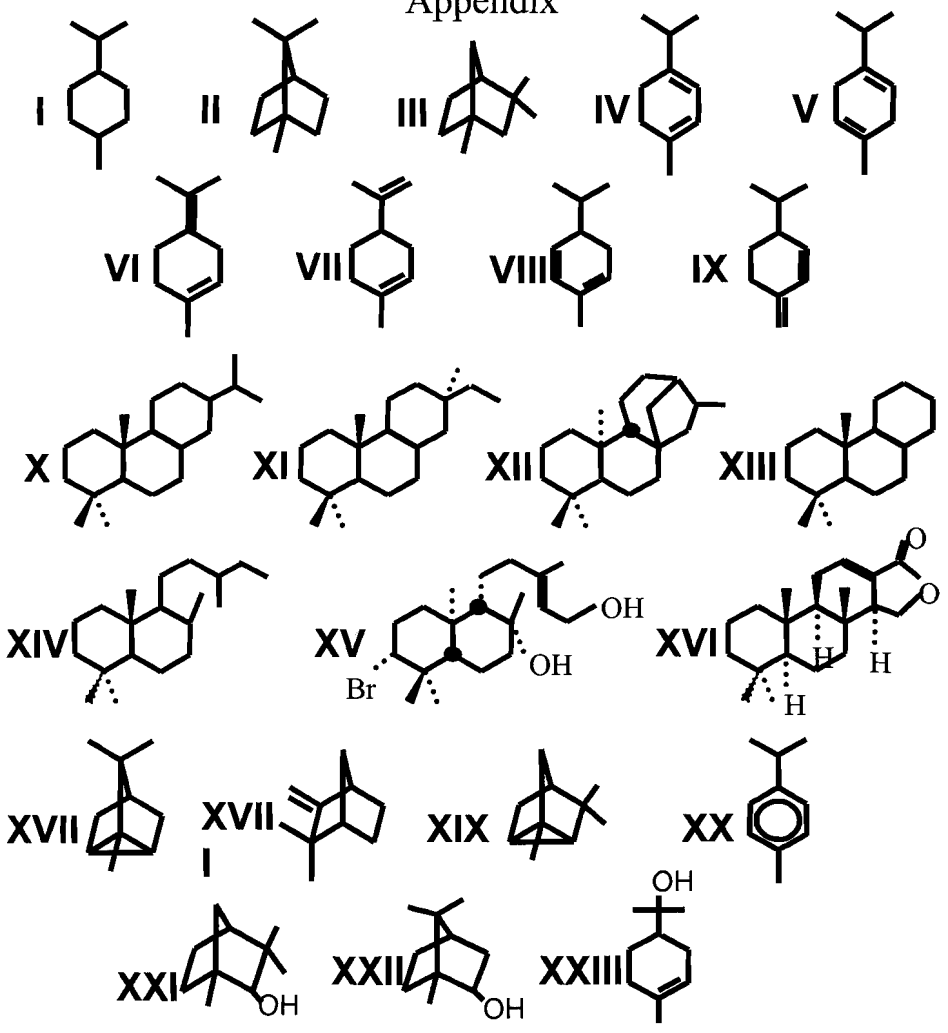

REFERENCES

Adam P., Philippe E. and Albrecht P. (1998) Photochemical sulfurization of sedimentary organic matter: A widespread process occurring at early diagenesis in natural environments? *Geochimica et Cosmochimica Acta* **62**, 265-272.

Ahmed M., Schouten S., Baas M. and de Leeuw J.W. (1999) Bound lipids in kerogens from the Miocene Monterey Formation: In *The Monterey Formation: From Rock to Molecule* (Ed. by J. Rullkötter & C. M. Isaacs), Colombia University Press, in press.

Aley A.A, Nash D.F., 1984. A summary of the geology and oil habitat of the eastern flank hydrocarbon province of South Oman. Proceedings OAPEC Seminar "Source and Habitat of Petroleum in the Arab countries", Kuwait, October, 1984.

Banks, H.P. (1975) Early vascular land plants: proof and conjecture. *Bioscience* **25**, 730-737.

Barnes M.A. and Barnes W.C. (1983) Oxic and anoxic diagnesis of diterpenes in lacustrine sediments. In *Advances in Organic Geochemsitry 1981* (Ed. by M. Bjoroy). Wiley, Chichester, pp. 289-298.

Behar F. and Pelet R. (1985) Pyrolysis-gas chromatography applied to organic geochemistry. Structural similarities between kerogens and asphaltenes from related rock extracts and oils. *Journal of Analytical and Applied Pyrolysis* **8**, 173-187.

Behar F., Derenne S. and Largeau C. (1995) Closed pyrolyses of the isoprenoid algaenan of *Botryococcus braunii, L* race: Geochemical implications for derived kerogens. *Geochimica et Cosmochimica Acta* **59**, 2983-2997.

Berkaloff C., Casadevall E., Largeau C., Metzger P., Peracca S. and Virlet J. (1983) The resistant polymer of the walls of the hydrocarbon-rich alga *Botryoccus Braunii. Phytochemistry* **22**, 389-397.

Beynon J.H. (1960) *Mass Spectrometry and its Application to Organic Chemistry.* Elsevier, Amsterdam, pp. 334.

Beynon J.H., Saunders R.A. and Williams A.E. (1968) *The Mass Spectra of Organic Molecules.* Elsevier, Amsterdam, pp. 103.

Blanc-Valleron M.-M. (1986) Enseignement géologiques tirés de l'étude systématique da la matière organique d'un bassin salifère. Le basin potassique de Mulhouse

(Alsace, France). *Comptes Rendus de l'Academie des Sciences Paris* **302**, 825-830.

Blokker P., Schouten S., van der Ende H., de Leeuw J.W., Hatcher P.G. and Sinninghe Damsté J.S. (1998) Chemical structure of algaenans from the fresh water algae *Tetraedron minimum, Scenedesmus communis* and *Pediastrum boryanum*. *Organic Geochemistry* **29**, 1453-1468.

Boon J.J. and de Leeuw J.W. (1987) Organic geochemical aspects of cyanobacterial mats. In: *The Cyanobacteria* (Ed. by F. Fay & C. v. Baalen), pp. 471-492. Elsevier, Amsterdam.

Boussafir M., Gelin F., Lallier-Vergès E., Derenne S., Bertrant P. and Largeau C. (1995) Electron microscopy and pyrolysis of kerogens from the Kimmeridge Clay Formation (U.K.): Source organisms, preservation processes and origin of microcycles. *Geochimica et Cosmochimica Acta* **59**, 3731-3748.

Brassell S.C., Eglinton G. and Maxwell J.R. (1983) The geochemistry of terpenoids and steroids. *Biochemical Society Transactions* **11**, 575-586.

Brassell S.C., Lewis C.A., de Leeuw J.W., de Lange F. and Sinninghe Damsté (1986) Isoprenoid thiophenes: novel diagenetic products in sediments? *Nature* **320**, 160-162.

Brassell S.C. (1993) Applications of biomarkers for delineating marine palaeoclimatic fluctuations during the Pleistocene. In *Organic Geochemistry: Principles and Applications* (Ed. by M.H. Engel and S.A. Macko), pp 699-738. Plenum Press, New York.

Bréhéret J.-G. (1994) The mid-Cretaceous organic-rich sediments from the Vocontian zone of the French Southeast Basin. *Hydrocarbon and Petroleum Geology of France, Special Publication of the European Association of Petroleum Geoscientists* **4**, 295-320.

Burnham A.K. (1989) On the validity of the Pristane Formation Index. *Geochimica et Cosmochimica Acta* **53**, 1693-1697.

Cardoso J., Watts C.D., Maxwell J.R., Goodfellow R., Eglinton G., Golubic S. (1978) A biochemical study of the Abu Dhabi algal mats: a simplified ecosystem. *Chemical Geology* **23**, 273-291.

Chappe B., Albrecht P. and Michaelis W. (1982) Polar lipids of archaebacteria in sediments and petroleum. *Science* **217**, 65-66.

Cox B.M. and Gallois R.W. (1981) The stratigraphy of the Kimmeridge Clay of the Dorset type area and its correlation with some other Kimmeridgian sequences. *Report Institute of Geological Sciences*, 1-44.

Craig H. (1957) Isotopic standards for carbon and oxygen and correction factors for massspectrometric analysis of carbon dioxide. *Geochimica et Cosmochimica Acta* **12**, 133-149.

Cranwell P.A. (1973) Branched-chain and cyclopropanoid acids in a recent sediment. *Chemical Geology* **11**, 307-313.

Curtis C.W., Guin J.A., Kwon K.C., Smith N.L., Mattson G.A., Rice A. and Worley S.D. (1983) Selectivity of coal minerals using cyclohexene as a probe reactant. *Fuel* **62**, 1341-1346.

Day W.C. and Erdman J.G. (1963) Ionene: A thermal degradation product of β-carotene. *Science* **141**, 808-810.

Derenne S., Largeau C., Casadevall E. and Berkaloff C. (1989) Occurrence of a resistant biopolymer in the L race of *Botryococcus Braunii*. *Phytochemistry* **28**, 1137-1142.

Derenne S., Largeau C., Casadevall E. and Sellier N. (1990) Direct relationship between the resistant biopolymer and the tetraterpenic hydrocarbon in the lycopadiene race of *Botryococcus Braunii*. *Phytochemistry* **29**, 2187-2192.

Derenne S., Largeau C., Casadevall E., Berkaloff C. and Rousseau B. (1991) Chemical evidence of kerogen formation in source rocks and oil shales via selective preservation of thin resistant outer walls of microalgae: Origin of ultralaminae. *Geochimica et Cosmochimica Acta* **55**, 1041-1050.

Derenne S., Berre F.L., Largeau C., Hatcher P., Connan J. and Raynaud J.F. (1992a) Formation of ultralaminae in marine kerogens via selective preservation of thin resistant outer walls of microalgae. *Organic Geochemistry* **19**, 345-350.

Derenne S., Largeau C., Berkaloff C., Rousseau B., Wilhelm C. and Hatcher P.G. (1992b) Non- hydrolyzable macromolecular constituents from outer walls of chlorella fusca and nanochlorum eucaryatum. *Phytochemistry* **31**, 1923-1929.

Derenne S., Metzger P., Largeau C., van Bergen P.F., Gatellier J.P., Sinninghe Damsté J.S., de Leeuw J.W. and Berkaloff C. (1992c) Similar morphological and chemical variations of *Gloeocapsomorpha prisca* in Ordovician sediments and cultured *Botryococcus braunii* as a response to changes in salinity. *Organic Geochemistry* **19**, 299-313.

Derenne S., Largeau C. and Behar F. (1994) Low polarity pyrolysis products of Permian to Recent Botryococcus-rich sediments: First evidence for the contribution of an isoprenoid algaenan to kerogen formation. *Geochimica et Cosmochimica Acta* **58**, 3703-3711.

DeRosa, M., and A. Gambacorta (1988) The lipids of archaebacteria. *Progression in Lipid Research* **27**, 153-175.

Dowling N.J.E., Widdel F., White D.C. (1986) Phospholipid ester-linked fatty acid biomarkers of acetate-oxidising sulphate reducers and other sulphide-forming bacteria. *Journal of General Microbiology* **132**, 1815-1825.

Dubreuil C., Derenne S., Largeau C., Berkaloff C. and Rousseau B. (1989) Mechanism of formation and chemical structure of Coorongite-I. Role of the resistant biopolymer and of the hydrocarbons of *Botryococcus braunii. Organic Geochemistry* **14**, 543-553.

Durand B. (1980) Sedimentary organic matter and kerogen. Definition and quantitative importance of kerogen. In: *Kerogen-Insoluble Organic Matter from Sedimentary Rocks* (Ed. by B. Durand), pp. 13-34. Editions Technip, Paris.

Durand B. and Nicaise G. (1980) Procedures for kerogen isolation. In: *Kerogen-Insoluble Organic Matter from Sedimentary Rocks* (Ed. by B. Durand), pp. 35-54. Editions Technip, Paris.

Eglinton T.I. (1988) An investigation into kerogens using pyrolysis methods. *PhD-dissertation.* University of Newcastle upon Tyne (UK), pp. 180.

Eglinton T.I., Sinninghe Damsté J.S., Kohnen M.E.L. and de Leeuw J.W. (1990) Rapid estimation of organic sulfur content of kerogens, coals and asphaltenes by flash pyrolysis-gas chromatography. *Fuel* **69**, 1394-1404.

Eglinton T., Fry B.D., Freeman K.H. and Hayes J.M. (1991) Carbon-isotopic compositions of products from flash pyrolysis of kerogens. In: *Organic Geochemistry. Advances and Applications in Energy and the Natural Environment.* (Ed. by D. A. C. Manning), pp. 411-416, Manchester University Press, Manchester.

Eglinton T.I. (1994) Carbon isotopic evidence for the origin of macromolecular aliphatic structures in kerogen. *Organic Geochemistry* **21**, 721-735.

Fenical W. (1978) Diterpenoids. In *Marine Natural Products. Chemical and Biological Perspectives 2* (Ed. by P. J. Scheuer). Academic Press, pp. 173-245.

Flesch G. and Rohmer M. (1988) Prokaryotic hopanoids: the biosynthesis of bacteriohopane skeleton. *European Journal of Biochemistry* **175**, 405-411.

Fowler M.G. and Douglas A.G. (1987) Saturated hydrocarbon biomarkers in oils of Late Precambrian age from Eastern Siberia. *Organic Geochemistry* **11**, 201-213.

Freeman K.H., Hayes J.M., trendel J-M. and Albrecht P. (1990) Evidence from GC-MS carbon-isotopic measurements for multiple origins of sedimentary hydrocarbons. *Nature* **353**, 254-256.

Freeman K.H., Boreham C.J., Summons R.E. and Hayes J.M. (1994) the effect of aromatization on the isotopic compositions of hydrocarbons during early diagenesis. Organic Geochemistry **21**, 1037-1049.

Fry B. and Sherr E. (1984) Delta ^{13}C measurements as indicators of carbon flow in marine and freshwater ecosystems. *Contribibutions to Marine Sciences* **27**, 13-47.

Fry B., Brand W., Mensch F.J., Tholke K. and Garritt R. (1992) Automated analysis system for coupled ^{13}C and ^{15}N measurements. *Analytical Chemistry* **64**, 288-291.

Fukushima K., Yasukawa M., Muto N., Uemera H. and Ishiwatari R. (1992) formation of C_{20} isoprenoid thiophenes in modern sediments. *Organic Geochemistry* **18**, 83-92.

Gearing J.N. (1988) The use of stable isotope ratios for tracing nearshore-offshore exchange of organic matter. In: *Lecture Notes on Coastal and Estuarine Studies, Vol. 22. Coastal-Offshore Ecosystems Interactions* (Ed. by B.-O. Jansson), pp. 69-101 Springer, Berlin.

Gelin F., Gatelier J.-P.L.A., Sinninghe Damsté J.S., Metzger P., Derenne S., Largeau C. and de Leeuw J.W. (1993) Mechanisms of flash pyrolysis of ether lipids isolated from the green microalgae *Botryococcus braunii* race L. *Journal of Analytical and Applied Pyrolysis* **27**, 155-168.

Gelin F., Sinninghe Damsté J.S., Derenne S., Largeau C., Metzger P. and de Leeuw J.W. (1994) Scope and limitations of flash pyrolysis-gas chromatography/mass spectrometry as revealed by the thermal behaviour of high-molecular-weight lipids derived from the green microalga *Botyococcus braunii. Journal of Analytical and Applied Pyrolysis* **28**, 183-204.

Gelin F., Sinninghe Damsté J.S., Harrison W.N., Maxwell J.R. and de Leeuw J.W. (1995) Molecular indicators for palaeoenvironmental change in a Messinian evaporitic sequence (Vena del Gesso, Italy): III. Stratigraphic changes in the molecular structure of kerogen in a single marl bed as revealed by flash pyrolysis. *Organic Geochemistry* **23**, 555-566.

Gelin F., Boogers I., Noordeloos A.A.M., Sinninghe Damsté J.S., Hatcher P.G. and de Leeuw J.W. (1996a) Novel, resistant microalgal polyethers: An important sink of organic carbon in the marine environment. *Geochimica et Cosmochimica Acta* **60**, 1275-1280.

Gelin F., Sinninghe Damsté J.S., Harrison W.N., Reis C., Maxwell J.R. and de Leeuw J.W. (1996b) Variations in origin and composition of kerogens constituents as revealed by analytical pyrolysis of immature kerogens before and after desulphurization. *Organic Geochemistry* **24**, 705-714.

Gelin F., Boogers, I., Noordeloos, A.A.M., Sinninghe Damsté J.S., Riegman R. and de Leeuw, J.W. (1997) Resistant biomacromolecules in marine microalgae of the classes Eustigmatophyceae and Chlorophyceae: geochemical implications. *Organic Geochemistry* **26**, 659-675.

Gelin F., Volkman J.K., Largeau C., Derenne S., Sinninghe Damsté J.S. and de Leeuw J.W. (1999) Distribution of aliphatic, nonhydrolyzable biopolymers in marine microalgae. *Organic Geochemstry* **30**, 147-159.

Gelpi E., Schneider H., Mann J., Oro J. (1970) Hydrocarbons of geochemical significance in microscopic algae. *Phytochemistry* **9**, 603-612.

Gibbons M.J. (1978) The geochemistry of sabkha and related deposits. Ph.D. thesis, University of Newcastle-upon-Tyne.

Gillan F.T. and Johns R.B. (1980) Input and early diagenesis of chlorophylls in a temperate intertidal sediment. *Marine Chemistry* **9**, 243-253.

Goericke R., Montoya J.P. and Fry B. (1994) Physiology of isotope fractionation in algae and cyanobacteria. In: *Stable Isotopes in Ecology and Environmental Science* (Ed. by K. Lajtha and R. H. Michener), pp. 187-221. Blackwell Scientific Publications, Oxford.

Goldfine H. (1972) Comparative aspects of bacterial lipids. *Advanced Microbiological Physiology* **8**, 1-58.

Goossens H., de Leeuw J.W., Schenck P.A. and Brassell S.C. (1984) Tocopherols as likely preursors of pristane in ancient sediments and crude oils. *Nature* **312**, 440-442.

Goossens H., Due A., de Leeuw J.W. , van de Graaf B. and Schenck P.A. (1988) A simple method to assess maturity by pyrolysis/evaporation-gas chromatography of unextracted samples. *Geochimica et Cosmochimica Acta* **52**, 1189-1193.

Goossens H., de Leeuw J.W., Rijpstra W.I.C., Meyburg G.J. and Schenck P.A. (1989) Lipids and their mode of occurrence in bacteria and sediments - I. A methodological study of the lipid composition of *Acinetobacter calcoaceticus* LMD 79-41. *Organic Geochemistry* **14**, 15-25.

Gorin G.E., Racz L.G., Walter M.R. (1982) Late Precambrian-Cambrian sediments of Huqf group, Sultanate of Oman. *The American Association of Petroleum Geologists Bulletin* **66**, 2609-2627.

Goth K., de Leeuw J.W., Püttmann W. and Tegelaar E.W. (1988) Origin of Messel Oil Shale kerogen. *Nature* **336**, 759-761.

de Graaf W., Sinninghe Damsté J.S. and de Leeuw J.W. (1992) Laboratory simulation of natural sulfurization I. Formation of monomeric and oligomeric isoprenoid polysulphides by low-temperature reactions of inorganic polysulphides with phytol and phytadienes. *Geochimica et Cosmochimica Acta* **56**, 4321-4328.

de Graaf W., Sinninghe Damsté J.S. and de Leeuw J.W. (1995) Low-temperature addition of hydrogen polysulphides to olefins: Formation of 2,2'-dialkyl polysulphides from alk-1-enes and cyclic (poly)sulfides and polymeric organic sulphur compounds from α,ω-dienes. *Journal of the Chemical Society Perkins Trans I*, 635-640.

van Graas G., de Leeuw J.W. and Schenck P.A. (1980) Characterization of coals and sedimentary organic matter by Curie-point pyrolysis-mass spectrometry. Part I. *Journal of Analytical and Applied Pyrolysis* **2**, 265-276.

van Graas G., de Leeuw J.W. and Schenck P.A. (1981) Kerogen of Toarcian shales of the Paris Basin. A study of its maturation by flash pyrolysis techniques. *Geochimica et Cosmochimica Acta* **45**, 2465-2474.

Grantham P.J. (1986) The occurrence of unusual C_{27} and C_{29} sterane predominances in two type of Oman crude oil. *Organic Geochemistry* **9**, 1-10.

Grantham P.J., Lijmbach G.W.M., Posthuma J., Clarke M.W.H, Willink R.J. (1988) Origin of crude oils in Oman. *Journal of Petroleum Geology* **11**, 61-80.

Gray N.R., Lancaster C.J. and Gethner J. (1991) Chemometric analysis of pyrolysis compositions: A model for predicting the organic matter type of source rocks using pyrolysis-gas chromatography. *Journal of Analytical and Applied Pyrolysis* **20**, 87-106.

Grimalt J.O., Simoneit B.R.T., Hatcher P.G. and Nissenbaum A. (1988) The molecular composition of ambers. *Organic Geochemistry* **13**, 677-690.

Hagemann H.W. and Hollerbach A. (1980) Relationship between the macropetrographic and organic geochemical composition of lignites. In *Advances in Organic Geochemistry 1979* (Ed. by A. G. Douglas and J. R. Maxwell). Pergamon, Oxford, pp. 631-638.

Hartgers W.A., Sinninghe Damsté J.S. and de Leeuw J.W. (1992) Identification of C_2-C_4 alkylated benzenes in flash pyrolysates of kerogens, coals and asphaltenes. *Journal of Chromatography* **606**, 211-220.

Hartgers W.A., Sinninghe Damsté J.S. and de Leeuw J.W. (1994a) Geochemical significance of alkylbenzene distributions in flash pyrolysates of kerogen. *Geochimica et Cosmochimica Acta* **58**, 1759-1775.

Hartgers W.A., Sinninghe Damsté J.S., Requejo A.G., Allan J., Hayes J.M. Ling Y., Xie T-M., Primack J. and de Leeuw J.W. (1994b) A molecular and carbon isotope study towards the origin and diagentic fate of diaromatic carotenoids. *Organic Geochemistry* **22**, 703-725.

Hartgers W.A., Sinninghe Damsté J.S., de Leeuw J.W., Ling Y. and Dyrkacz G.R. (1994c) Molecular characterization of flash pyrolysates of two carboniferous coals and their constituting maceral fracions. *Energy Fuels* **8**, 1055-1067.

Hartgers W.A., Sinninghe Damsté J.S. and de Leeuw J.W. (1995) Curie Point pyrolysis of sodium salts of functionalized fatty acids. *Journal of Analytical and Applied Pyrolysis* **34**, 191-217.

Hatcher P.G., Spiker E.C., Szeverenyi N.M. and Maciel G.E. (1983) Selective preservation and origin of petroleum-forming aquatic kerogen. *Nature* **305**, 498-501.

Hayes J.M. (1993) Factors controlling ^{13}C contents of sedimentary organic compounds: Principles and evidence. *Marine Geology* **113**, 111-125.

ten Haven H.L., de Leeuw J.W., Peakman T.M. and Maxwell J.R. (1986) Anomalies in steroid and hopanoid maturity indices. *Geochimica et Cosmochimica Acta* **50**, 853-855.

ten Haven H.L., Baas M., de Leeuw J.W. and Schenck P.A. (1987) Late Quarternary Mediterranean Sapropels. I-On the origin of organic matter in Sapropel S_7. *Marine Geology* **75**, 137-156.

ten Haven H.L., Eglinton G., Farrimond P., Kohnen M.E.L., Poynter J.G., Rullkötter J. and Welte D.H. (1992) Variations in the content and composition of organic matter in sediments underlying active upwelling regimes: a study from ODP Legs 108, 112 and 117. In *Upwelling Systems: Evolution Since the early*

Miocene 64 (Ed. by C. P. Summerhayes, W. L. Prell and K. C. Emeis), pp. 229-246. Geological Society Special Publications.

Hefter J., Hauke V., Richnow H.H. and Michaelis W. (1995) Alkanoic subunits in sulphur-rich geomacromolecules. *ACS Symposium Series* **612**, 93-109.

Heppenheimer H., Steffens K., Püttmann W. and Kalkreuth W. (1992) Comparison of resinite-related aromatic biomarker distributions in Cretaceous-Tertiary colas form Canada and Germany. *Organic Geochemistry* **18**, 273-287.

Hoefs M.J.L., van Heemst J.D.H., Gelin F., Koopmans M.P. van Kaam-Peters H.M.E., Schouten S., de Leeuw J.W. and Sinninghe Damsté J.S. (1995) Alternative biological sources for 1,2,3,4-tetramethylbenzene in flash pyrolysates of kerogen. *Organic Geochemistry* **23**, 975-979.

Hoefs M.J.L., Schouten S., de Leeuw J.W., King L.L., Wakeham S.G. and Sinninghe Damsté J.S. (1997) Ether lipids of planktonic archae in marine water column. *Applied and Environmental Microbiology* **63**, 3090-3095.

Hoering T.C. (1976) Molecular fossils from the Precambrian Nonesuch Shale. *Carnegie Institute Washington Yearbook* **72**, 682-690.

Hoering T.C. (1981) Monomethyl, acyclic hydrocarbons in petroleum and rock extracts. *Carnegy Institute Washington Yearbook* **80**, 389-393.

Hoffman I.C., Hutchison J., Robson J.N., Chicarelli M.I. and Maxwell J.R. (1992) Evidence for sulphide links in a crude oil asphaltene and kerogens from reductive cleavage by lithium in ethylamine. *Organic Geochemistry* **19**, 371-388.

Hofmann K., Lucas R.A., Sax S.M. (1952) The chemical nature of the fatty acids of Lactobacillus arobinosus. *Journal of Biological Chemistry* **195**, 473-485.

Hofmann P., Huc A.Y., Carpentier B., Schaeffer P., Albrecht P., Keely B., Maxwell J.R., Sinninghe Damsté J.S., de Leeuw J.W. and Leythauser D. (1993) Organic matter of the Mulhouse Basin, France: a synthesis. *Organic Geochemistry* **20**, 1105-1123.

Höld I.M., Schouten S., van Kaam-Peters H.M.E. and Sinninghe Damsté J.S. (1998a) Recognition of *n*-alkyl and isoprenoid biopolymers in marine sediments by stable carbon isotopic analysis of pyrolysis products of kerogens. *Organic Geochemistry* **28**, 179-195.

Höld I.M., Brussee N.J., Schouten S., Sinninghe Damsté J.S. (1998b) Changes in the molecular structure of a type II-S kerogen (Monterey Formation, USA) during sequential chemical degradation. *Organic Geochemistry* **29**, 1403-1417.

Höld, I.M., Schouten, S., Van der Gaast, S.J. and Sinninghe Damsté, J.S., 1999. On the origin of prist-1-ene and prist-2-ene in kerogen pyrolysates. Submitted.

Höld I.M., Schouten S., Hargers W.A. and Sinninghe Damsté J.S. (2000) Evidence for sequestered non-aromatic carotenoids in kerogens. *In prep.*

Hollander D.J., Sinninghe Damsté J.S., Hayes J.M., de Leeuw J.W. and Huc A.Y. (1993) Molecular and bulk isotopic analysis of organic matter in marls of the Mulhouse Basin (Tertiary, Alsace, France). *Organic Geochemistry* **20**, 1253-1263.

Horsfield B. (1989) Practical criteria for classifying kerogens: some observations from pyrolysis-gas chromatography. *Geochimica et Cosmochimica Acta* **53**, 891-901.

Huang D., Daijang Z., Jinchao L. (1994) The origin of 4-methyl steranes and pregnanes from Tertiary strata in the Qaidam Basin, China. *Organic Geochemistry* **22**, 343-348.

Ioppolo-Armanios M., Alexander P. and Kagi R.I. (1994) Identification and origins of isopropylmethylphenols in crude oils. *Organic Geochemistry* **22**, 815-823.

Isaacs C.M., Thomson J.H., Lewan M.D., Arends R.G., Cotton M.L. and Filewicz M.V. (1992) Preliminary correlation and age of rock samples (KG-1 to KG-24) in the cooperative Monterey organic geochemistry study, Santa Barbara and Santa Barbara-Ventura basins, California. *U.S. Geological Survey Internal Report*, pp. 1-12.

Ishiwatari M. (1991) Pyrolysis of chlorophyll a after preliminary heating at a moderate temperature: implications for the origin of prist-1-ene on kerogen pyrolysis. *Journal of Analytical and Applied Pyrolysis* **18**, 207-218.

Jackson M.J., Powell T.G., Summons R.E., Sweet I.P. (1986) Hydrocarbon shows and petroleum source rocks in sediments as old as 1.7 x 10^9 years. *Nature* **322**, 727-729.

Jacques N.A. and Hunt A.L. (1980) Studies on cyclopropane fatty acid synthesis-effect of carbon source and oxygen tension on cyclopropane fatty acid synthesis activity in Pseudomanas dentrificans. *Biochimica et Biophysica Acta* **619**, 453-470.

Jenisch A., Richnow H.H. and Michaelis W. (1990) Chemical structural units of macromolecular coal components. *Organic Geochemistry* **16**, 917-929.

Jensich-Anton A., Adam P., Schaeffer P. and Albrecht P. (1999) Oxygen-containing subunits in sulfur-rich nonpolar macromolecules. *Geochimica et Cosmochimica Acta* **63**, 1059-1074.

Johns R.B. (1986) Biological markers in the sedimentary record. In: *Methods in Geochemistry and Geophysics* **24**, Elsevier, Amsterdam, pp. 286.

van Kaam-Peters H.M.E., Schouten S., Köster J., de Leeuw J.W. and Sinninghe Damsté J.S. (1997a) A molecular and carbon isotope biogeochemical study of biomarkers and kerogen pyrolysate of the Kimmeridge Clay Formation: Paleoenvironmental implications. *Organic Geochemistry* **27**, 399-422.

van Kaam-Peters H.M.E. and Sinninghe Damsté J.S. (1997b) Characterization of an extremely organic sulfur-rich, 150 Ma old carbonaceous rock: Palaeoenvironmental implications. *Organic Geochemistry* 27, 371-397.

van Kaam-Peters H.M.E., Schouten S., Köster J., Brüchert V. and Sinninghe Damsté J.S. (1997c) Palaeoclimatical control on the bulk, molecular, carbon and sulfur isotopic composition of organic matter of the Kimmeridge Clay facies. 18th International Meeting on Organic Geochemistry, Maastricht, Abstracts Part II, pp. 655-656.

van Kaam-Peters H.M.E., Köster J., de Leeuw J.W., Sinninghe Damsté J.S. (1997d) Occurrence of two novel benzothiophene hopanoid families in sediments. *Organic Geochemistry* **23**, 607-616.

van Kaam-Peters H.M.E., Köster J., van der Gaast S.J., Sinninghe Damsté J.S. and de Leeuw J.W. (1998) The effect of clay minerals on diasterane/sterane ratios. *Geochimica et Cosmochimica Acta* **62**, 2969-2975.

Kadouri A., Derenne S., Largeau C., Casadevall E. and Berkaloff C. (1988) Resistant biopolymer in the outer walls of *Botryococcus braunii*, B race. *Phytochemistry* **27**, 551-557.

Katayama T. (1955) The volatile constituents of seaweed, III-IV. *Ulva pertusa*, Enteromorpha species and *Sargassum* species. *Bull. JPN. Soc. Sci. Fish.* **21**, 412-428.

Katayama T. (1962) Volatile Constituents. In *Physiology and Biochemistry of Algae* (Edited by R. A. Lewis). Academic Press, New York, pp. 467-473

Kates M. (1978) The phytanyl ether linked polar lipids and isoprenoid neutral lipids of extremely halophilic bacteria. *Progress in Chemistry of Fats and Lipids* **15**, 301-342.

Keely B.J., Blake S.R., Schaeffer P. and Maxwell J.R. (1995) Distribution of pigments in the organic matter of marls from the Vena del Gesso evaporitic sequence. *Organic Geochemistry* **23**, 527-539.

Kenig F., Sinninghe Damsté J.S., Kock-van Dalen A.C., Rijpstra W.I.C., Huc. A.Y., de Leeuw J.W. (1995) Occurrence and origin of mono-, di, and trimethylalkanes in modern and holocene cyanobacterial mats from Abu Dhabi, United Arab Emirates. *Geochimica et Cosmochimica Acta* **59**, 2999-3015.

Kissin Y.V., Feulmer G.P. and Payne W.B. (1986a) Gas chromatographic analysis of polymethyl-substituted alkanes. *Journal of Chromatographic Science* **24**, 164-169.

Kissin Y.V. (1986b) Catagenisis and composition of petroleum: Origin of n-alkanes and isoalkanes in petroleum crudes. *Geochimica et Cosmochimica Acta* **51**, 2445-2457.

Klok J., Baas M., Cox H.C., de Leeuw J.W., Rijpstra W.I.C. and Schenck P.A. (1984) Qualitative and quantitative characterization of the total organic matter in a recent marine sediment (Part II). *Organic Geochemistry* **6**, 265-278.

Klomp U.C. (1986) The chemical structure of a pronounced series of iso-alkanes in South Oman crudes. *Organic Geochemistry* **10**, 807-814.

Koga Y., Nishihara M., Morii H. and Akagawa-Matsushita M. (1993) Ether lipids of methanogenic bacteria: Structures, comparitative aspects and biosyntheses. *Microbiological Reviews* **57**, 164-182.

Kohnen M.E.L., Schouten, S., Sinninghe Damsté J.S., de Leeuw J.W., Merrit D.A. and Hayes J.M. (1992) Rcognition of papaeobiochemicals by a combine molecular sulfur and isotope geochemical approach. *Science* **256**, 358-362.

Kok M.D., Osinga R., Schouten S. and Sinninghe Damsté J.S. (1997) Formation of sulphur-rich kerogen by the incorporation of inorganic sulphur species into algal sugars. 18th International Meeting on Organic Geochemistry, Maastricht, Abstracts Part II, pp. 665-666.

Koopmans M.P., de Leeuw J.W., Lewan M.D. and Sinninghe Damsté J.S. (1996a) Impact of dia- and catagenesis on sulphur and oxygen sequestration of biomarkers as revealed by artificial maturation of an immature sedimentary rock. *Organic Geochemistry* **25**, 391-426.

Koopmans M.P., Köster J., van Kaam-Peters H.M.E., Kenig F., Schouten S., Hartgers W.A., de Leeuw J.W. and Sinninghe Damsté J.S. (1996b) Diagenetic and catagenetic products of isorenieratene: Molecular indicators for photic zone anoxia. *Geochimica et Cosmochimica Acta* **60**, 4467-4496.

Koopmans M.P., Reiss-Schaeffer C., de Leeuw J.W., Lewan M.D., Maxwell J.R., Schaeffer P. and Sinninghe Damsté J.S. (1997a) Sulphur and oxygen sequestration of n-C_{37} and n-C_{38} unsaturated ketones in an immature kerogen and the realease of their carbon skeletons during early stages of thermal maturations. *Geochimica et Cosmochimica Acta* **61**, 2397-2408.

Koopmans M.P., de Leeuw J.W. and Sinninghe Damsté J.S. (1997) Novel cyclised and aromatised diagentic products of β-carotene in the Green River Shale. *Organic Geochemistry* **26**, 451-466.

Koopmans M.P., Rijpstra W.I.C., de Leeuw J.W., Lewan M.D., Sinninghe Damsté J.S. (1998) Artificial maturation of an immature sulphur- and organic-rich limestone from the Ghareb Formation, Jordan. *Organic Geochemistry* **28**, 503-521.

Koopmans M.P., Rijpstra W.I.C., Klapwijk M.M., de Leeuw J.W., Lewan M.D. and Sinninghe Damsté J.S. (1999) A thermal and chemical degradation approach to decipher pristane and phytane precursors in sedimentary organic matter. *Organic Geochemistry* in press.

Köster J., van Kaam-Peters H.M.E., Koopmans M.P., de Leeuw J.W., Sinninghe Damsté J.S. (1997) Sulphurisation of homohopanois: Effects on carbon number distribution, speciation, and 22S/22R epimer ratios. *Geochimica et Comochimica Acta* **61**, 2431-2452.

Krein E.B. and Aizenshtat Z. (1994) The formation of isoprenoid sulfur compounds during diagenesis: Simulated sulfur incorporation and thermal transformation. *Organic Geochemistry* **21**, 1015-1025.

Krein E.B. and Aizenshtat Z. (1995) Proposed thermal pathways for sulfur transformations in organic macromolecules: Laboratory simulation experiments. In *Geochemical Transformations of Sedimentary Sulfur* (Ed. by M.A. Vairavamurthy and M.A. Schoonen), *ACS Symposium Series 612*, pp. 110-137. Amer. Chem. Soc., Washington.

LaFlamme R.E. and Hites R.A. (1978) The global distribution of polycyclic aromatic hydrocarbons in Recent seidments. *Geochimica et Cosmochimica Acta* **42**, 289-303.

Langenheim J.H. (1969) Amber: a botanical inquiry. *Science* **163**, 1157-1168.

Largeau C., Casadevall E., Kadouri A. and Metzger P. (1984) Formation of *Botryococcus*-derived kerogens-Comparitive study of immature torbanites and of the extant alga *Botryococcus braunii*. *Organic Geochemistry* **6**, 327-332.

Largeau C., Derenne S., Casedevall E., Kadouri A. and Sellier N. (1986) Pyrolysis of immature Torbanite and of the resistant biopolymer (PRB A) isolated from extant alga *Botryococcus braunii*. Mechanism of formation and structure of Torbanite. *Organic Geochemistry* **10**, 1023-1032.

Largeau C., Derenne S., Casedevall E., Berkaloff C., Corolleur M., Lugardon B., Raynaud J.F. and Connan J. (1990a) Occurrence and origin of "ultralaminar" structures in "amorphous" kerogens of various source rocks and oil shales. *Organic Geochemistry* **16**, 889-895.

Largeau C., Derenne S., Clairay C., Casedevall E., Raynaud J.F., Lugardon B., Berkaloff C., Corolleur M. and Rousseau B. (1990b) Characterization of various kerogens by Scanning Electron Microscopy (SEM) and Transmission Electron Microscopy (TEM). Morphological relationships with resistant outer walls in extant micro-organisms. *Mededelingen Rijks Geologische Dienst* **45**, 91-101.

Larter S.R., Solli H., Douglas A.G., de Lange F. and de Leeuw J.W. (1979) Occurrence and significance of prist-1-ene in kerogen pyrolysates. *Nature* **279**, 405-408.

Larter S.R., Solli H. and Douglas A.H. (1983) Phytol containing melanoidins and their bearing on the fate of isoprenoid structures in sediments. In: *Avances in Organic Geochemistry 1981* (Ed. by M. Bjoroy et al.), John Wiley, Chichester, England, pp. 513-521.

Larter S.R. (1984) Application of analytical pyrolysis techniques to kerogen characterizations and fossil fuel exploration/exploitation. In: *Analytical pyrolysis*, (Ed. by K. J. Voorhees), pp. 212-275. Butterworths, London.

Larter S.R. and Horsfield B. (1993) Determination of structural components of kerogens using analytical pyrolysis methods. In: *Organic Geochemistry, Principles and Applications*, (Ed. by M. Engel and S. Macko), pp. 271-287. Plenum Press, New York.

Laws F.A., Popp B.N., Bigidare R.R., Kennicutt M.C. and Macko S.A. (1995) Dependence of phytoplankton isotopic composition on growth rate and $[CO_2]_{aq}$: Theoretical considerations and experimental results. *Geochimica et Cosmochimica Acta* **59**, 1131-1138.

de Leeuw J.W., Rijpstra W.I.C. and Schenck P.A. (1981) The occurence and identification of C_{30}, C_{31} and C_{32} alkan-1,15-diols and alkan-15-one-1-ols in Unit I and unit II Black Sea sediments. *Geochimica et Cosmochimica Acta* **45**, 2281-2285.

de Leeuw J.W., Sinninghe Damsté J.S., Schenck P.A., Boon J.J. (1985) Biogeochemistry of Gavish Sabkha sediments I. Studies on neutral reducing sugars and lipid moieties by gas chromatography-mass spectrometry. In: *Hypersaline ecosystems. The Gavish Sabkha* (Ed. by G. M. Friedman & W. E. Krumbein), pp. 350-367. Springer, Heidelberg.

de Leeuw J.W., van Bergen P.F., van Aarssen B.G.K., Gatelier J.-P.L.A., Sinninghe Damsté J.S. and Collinson M.E. (1991) Resistant biomacromolecules as major contributors to kerogen. *Philosophical Transactions of the Royal Society of London B* **333**, 329-337.

de Leeuw J.W. and Largeau C. (1993) A review of macromolecular organic compounds that comprise living organisms and their role in kerogen, coal and petroleum formation. In: *Organic Geochemistry. Principles and Applications* (Ed. by M. H. Engel & S. A. Macko), pp. 23-72. Plenum Press, New York.

Li M., Johns R.B. and Mei B. (1990) A study in early diageniesis: biomarker compositon of a suite of immature coals and coaly shales. *Organic Geochemstry* **16**, 1067-1075.

Li M., Larter S.R., Taylor P., Jones D.M., Bowler B. and Bjorøy M. (1995) Biomarkers or not biomarkers? A new hypothesis for the origin of pristane involving derivation from methytrimethyldridecylchromans (MTTCs) formed during diagenesis form chlorophyll and alkylphenols. *Organic Geochemistry* **23**, 159-167.

Lichtenthaler H.K., Schwender J., Disch A. and Rohmer M. (1997) Biosynthesis of isoprenoids in higher plant chloroplasts proceeds via a mevalonate-independent pathway. *FEBS Letters* **400**, 271-274.

Mackenzie A.S., Patience R.L. and Maxwell J.R. (1980) Molecular parameters of maturation in the Toarcian shales, Paris Basin, France-I. Changes in the configurations of acyclic isoprenoid alkanes, steranes and triterpanes. *Geochimica et Cosmochimica Acta* **44**, 1709-1721.

Makushina V.M., Aref'ev O.A., Zabrodina M.N., Petrov A.A. (1978) New relic alkanes of petroleums. *Neftekhiyma* **18**, 847-854 (in Russian).

March J. (1985) *Advanced Organic Chemistry: Reactions, Mechanisms, and structure.* John Wiley & Sons, Inc, New York.

Maters W.L., Meent D.V.D., Schuyl P.J.W. and de Leeuw J.W. (1977) Curie-point pyrolysis in organic geochemistry. In: *Analytical Pyrolysis*, (Ed. by C.E.R. Jones and C.A. Cramers), pp 203-216. Elsevier, Amsterdam.

McKelvey V.E. (1959) The Phosphoria, Park City and Shedhorn Formation in the Western Phosphate Field. *U.S. Geological Survey Professional Paper* **313-A**, 1-47.

McKirdy D.M., Kantsler A.J., Emmett J.K. and Aldridge A.K. (1984) Hydrocarbon genesis and organic matter facies in Cambrian carbonates of the eastern Officer Basin, South Australia. In: *Petroleum Geochemistry and Source Rock Potential of Carbonate Rocks*, (Ed. by J. G. Palacas), pp. 13-31. American Association of Petroleum Geologists, Tulsa, Oklahoma.

McKirdy D.M., Imbuss S.W. (1992) Precambrian petroleum: A decade of changing perceptions. In: *Early Organic Evolution: Implications for Mineral and Energy Resources* (Ed. by M. Schidlowski). Springer-Verlag, Berlin Heidelberg.

van der Meent D, Brown S.C., Philp R.P., Simoneit B.R.T. (1980) Pyrolysis-high resolution gas chromatography and pyrolysis gas chromatography-mass spectrometry of kerogens and kerogen precursors. *Geochimica et Cosmochimica Acta* **44**, 999-1013.

Merrit D.A., Brand W.A. and Hayes J.M. (1994) Isotope-ratio-monitoring gas chromatography: Methods for isotopic calibration. *Organic Geochemistry* **21**, 573-584.

Meunier-Christman C. (1988) Géochimie organique de phosphates et schistes bitumineux marocains: étude du processus de phophatogénèse. PhD Dissertation. University of Strasbourg, pp. 133.

Meyer H. and Holz G.G. (1966) Biosynthesis of lipids by kinetoplastic flagellates. *Journal of Biological Chemistry* **241**, 5000-5007.

Michaelis J.M. and Albrecht P. (1979) Molecular fossils of archaebacteria in kerogen. *Naturwissenschaften* **66**, 420-422.

Mills J.S., White R. and Gough L.J. (1984) The chemical composition of Balic amber. *Chemical Geology* **47**, 15-39.

Mycke B., Narjes F. and Michaelis W. (1987) Bacteriohopanetetrol from chemical degradation of an oil shale kerogen. *Nature* **326**, 179-181.

Naylor S., Hanke F.J., Manes L.V. and Crews P. (1983) Chemical and biological aspects of marine monoterpenes. *Prog. Chem. Org. Nat. Prod.* **44**, 189-241.

Nip M., Tegelaar E.W., Brinkhuis H., de Leeuw J.W., Schenck P.A. and Holloway P.J. (1986a) Analysis of modern and fossil plant cuticles by Curie point Py-GC and Curie point Py-GC-MS: Recognition of a new, highly aliphatic and resistant biopolymer. *Organic Geochemistry* **10**, 769-778.

Nip M., Tegelaar E.W., de Leeuw J.W. and Schenck P.A. (1986b) A new non-saponifiable highly aliphatic and resistant biopolymer in plant cuticles. *Naturwissenschaften* **73**, 579-585.

Otto A., Walther H. and Püttmann W. (1997) Sisqui-and diterpenoid biomarkers preserved in *Taxodium*-rich Oligocen oxbow lake clays, Weisselster basin, Germany. *Organic Geochemistry* **26**, 105-115.

Ourisson G., Albrecht P. and Rohmer M. (1979) The hopanoids. Palaeochemistry and biochemistry of a group of natural products. *Pure and Applied Chemistry* **51**, 709-729.

Ourisson G., Albrecht P. and Rohmer M. (1982) Predictive microbial biochemistry from molecular fossils to procaryotic membranes. *Trends in Biochemical Sciences* **7**, 236-239.

Peters, K.E. and Moldowan, J.M. (1993). The Biomarker Guide. Englewood Cliffs, New Jersey, Prentice Hall, pp. 363.

Peters K.E., Clark M.E., Das Gupta U., McCaffrey M.A., Lee C.Y. (1995) Recognition of an Infracambrian source rock based on biomarkers in the Baghewala-1 Oil, India. *American Association of Petroleum Geologists Bulletin* **79**, 1481-1494.

Philp R.P. and Calvin M. (1976) Possible origin for insoluble organic (kerogen) debris in sediments from insoluble cell-wall materials of algae and bacteria. *Nature* **262**, 134-136.

Ratledge C. and Wilkinson S.G. (1988) Terpenoid Lipids. In: *Microbial Lipids I* (Ed. by C. Ratledge and S.G. Wilkinson), pp 623. Academic Press, London.

Regtop R.A., Ellis J., Crisp P.T, Ekstrom A. and Fookes C.J.R. (1985) Pyrolysis of model compounds on spent oil shales, minerals and charcoal: implications for shale oil composition. *Fuel* **64**, 1640-1646.

Regtop R.A., Crisp P.T., Ellis J. and Fookes C.J.R. (1986) 1-Pristene as a precursor for 2-pristene in pyrolysates of oil shale from Condor, Australia. *Organic Geochemistry* **9**, 233-236.

Requejo A.G. (1997) Short-chain C_{21} and C_{22} diasteranes in petroleum and source rocks as indicators of maturity of depositional environment. *Geochimica et Cosmochimica Acta* **61**, 2653-2668.

Richnow H.H., Jenisch A. and Michaelis W. (1992) Structural investigations of sulphur-rich macromolecular oil fractions and a kerogen by sequential chemical degradation. *Organic Geochemistry* **19**, 351-370.

Richnow H.H., Jenisch A. and Michaelis W. (1993) The chemical structure of macromolecular fractions of a sulfur-rich oil. *Geochimica et Cosmochimica Acta* **57**, 2767-2780.

Risatti J.B., Rowland S.J., Yon D.A. and Maxwell J.R. (1984) Stereochemical studies of acyclic isoprenoids-XII. Lipids of methanogenic bacteria and possible contributors to sediments. In: *Advances in Organic Geochemistry 1983,* (Ed. by P.A. Schenk, J.W. de Leeuw and G.W.M. Lijmbach), pp. 105-114. Pergamon Press, Oxford.

Robinson N. and Eglinton G. (1990) Lipid chemistry of Iceland hot spring microbial mats. *Organic Geochemistry* **15**, 291-298.

Rohmer M., Bisseret P. and Neunlist S. (1992) The hopanoids, prokaryotic triterpenoids and precursors of ubiquitous molecular fossils. In *Biological Markers in Sediments and Petroleum* (Ed. by J. M. Moldowan, P. Albrecht & R. P. Philp), pp. 1-17. Prentice Hall, Englewood Cliffs, New York.

Rohmer M., Knani M., Simonin P., Sutter B. and Sahm H. (1993) Isoprenoid biosynthesis in bacteria: a novel pathway for the early steps leading to isopentyl diphosphate. *Biochemical Journal* **295**, 517-524.

Rohmer M., Seemann M., Horbach S., Bringer-Meyer S. and Sahm H. (1996) Glyceraldehyde 3-phosphate and pyruvate as precursors of isoprenic units in an alternative non-mevalonate pathway for terpenoid biosynthesis. *Journal of the American Chemical Society* **118**, 2564-2566.

Rontani J.-F., Giral P.J.-P., Baillet G. and Raphael D. (1992) "Bound" 6,10,14-trimethylpentadecan-2-one: a useful marker for photodegradation of chlorophylls with a phytol ester group in seawater. *Organic Geochemistry* **18**, 139-142.

Rowland S.J., Rockey C., Al-Lihaibi S.S. and Wolff G.A. (1993) Incorporation of sulphur into phytol derivatives during simulated early diagenesis. *Organic Geochemistry* **20**, 1-5.

Rupert J.P., Granquist, W.T. and Pinnavaia T.J. (1987) Catalytic properties of clay minerals. In: A.C.D. Newman (Editor) Chemistry of clays and clay minerals. Mineralogical Society (Ed. by A.C.D. Newman), pp 275-318.

Schaeffer P., Ocampo R., Callot H.J. and Albrecht P. (1993) Extraction of bound porphyrins from sulfur-rich sediments and their use for reconstruction of palaeoenvironment. *Nature* **364**, 133-135.

Schaeffer P., Harrison W.N., Keely B.J. and Maxwell J.R. (1995) Product distributions from chemical degradation of kerogens from a marl from a Miocene evaporitic sequence (Vena del Gesso, N. Italy). *Organic Geochemistry* **23**, 541-554.

Schidlowski M., Matzigkeit U. and Krumbein W.E. (1984) Superheavy organic carbon from hypersaline mcirobial mats. Assimilatory pathway and geochemical implications. *Naturwissenschaften* **71**, 303-308.

Schoell M. (1984) Stable isotopes in petroleum research. In: *Advances in Petroleum Geochemistry 1* (Ed. by J. Brooks & D. H. Welte), pp. 215-245. Academic Press, London.

Schouten S., Pavlovic D., Sinninghe Damsté J.S. and de Leeuw J.W. (1993) Nickel Boride: An improved desulphurization agent for sulphur-rich geomacromolecules in polar and asphaltene fractions. *Organic Geochemistry* **20**, 901-910.

Schouten S., de Graaf W., Sinninghe Damsté J.S., van Driel G.B. and de Leeuw J.W. (1994) Laboratory simulation of natural sulphurization: II. Reaction of multi-functionalized lipids with inorganic polysulphides at low-temperatures. *Organic Geochemstry* **22**, 825-834.

Schouten S., Sinninghe Damsté J.S. and de Leeuw J.W. (1995) A novel triterpenoid carbon skeleton in immature sulphur-rich sediments. *Geochimica et Cosmochimica Acta* **59**, 953-958.

Schouten S., Schoell M., Rijpstra W.I.C., Sinninghe Damsté J.S. and de Leeuw J.W. (1997) A molecular stable carbon isotope study of organic matter in immature Miocene Monterey sediments (Pismo Basin). *Geochimica et Cosmochimica Acta* **61**, 2065-2082.

Schouten S., Hoefs M.J.L., Koopmans M.P., H-J B. and Sinninghe Damsté J.S. (1998a) Structural characterization, occurrence and fate of archaeal ether-bound acyclic and cyclic biphytanes and corresponding diols in sediments. *Organic Geochemistry* **29**, 1305-1319.

Schouten, S., de Loureiro, M.R.B., Sinninghe Damsté, J.S. and Leeuw, J.W. (1999). Molecular biogeochemistry of Montery sediments (Naples Beach, USA). I Distributions of hydrocarbons and organic sulfur-bound compounds. In *The Monterey Formation: From Rock to Molecule* (Ed. by J. Rullkötter & C. M. Isaacs), Colombia University Press, in press.

Schwender J., Seemann M., Lichtenthaler H.K. and Rohmer M. (1996) Biosynthesis of isoprenoids (carotenoids, sterols, prenyl side-chains of chlorophylls and plastoquinone) via a novel pyruvate/glyceraldehyde 3-phosphate non-mevalonate pathway in the green alga *Scenedesmus obliquus*. *Biochemical Journal* **316**, 73-80.

Sharkey T.D. and Berry J.A. (1985) Carbon isotope fractionation of algae as influenced by an inducible CO_2 concentrating mechanism. In: *Inorganic Carbon Uptake by Aquatic Photosynthetic Organisms* (Ed. by W.J. Lucas & J.A. Berry), American Society of plant Physiology, Rockville, Maryland.

Shiea J., Brassell S.C., Ward D.M. (1990) Mid-chain branched mono-and dimethyl alkanes in hot spring cyanobacterial mats: A direct biogenic source for branched alkanes in ancient sediments? *Organic Geochemistry* **15**, 223-231.

Sieskind O., Joly G. and Albrecht P. (1979) Simulation of the geochemical transformations of sterols: superacid effect of clay minerals. *Geochimica et Cosmochimica Acta* **43**, 1675-1679.

Simoneit B.R.T. (1977) Diterpenoid compounds and other lipids in deep-sea sediments and their gechemical significance. *Geochimica et Cosmochimica Acta* 41, 463-476.

Simoneit B.R.T., Grimalt J.O., Wang T.G., Cox R.E., Hatcher P.G. and Nissenbaum A. (1986) Cyclic terpenoids of contemporary resinous plant detritus and of fossil woods, ambers and coals. *Organic Geochemistry* 10, 877-889.

Sinninghe Damsté J.S., Kock-van Dalen A.C., de Leeuw J.W. and Schenck P.A. (1988) The identification of homologous series of alkylated thiophenes, thiolanes, thianes and benzothiophenes present in pyrolysates of sulphur-rich kerogens. *Journal of Chromatography* **435**, 435-452.

Sinninghe Damsté J.S., Rijpstra W.I.C., de Leeuw J.W. and Schenck P.A. (1989) The occurrence and identification of series of organic sulphur compounds in oils and sediments extracts II. Their presence in samples from hypersaline and non-hypersaline depositional environments and their possible applications as source, paleoenvironmental and maturity indicators. *Geochimica et Cosmochimica Acta* **53**, 1323-1341.

Sinninghe Damsté J.S. and de Leeuw J.W. (1990a) Analysis, structure and geochemical significance of organically-bound sulphur in the geosphere: State of the art and future research. *Organic Geochemistry* **16**, 1077-1101

Sinninghe Damsté J.S., Eglinton T.I., Rijpstra W.I.C. and de Leeuw J.W. (1990b) Characterization of sulphur-rich high molecular weight substances by flash pyrolysis and Raney Ni desulfurisation. In: *Geochemistry of Sulphur in Fossil*

Fuels., *ACS Symposium Series 249* (Ed. by W. L. Orr & C. M. White), pp. 486-528. Amer. Chem. Soc, Washington DC.

Sinninghe Damsté J.S., Eglinton T.I. and de Leeuw J.W. (1992) Alkylpyrroles in a kerogen pyrolysate: Evidence for abundant tetrapyrrole pigments. *Geochimica et Cosmochimica Acta* **56**, 1743-1751.

Sinninghe Damsté J.S., Betts S., Ling Y., Hofmann P.M. and de Leeuw J.W. (1993) Hydrocarbon biomarkers of different lithofacies of the Salt IV Formation of the Mulhouse Basin, France. *Organic Geochemistry* **20**, 1187-1200.

Sinninghe Damsté J.S., Rijpstra W.I.C., de Leeuw J.W., Lijmbach G.W.M. (1994) Molecular characterization of organically-bound sulfur in crude oils. *Journal of High Resolution Chromatography* **17**, 489-500.

Sinninghe Damsté J.S., Hollander D., Kohnen M.E.L., de Leeuw J.W. (1995a) Early diagenesis of bacteriohopanetetrol derivatives: Formation of fossil homohopanoids. *Geochimica et Cosmochimica Acta* **59**, 5141-5157.

Sinninghe Damsté J.S. and de Leeuw J.W. (1995b) Comments on Biomarkers or not Biomarkers. A new hypothesis for the origin of pristane involving derivation from methyltrimethyltridecylchromans (MTTC'S) formed during diagenesis from chlorophyll and alkylphenols" from M. Li, S.R. Larter, D. Taylor, D.M. *Organic Geochemistry* **23**, 1085-1087.

Sinninghe Damsté J.S. and Koopmans M.P. (1997). The fate of carotenoids in sediments: An overview. *Pure & Applied Chemistry* **69**, 2067-2074.

Sinninghe Damsté J.S., Baas M., Koopmans M.P. and Geenevasen J.A.J. (1997) Cyclisation, aromatisation, and expulsion reactions of β-carotene during sediment diagensis. *Tetraedron Letters* **38**, 2347-2350.

Sinninghe Damsté J.S. (1999) Sulfurized carbohydrates: An important sedimentary sink for organic carbon? *Earth and Planetary Science Letters* **164**, 7-14.

Solli H. and Leplat P. (1986) Pyrolysis-gas chromatography of asphaltenes and kerogens from source rocks and coals-A comparative structural study. *Organic Geochemistry* **10**, 313-329.

Standen G., Boucher R.J., Rafalska-Bloch J. and Eglinton G. (1991) Ruthenium tetroxide oxidation of natural organic macromolecules: Messel kerogen. *Chemical Geology* **91**, 297-313.

Standen G., Boucher R.J., Eglinton G., Hansen G., Eglinton T.I. and Larter S.R. (1992) Differentiation of German Tertiary brown coal lithotypes ('amorphous'

and 'woody' kerogens) using ruthenium tetraoxidation and pyrolysis-GC-MS. *Fuel* **71**, 31-36.

Summons R.E. (1987) Branched alkanes from ancient and modern sediments: Isomer discrimination by GC/MS with multiple reaction monitoring. *Organic Geochemistry* **11**, 281-289.

Summons R.E., Brassell S.C., Eglinton G., Evans E., Horodyski R.J., Robinson N., Ward D.M. (1988a) Distinctive hydrocarbon biomarkers from fossiliferous sediment of the Late Proterozoic Walcott Member, Chuar Group, Grand Canyon, Arizona. *Geochimica et Cosmochimica Acta* **52**, 2625-2637.

Summons R.E., Powell T.G., Boreham C.J. (1988b) Petroleum geology and geochemistry of the Middle Proterozoic Mc Arthur Bassin, Northern Australia: III. Composition of extractable hydrocarbons. *Geochimica et Cosmochimica Acta* **52**, 1747-1763.

Summons R.E. and Powell T.G. (1992) Hydrocarbon composition of the Late Proterozoic oils of the Siberian Platform: Implications for the Depositional Environment of Source Rocks. In: *Early Organic Evolution: Implications for Mineral and Energy Resources* (Ed. by M. Schidlowski). Springer-Verlag, Berlin Heidelberg.

Tang Y.C. and Stauffer M. (1995) Formation of pristene, pristane and phytane: Kinetic study by laboratory pyrolysis of Monterey Source Rock. *Organic Geochemistry* **23**, 451-460.

Tegelaar E.W., de Leeuw J.W., Derenne S. and Largeau C. (1989) A reappraisal of kerogen. *Geochimica et Cosmochimica Acta* **53**, 3103-3106.

Thiel V. and Michaelis W. (1999) Mid-chain branched alkanoic-acids from "living fossil" demosponges: a link to ancient sedimentary lipids? *Organic Geochemistry* **30**, 1-14.

Tissot B.P. and Welte D.H. (1984) *Petroleum Formation and Occurrence*. Springer-Verlag, Heidelberg, pp. 538.

Vairamurthy A. and Mopper K. (1987) Geochemical formation of organosulphur compounds (thiols) by addition of H_2S to sedimentary organic matter. *Nature* **329**, 623-625.

Valisolalao J., Perakis N., Chappe B. and Albrecht P. (1984) A novel sulphur containing C_{35} hopanoid in sediments. Tetraedron Letters **25**, 1183-1186.

Van der Gaast S.J. and Vaars A.J. (1981) A method to eliminate the background in X-ray diffraction patterns of oriented clay mineral samples. *Clay Mineralogy* **16**, 383-393.

Venema A. and Veurink J. (1985) A method for solvent-free application of polymers and inorganic materials to ferromagnetic wires used for pyrolysis-capillary gas chromatographic studies. *Journal of Analytical and Applied Pyrolysis* **7**, 207-213.

Vink A., Schouten S., Sephton M. and Sinninghe Damsté J.S. (1998) A newly discovered norisoprenoid, 2,6,15,19 tetramethylicosane, in Cretaceaous black shales. *Geochimica et Cosmochimica Acta* **62**, 965-970.

Volkman J.K. and Maxwell J.R. (1986) Acyclic isoprenoids as biological markers. In: *Biological Markers in the Sedimentary Record*, (Ed. by R. B. Johns, pp. 1-42. Elsevier, Amsterdam.

Volkman J.K., Barrett S.M., Dunstan G.A. and Jeffrey S.W. (1992) C_{30}-C_{32} alkyl diols and unsaturated alcohols in microalgae of the class Eustigmatophyceae. *Organic Geochemistry* **18**, 131-138.

Wade L.G. (1987) Organic Chemistry, pp. 434-435. Prentice-Hall, London.

Wang T.-G. and Simoneit B.R.T. (1995) Tricyclic terpanes in Precambrian bituminous sandstone from the eastern Yanshan region, North China. *Chemical Geology* **120**, 155-170.

West N., Alexander R. and Kagi R.I. (1990) The use of silicalite for rapid isolation of branched and cyclic alkane fractions of petroleum. *Organic Geochemistry* **15**, 499-501.

Whittaker D. (1972) The monoterpenoids. In *Chemistry of Terpenes and Terpenoids* (Ed. by A. A. Newman). Academic Press, London and New York, pp. 449.

Wu Q., Liu Z., Sheng G. and Fu J. (1986) Biomarkers originated from Precambrian algae. In: Biomarkers and Kerogens (Ed. by Shi Jiyang), Guizhou Peaople's Publishing House, Guiyang, pp. 111-121 (in Chineese).

Zheng Q.-H., Su J.-Y., Huang Q.-P., Wang Z.-C., Liu X., Gao B., Zeng L.-M. and Zheng D.-X. (1994) Biogenetic pathways for marine terpenoids. *Science in China (Series B)* **37**, 897-905.

This thesis is based on the following publications:

Chapter 2: Changes in the molecular structure of a type II-S kerogen (Monterey Formation, USA) during sequential chemical degradation.
Ingeborg M. Höld, Niels J. Brussee, Stefan Schouten, Jaap S. Sinninghe Damsté (1998) *Organic Geochemistry* **29**, 1403-1417.

Chapter 3: Recognition of *n*-alkyl and isoprenoid biopolymers in marine sediments by stable carbon isotopic analysis of pyrolysis products of kerogens.
Ingeborg M. Höld, Stefan Schouten, Heidy M.E. van Kaam-Peters and Jaap S. Sinninghe Damsté (1998) *Organic Geochemistry* **28**, 179-195.

Chapter 4: On the origin of prist-1-ene and prist-2-ene in kerogen pyrolysates.
Ingeborg M. Höld, Stefan Schouten, Sjerry J. Van der Gaast and Jaap S. Sinninghe Damsté *Chemical Geology*, accepted.

Chapter 5: Evidence for sequesterd non-aromatic carotenoids in kerogen
Ingeborg M. Höld, Stefan Schouten, Walter A. Hartgers and Jaap S. Sinninghe Damsté, in preparation.

Chapter 6: Origin of free and bound mid-chain methyl alkanes in oils, bitumens and kerogens of the marine, Infracambrian Huqf Formation (Oman).
Ingeborg M. Höld, Joyce Jellema, Stefan Schouten and Jaap S. Sinninghe Damsté (1999) *Organic Geochemistry* **30**, 1411-1428.

DANKWOORD

Het is moeilijk uit te leggen waar het verichten van wetenschappelijk onderzoek en het schrijven van een proefschrift mee te vergelijken zijn. Sommigen vergelijken het met een voetbalwedstrijd, andere met zwemmen naar een eiland. Enige jaren geleden kwam ik in een folder van bergsportartikelen het onderstaande gedicht tegen.

> In a sense everything that is exists to climb. All evolution is a climbing toward a higher form. Climbing is a metaphor for life as it reaches toward consciousness, toward the spirit.
>
> We have always honored the high places because we sense them to be homes of gods. In the mountains there is a promise of .....something inexplicable. A higher plane of awareness, a spirit that soars.
>
> So we climb. And in the climbing there is more than a metaphor: there is a means of discovery.
>
> And what about exploring caves, descending into great holes in the Earth? It is another means to the same end, as well as another metaphor - for going inside to explore the mysteries that reside within the Self.

Een ieder die wel eens een berg beklommen heeft weet dat het hard werken is om boven en om weer veilig beneden te komen. Soms als de berg erg hoog en moeilijk is wil je opgeven, denk je ik haal het niet, ik kan het niet, ik draai om. Dan is het goed om een gids mee hebben die je een duuwtje in de rug kan geven. Zodat je er weer even tegenaan kan op weg naar boven. Daarom wil ik, al mijn gidsen binnen en buiten het NIOZ hierbij bedanken. Zonder jullie had ik het niet gered!

CURRICULUM VITAE

Ingeborg Maria Höld werd geboren op 20 oktober 1968 te Den Haag. In 1987 behaalde zij het VWO diploma aan het Aloysius College ook te Den Haag en begon met de studie Scheikunde aan de Rijksuniversiteit Leiden. Tijdens de doctoraalfase verrichtte ze onderzoek naar Gasfase reacties van H, OH en $O(^3P)$ radikalen met benzeenderivaten bij de vakgroep Milieuchemie van Prof. R. Louw (Universiteit Leiden). Daarna verrichtte ze gedurende een half jaar onderzoek naar de synthese van pyrrolidine-phospholane ring systemen bij de vakgroep Organische Chemie van Prof. A. Brandi (Università di Firenze, Italië). Begin 1993 startte zij met haar promotieonderzoek bij de afdeling Mariene Biogeochemie en Toxicologie (MBT) van het Nederlands Instituut voor Onderzoek der Zee op Texel. Hier werd het in dit proefschrift beschreven onderzoek uitgevoerd onder leiding van Dr. Jaap. S. Sinninghe Damsté. Sinds oktober 1998 is zij werkzaam als wetenschappelijk onderzoeker bij de afdeling Milieu van het Nederlands Forensisch Instituut te Rijswijk.